DUDLEY KNOX LIBRARY
NAVAL POSTGRADUATE SCHOOL
MONTEREY CA 93943-5101

Approved for public release; distribution is unlimited.

DETERMINING THE EFFECT OF ENDWALL BOUNDARY LAYER SUCTION IN A LARGE SCALE SUBSONIC COMPRESSOR CASCADE

by

Matthew Allen Webber
Lieutenant, United States Navy
B.S., University of Kansas

Submitted in partial fulfillment
of the requirements for the degree of

MASTER OF SCIENCE IN AERONAUTICAL ENGINEERING

from the

NAVAL POSTGRADUATE SCHOOL
March 1993

REPORT DOCUMENTATION PAGE

eport Security Classification: Unclassified		1b Restrictive Markings		
ecurity Classification Authority		3 Distribution/Availability of Report		
)eclassification/Downgrading Schedule		Approved for public release; distribution is unlimited.		
rforming Organization Report Number(s)		5 Monitoring Organization Report Number(s)		
lame of Performing Organization 'al Postgraduate School	6b Office Symbol *(if applicable)* 31	7a Name of Monitoring Organization Naval Postgraduate School		
ddress *(city, state, and ZIP code)* nterey CA 93943-5000		7b Address *(city, state, and ZIP code)* Monterey CA 93943-5000		
lame of Funding/Sponsoring Organization	6b Office Symbol *(if applicable)*	9 Procurement Instrument Identification Number		
:ess *(city, state, and ZIP code)*		10 Source of Funding Numbers		
		Program Element No	Project No	Task No	Work Unit Accession No

'itle *(include security classification)* DETERMINING THE EFFECT OF ENDWALL BOUNDARY LAYER SUCTION IN A RGE SCALE SUBSONIC COMPRESSOR CASCADE

'ersonal Author(s) Matthew Allen Webber

Type of Report	13b Time Covered	14 Date of Report *(year, month, day)*	15 Page Count
;ter's Thesis	From To	1993, March, 31	140

upplementary Notation The views expressed in this thesis are those of the author and do not reflect the official policy or position he Department of Defense or the U.S. Government.

'osati Codes			18 Subject Terms *(continue on reverse if necessary and identify by block number)*
l	Group	Subgroup	Boundary Layer, Cascade, Controlled-Diffusion, Axial Velocity Ratio, Displacement Thickness

.bstract *(continue on reverse if necessary and identify by block number)*

An arrangement of suction slots was installed in the Naval Postgraduate School's subsonic cascade id tunnel. The aim was to improve flow two-dimensionality to enable flow separation of the installed itrolled-diffusion blades at high incidence. The slots were located 17.25 inches upstream of the test tion. Pressure and laser-Doppler velocimetry measurements were made, for a Reynolds number of .000 and an inlet flow angle of 44.4°, upstream and downstream of the test section to determine the effects varying suction. The set of baseline inlet flow field measurements was to be used for comparison poses in future tunnel modifications. The results showed that the tunnel endwall boundary layers were mmetric for the baseline configuration. Uniform suction was not achieved in both the pitchwise and nwise directions. However, the axial velocity ratio was reduced by 1.9% and the blade loading increased ;htly with increased suction.

)istribution/Availability of Abstract unclassified/unlimited __ same as report __ DTIC users		21 Abstract Security Classification Unclassified	
Name of Responsible Individual th V. Hobson		22b Telephone *(include Area Code)* (408) 656-2888	22c Office Symbol Code 31/Sc

FORM 1473,84 MAR 83 APR edition may be used until exhausted security classification of this pag
All other editions are obsolete Unclassifie

ABSTRACT

An arrangement of suction slots was installed in the Naval Postgraduate School's subsonic cascade wind tunnel. The aim was to improve flow two-dimensionality to enable flow separation of the installed controlled-diffusion blades at high incidence. The slots were located 17.25 inches upstream of the test section. Pressure and laser Doppler velocimetry measurements were made, for a Reynolds number of 711000 and an inlet flow angle of 44.4°, upstream and downstream of the test section to determine the effects of varying suction. The set of baseline inlet flow field measurements was to be used for comparison purposes in future tunnel modifications. The results showed that the tunnel endwall boundary layers were asymmetric for the baseline configuration. Uniform suction was not achieved in both the pitchwise and spanwise directions. However, the axial velocity ratio was reduced by 1.9% and the blade loading increased slightly with increased suction.

Thesis
W33015
c.1

TABLE OF CONTENTS

I. INTRODUCTION 1

A. BACKGROUND 1

B. CASCADE MODIFICATION EXAMPLES 2

C. PRIOR CONTROLLED DIFFUSION (CD) BLADE TESTS . . 4

D. PURPOSE 5

II. TEST FACILITY, INSTRUMENTATION AND INITIAL SETUP . 6

A. CASCADE BASE LINE CONFIGURATION 6

B. WIND TUNNEL MODIFICATION 6

1. SUCTION SLOT 8

2. BLOWER CONFIGURATION 11

C. INSTRUMENTATION 11

1. RAKE PROBE AND TRAVERSE 11

2. LDV SYSTEM 14

3. INSTRUMENTED CD BLADE 17

4. STATIC PRESSURES 17

D. DATA ACQUISITION 22

1. HARDWARE 22

2. SOFTWARE 22

III. EXPERIMENTAL PROCEDURE 23

A. BASE LINE CONFIGURATION 23

DUDLEY KNOX LIBRARY
NAVAL POSTGRADUATE SCHOOL
MONTEREY CA 93943-5101

B. SUCTION PROCEDURE 23

IV. RESULTS AND DISCUSSION 25

A. INLET SURVEYS 25

B. AVR 41

C. INSTRUMENTED BLADE 41

D. LDV SURVEYS 46

IV. CONCLUSIONS AND RECOMMENDATIONS 50

APPENDIX A. RECORDED DATA 52

A1. RAKE PROBE DATA 52

A2. INSTRUMENTED BLADE DATA 73

A3. MANOMETER DATA 76

A4. LDV DATA 83

APPENDIX B. DATA REDUCTION 106

B1. LIST OF EQUATIONS 106

B2. V_{REF} COMPUTATION AND PROGRAM 109

APPENDIX C. PROBE CALIBRATION 115

C1. YAW PROBE CALIBRATION 115

C2. STATIC PROBE CORRECTION 115

APPENDIX D. ENGINEERING DRAWINGS 121

LIST OF REFERENCES 129

INITIAL DISTRIBUTION LIST 131

LIST OF FIGURES

Figure 1. Rectilinear Subsonic Cascade Wind Tunnel . . 7

Figure 2. Top View of the Suction Configuration . . . 9

Figure 3. Suction Manifold Cross Section 10

Figure 4. Suction Slot Mounted to the South Endwall . 12

Figure 5. Blower Configuration 13

Figure 6. Rake Probe Plan View 15

Figure 7. Rake Probe Mounted to Downstream Traverse . 16

Figure 8. LDV Test Section Geometry 18

Figure 9. Instrumented Blade Pressure Tap Location . . 19

Figure 10. Manometer A. Pressure Tap Arrangement . . . 20

Figure 11. Manometer B. Pressure Tap Arrangement . . . 21

Figure 12. Inlet Flow Carpet Plot for Base Line Configuration 26

Figure 13. Inlet Flow Carpet Plot for Low Suction . . 27

Figure 14. Inlet Flow Carpet Plot for Medium Suction . 28

Figure 15. Inlet Flow Carpet Plot for High Suction . . 29

Figure 16. Superimposed Spanwise Pressure Distribution at 11.8 in. Pitch for Increased Suction . . 30

Figure 17. Superimposed Spanwise Pressure Distribution at 20 in. Pitch for Increased Suction . . . 31

Figure 18. Superimposed Spanwise Pressure Distribution at 22 in. Pitch for Increased Suction . . . 32

Figure 19. Superimposed Spanwise Pressure Distribution at 35.88 in. Pitch for Increased Suction . 33

Figure 20. Superimposed Spanwise Pressure Distribution at 50.9 in. Pitch for Increased Suction . . 34

Figure 21. Average Displacement Thickness for the North and South Endwalls, 20 to 23 in. Pitch . . 36

Figure 22. Pitchwise Manifold and Endwall Static Pressure Variations for Low Suction 38

Figure 23. Pitchwise Manifold and Endwall Static Pressure Variation for Medium Suction . . . 39

Figure 24. Pitchwise Manifold and Endwall Static Pressure Variation for High Suction 40

Figure 25. Suction Effects on the Axial Velocity Ratio for the Passage of 20 to 23 in. Pitch . . . 42

Figure 26. Instrumented Blade Pressure Distribution for Low Suction 43

Figure 27. Instrumented Blade Pressure Distribution for Medium Suction 44

Figure 28. Instrumented Blade Pressure Distribution for High Suction 45

Figure 29. Station 1 Inlet Velocity Comparison for Base Line Configuration and High Suction 47

Figure 30. Station 1 Inlet Flow Angle Comparison for Base Line Configuration and High Suction 48

Figure 31. Station 18 Outlet Flow Velocity Comparison for Base line Configuration and High Suction . 49

Figure A1. Manometer A for Low Suction Tests 78

Figure A2. Manometer B for Low Suction Tests 78

Figure A3. Manometer A for Medium Suction Tests . . . 80

Figure A4. Manometer B for Medium Suction Tests . . . 80

Figure A5. Manometer A for High Suction Tests 82

Figure A6. Manometer B for High Suction Tests 82

I. INTRODUCTION

A. BACKGROUND

Cascade experimentation continues to supply designers of axial flow turbo-machines with useful data. Frequently the objective of the measurements is to obtain two-dimensional flow around a particular blade shape since blading design is still carried out along quasi-three-dimensional or two-dimensional stream tubes. Therefore, the two-dimensionality of the flow within the cascade is important.

Flow two-dimensionality in compressor cascade experiments has received considerable attention. The degree of two-dimensionality has generally been determined by measuring the axial velocity density ratio (AVDR),or axial velocity ratio (AVR) for incompressible flow, across the blade row. There is experimental evidence showing that the AVR and aspect ratio of a cascade are important parameters in affecting flow deviation, losses and pressure distribution, i.e., stall point, of test blades [Ref. 1].

If a cascade has parallel solid end walls, the displacement effect of the endwall boundary layers causes a convergence of the stream-tube through the cascade. This will have two effects on the midspan boundary layers: first, the convergence alters the blade loading and thus the freestream

pressure field applied to the surface boundary layers; secondly, the spanwise convergence of the blade surface flow causes a thickening of the midspan boundary layer [Ref. 2]. Therefore, for a cascade with an aspect ratio less than three, provisions for end wall boundary layer removal should be incorporated. This can take two forms, first, provisions should be made for a porous wall or slots upstream of the blade row and, or, secondly, a porous wall within the blade row. For either compressor or turbine cascades, careful removal of the upstream endwall boundary layer will improve the two-dimensionality of the flow [Ref.3].

B. CASCADE MODIFICATION EXAMPLES

The work of some researchers to modify existing cascades is well documented in References 2, 4, 5 and 6. Reference 2 presents measurements for a large scale turbine cascade in which an arrangement of end-plates was incorporated to improve the two-dimensionality of the midspan flow. The endwall boundary layers were removed through slots located in the inlet section. Since the slots were a considerable distance ahead of the test section, the boundary layer grew to approximately 15mm by the time it reached the test section. Therefore, endwall slots were installed within the test section to further remove the boundary layer, resulting in the effective control of the AVR.

The effect of endwall suction on the flow in two-dimensional wind tunnels is examined in [Ref. 4]. The model that was used involved a flat plate airfoil in a tunnel with a suction window shaped to permit an analytic solution. The solution showed that the lift coefficient depended explicitly on the porosity parameter of the suction window and implicitly on the suction pressure differential.

Boundary layer control for a seven blade compressor cascade is described in [Ref.5]. In this study, a suction slot was placed ahead of the test section to allow optical access for laser-Doppler velocimetry measurements (LDV). The system required strong suction and a complex baffling system within the suction slot. Six suction ducts were located at a half blade spacing on either side of the blades. Each individual duct had a separate baffle control and was adjusted by changing the baffle position while examining the outlet flow. Presumably the control of the endwall suction distribution controlled the size of the endwall boundary layer at its intersection with the blade leading edge, thus controlling the origin of the corner disturbances. The AVDR was determined by averaging the local axial velocity ratio over three blade passages centered at the minimum velocity ratio point of the center blade wake. The average AVDR was found to be 1.0 with a day-to-day variation of ±3%.

The boundary layer control used in Reference 6 on a large scale compressor cascade having 7 blades consisted of three techniques. First, an endwall boundary layer suction scoop was placed ahead of the test section. This scoop was instrumented with static pressure taps to ensure the boundary layer was removed without contracting or diffusing the inlet flow. Secondly, an upper and lower bleed passage was used at the side walls between blade 1 and 7. Thirdly, corner suction was applied on each test blade to eliminate secondary flow caused by the corner disturbance.

C. PRIOR CONTROLLED DIFFUSION (CD) BLADE TESTS

Previous experiments at the Naval Postgraduate School Turbopropulsion Laboratory's Cascade Tunnel, using 20 CD blades designed by Sanger [Ref. 7], have not produced stall of the blade profile at high inlet flow angles. This is possibly due to the effects of three-dimensional flow in the endwall region of the cascade. Dreon, [Ref.8], performed wake measurements and blade surface pressure measurements at air inlet angles of 40.3° and 43.4°. The AVDR for these tunnel settings was 1.062 and 1.042 respectively. The measured blade surface pressures gave no evidence of flow separation.

Extensive LDV experiments by Elazar, [Ref. 9], were performed at inlet angles of 40°, 43.4°, and 46° which also did not show any flow separation on the suction surface. Five-hole pneumatic probe measurements were performed by

Classick [Ref.10] for an inlet flow angle of 48°. These measurements gave an AVDR of 1.108 and no flow separation occurred at this high incidence. More recently, Hobson and Shreeve [Ref. 11], performed detailed measurements at an inlet flow angle of 48°. Their results showed a steady pressure increase on the suction surface with no separation. However, the pressure gradient leveled off at the trailing edge, suggesting, possibly, the approach of flow separation.

D. PURPOSE

The present aim was to improve the two-dimensionality of the flow in the cascade using inlet boundary layer suction in order to allow an investigation of the onset of stall in the present installed CD blades at higher incidence angles. The effect of endwall suction was determined with probe and LDV measurements, with slots installed 17.25 inches ahead of the test section.

II. TEST FACILITY, INSTRUMENTATION AND INITIAL SETUP

A. CASCADE BASE LINE CONFIGURATION

A schematic diagram of the Rectilinear Subsonic Cascade Wind Tunnel facility is shown in Figure 1. A detailed description of its design and operation is found in an earlier thesis [Ref. 12]. Flow inlet conditions were investigated in detail by McGuire [Ref. 13]. Since that time, the inlet guide vanes were replaced with a new row of 60 blades. The design is given in Appendix D. The tunnel contained 20 CD blades with a chord of 5.01 inches and span of 10 inches. The blade spacing was set at 3 inches for a solidity of 1.67 and the setting angle was 14.1°. Blades 7 and 8, located at 20 to 23 inches pitch, were used for all LDV, AVR and boundary layer displacement thickness measurements. The instrumented blade was located at mid-pitch, 30 inches from the east sidewall.

B. WIND TUNNEL MODIFICATION

The ability to perform boundary layer control on the cascade endwalls was incorporated into the original design. Two manifolds with access to a blower were located on each endwall 17.25 inches ahead of the test section. The manifolds were equipped with blank-off plates for the base line tests. The present modifications to the cascade included the installation of suction slots and connections to a blower.

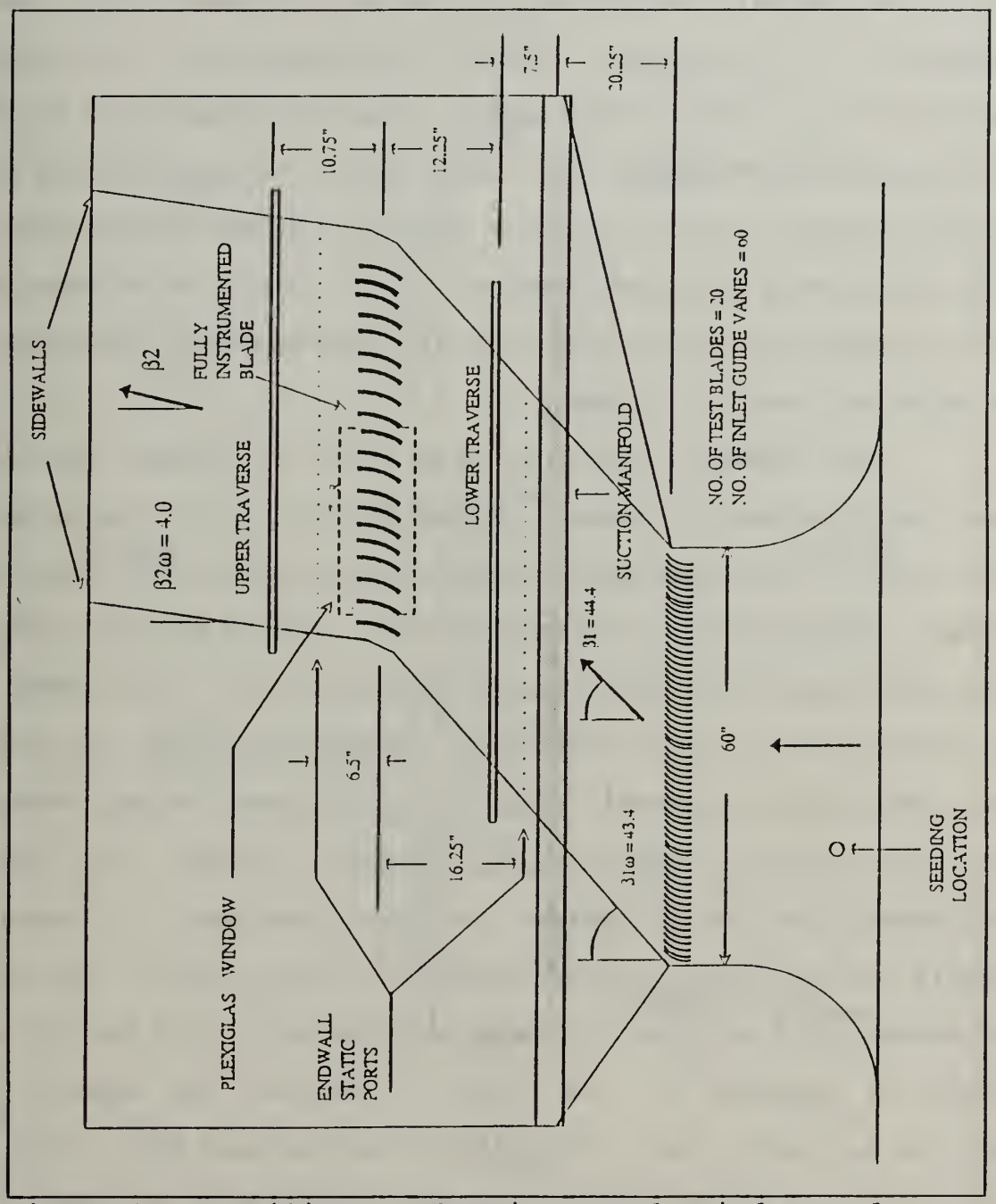

Figure 1. Rectilinear Subsonic Cascade Wind Tunnel

1. SUCTION SLOT

Flush mounted adjustable width slots were installed into the endwall manifolds. Figure 2 shows a top-down schematic of the tunnel suction configuration. A cross section of the slot, baffle and manifold arrangement is found in Figure 3. Each slot was comprised of two flat pieces of stock aluminum with a 5/8 inch radius machined on one edge. The pieces were attached together with machined cross-members that allowed for the variation of the slot height. A detailed drawing is found in Appendix D.

The endwall manifolds were each 120 inches and the test section was 60 inches. Since the inlet flow angle was set to 44.4°, the test section was not centered on the suction slots. Initial tests with the suction slot in the full open position showed that there was strong suction at the sidewall extremities but none at mid-pitch. Because of this, the slot was arbitrarily narrowed to one inch. Further testing showed that the suction improved in strength, however, the non-uniformity in the pitchwise direction remained. A porous baffle was attached to the backside of the slot to try and alleviate this problem. A detailed drawing of the baffle is found in Appendix D. In order to monitor the amount of suction applied across the manifold, eleven taps were drilled into the base of the manifold of which nine were attached to a water manometer. The nine pressure taps were centered on

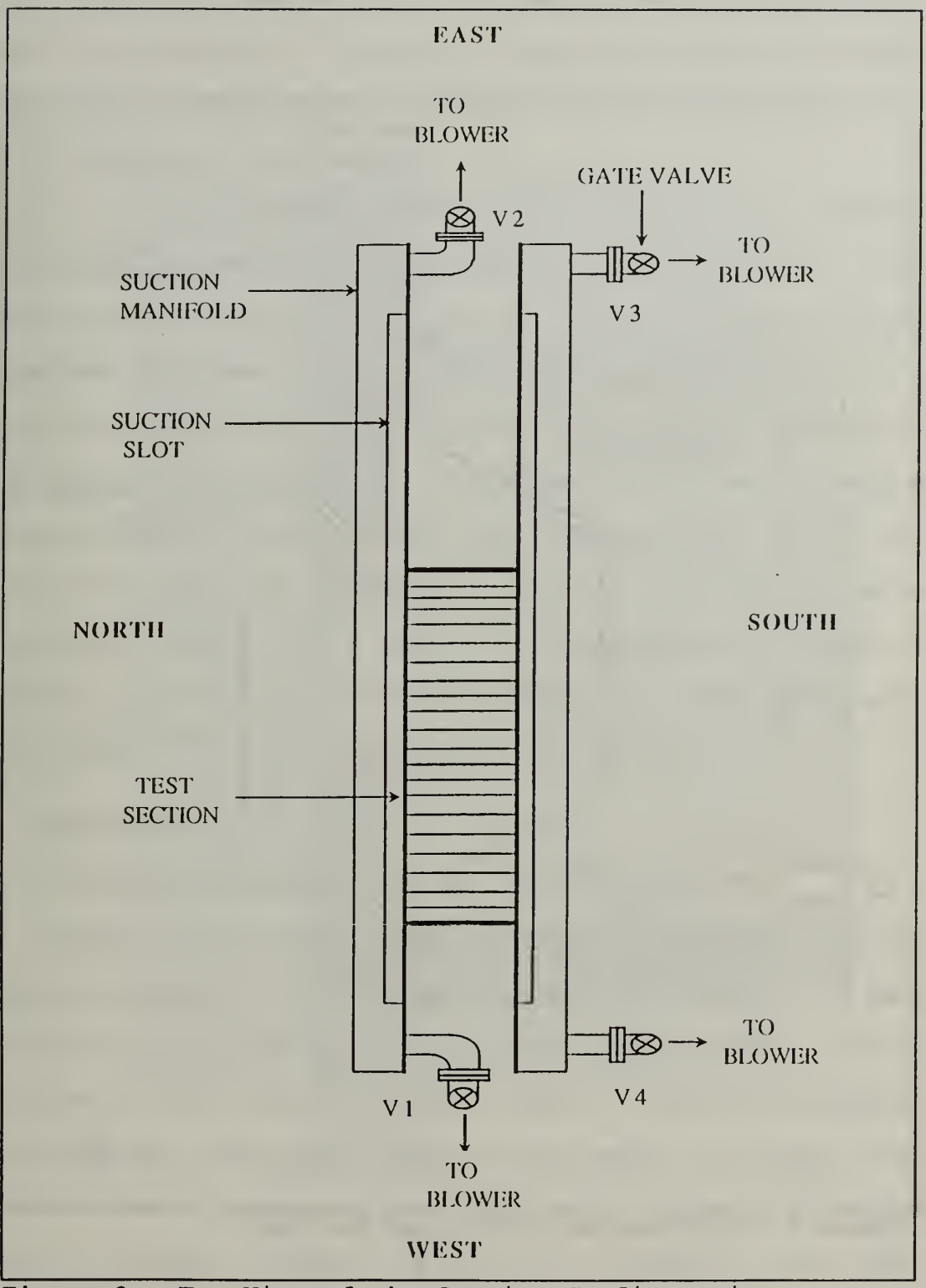

Figure 2. Top View of the Suction Configuration

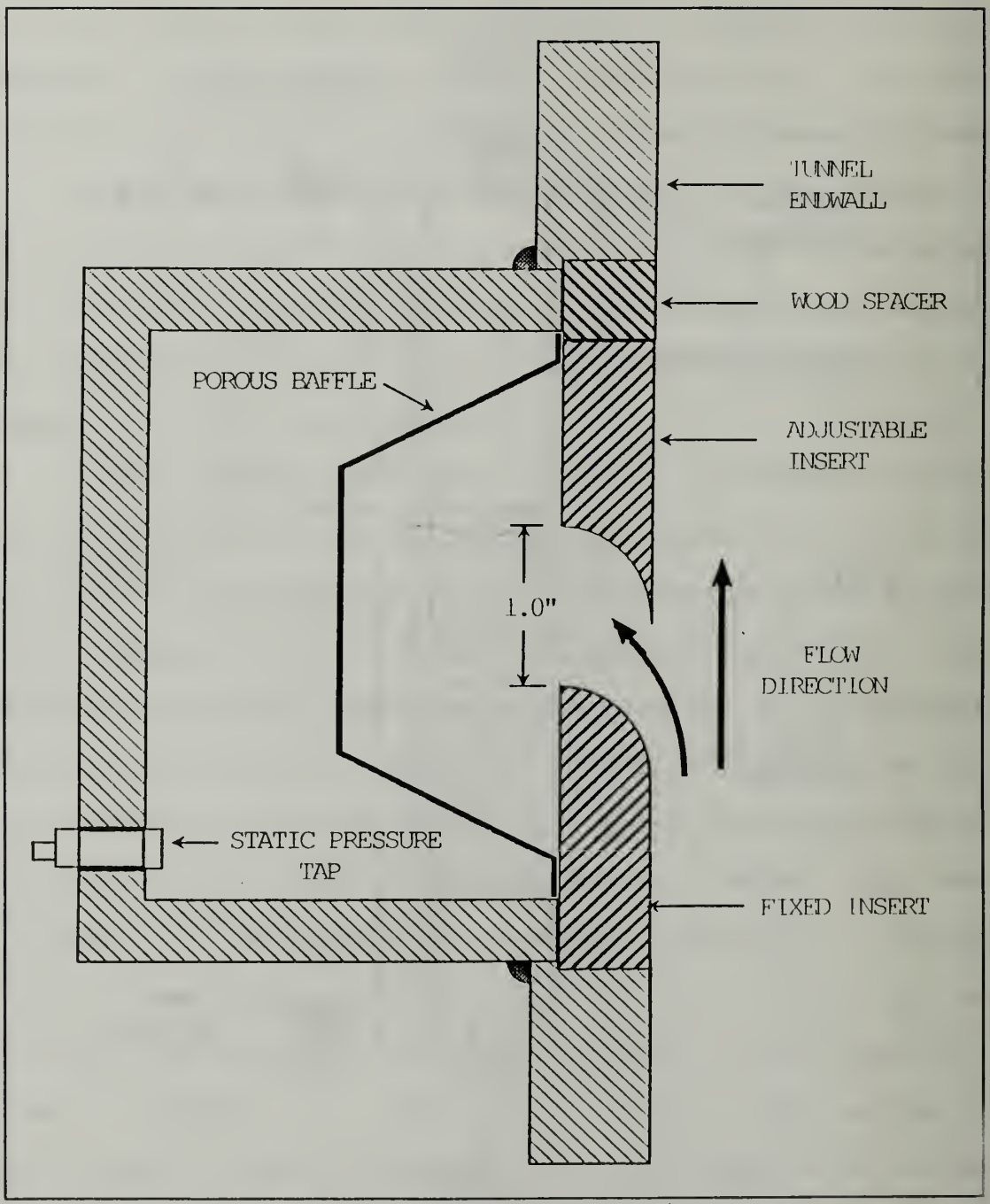

Figure 3. Suction Manifold Cross Section

the inlet to the test section. A dimensioned cross section is given in Appendix D. Figure 4 shows the end of the slot outside the tunnel which was taped over for the tests.

2. BLOWER CONFIGURATION

A 30 horsepower Allis Chalmers electric motor driven centrifugal blower was placed behind the south wall of the wind tunnel. A photograph of the blower configuration is given in Figure 5. The blower inlet was connected to a cylindrical plenum having 6 hook-ups, three at a third of the length and three at the end. The blower plenum was connected to the tunnel by mounting four gate valves to each end of the tunnel manifolds and running flex tubing from the valves to the blower plenum. The gate valves allowed the amount of suction to be varied within the manifolds. The two unused attachments of the blower plenum were capped.

C. INSTRUMENTATION

1. RAKE PROBE AND TRAVERSE

A ten inch rake probe was designed to take detailed pressure distribution measurements across the span of the test section with a finer resolution at each end to better record the size of the endwall boundary layer. The probe assembly contained 20 individual probes, of which 17 were total pressure ports, numbered from the north endwall. The two central probes, (numbers 10 and 11), formed a yaw probe located at the midspan with a static pressure port,

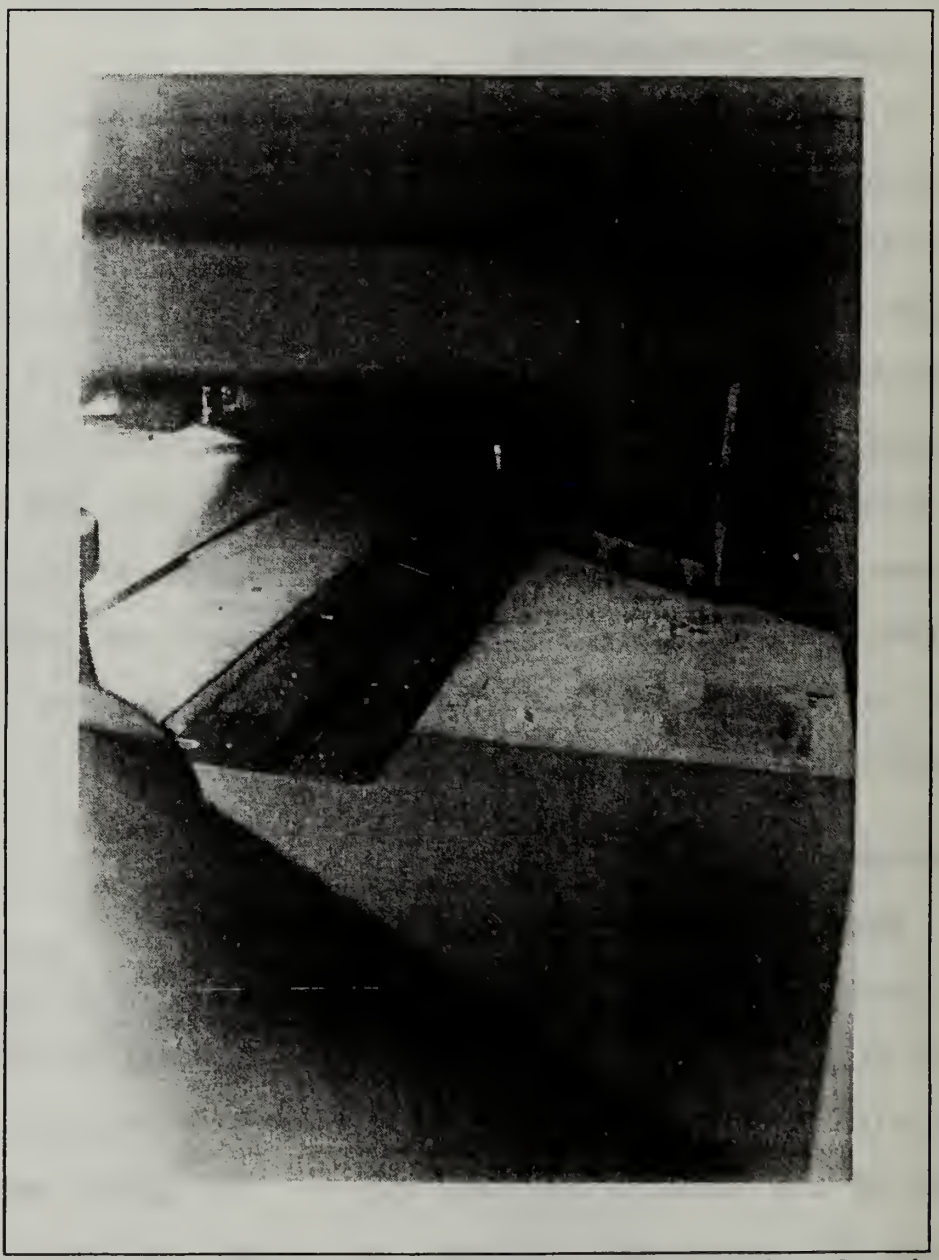

Figure 4. Suction Slot Mounted to the South Endwall

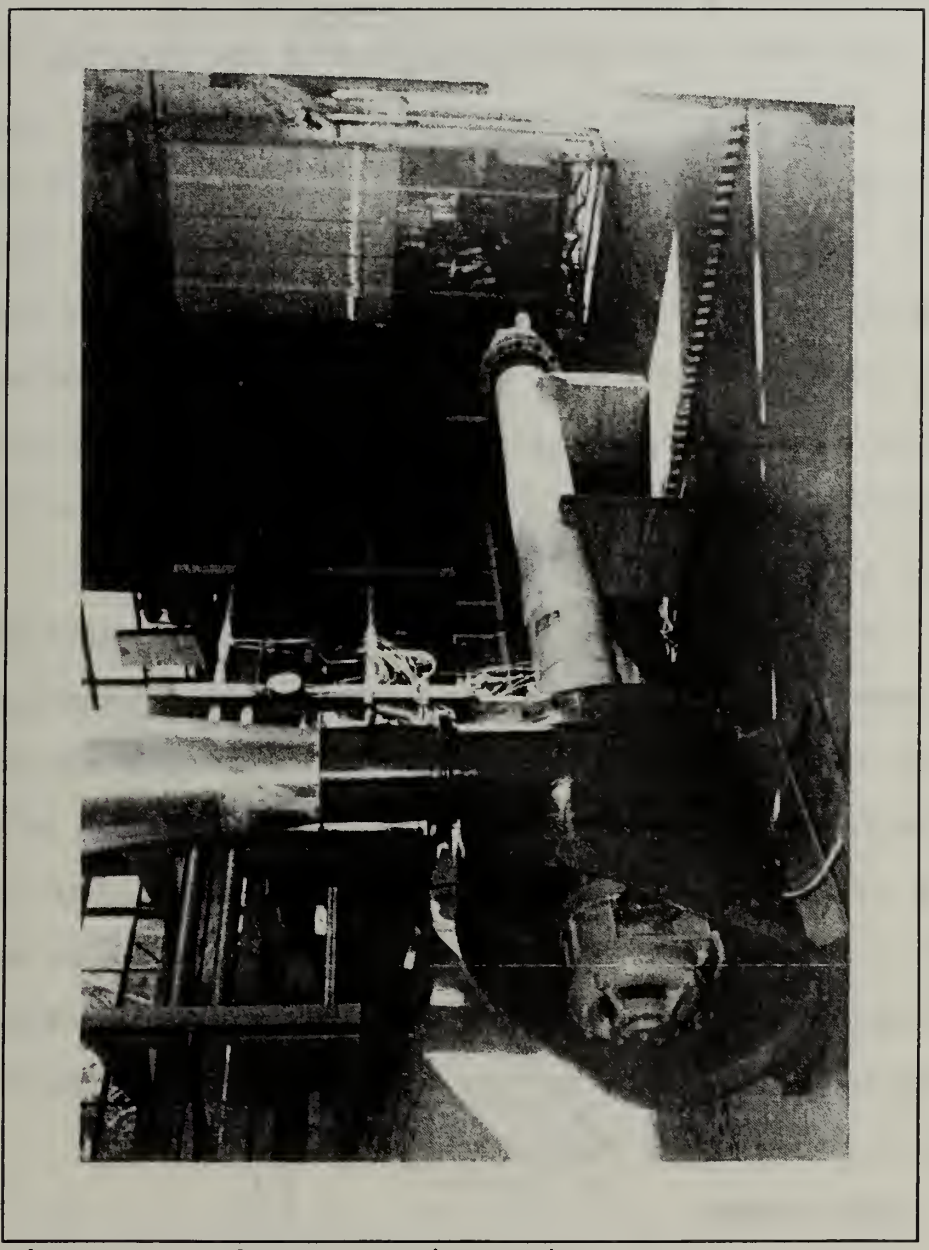

Figure 5. Blower Configuration

(numbered 9), one inch off midspan. A detailed drawing of the probe is found in Appendix D. Figure 6 shows a plan-view schematic of the probe.

The rake probe was calibrated in the free jet located at the Turbopropulsion Laboratory. This was done by subjecting the probe to three different levels of dynamic pressure and varying the angle of incidence to obtain a calibration curve for the yaw probe. It was noticed that the static pressure port was subject to probe interference. Therefore, a correction factor was calculated to account for this difference. The calibration data and curves are given in Appendix C.

The rake probe was traversed both upstream and downstream of the test section. This was accomplished by mounting it to a traverse assembly which in turn was mounted to the side of the south wall of the tunnel, as seen in Figure 1. The traverse was equipped with a geared counter used to measure the distance. Figure 7 shows the rake probe mounted to the upper traverse. It also shows the relative position of the suction manifold to the test section, upstream, downstream and manifold pressure taps.

2. LDV SYSTEM

The two component LDV system used for the base line tunnel configuration is described in detail by Murray [Ref.14].

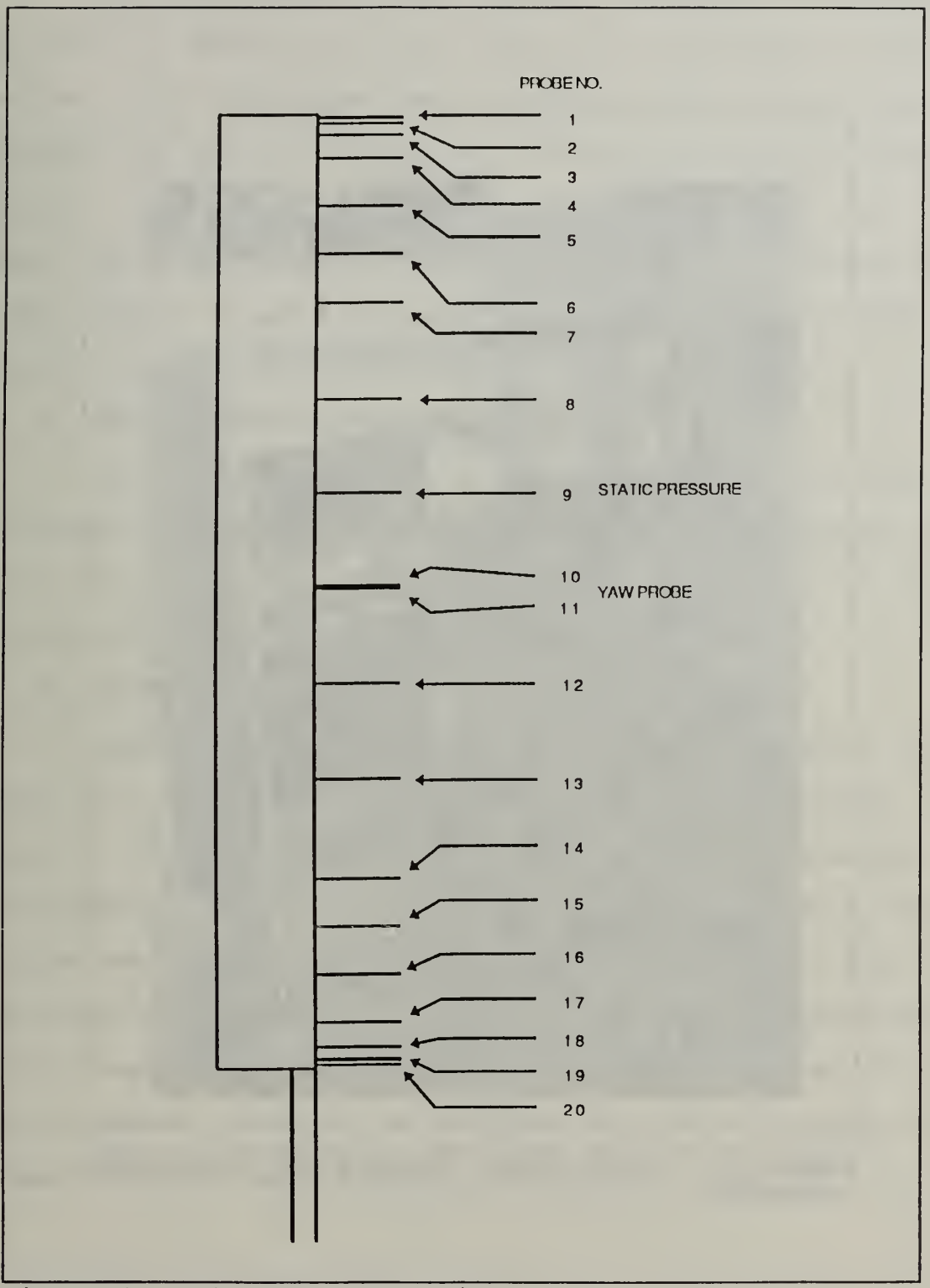

Figure 6. Rake Probe Plan View

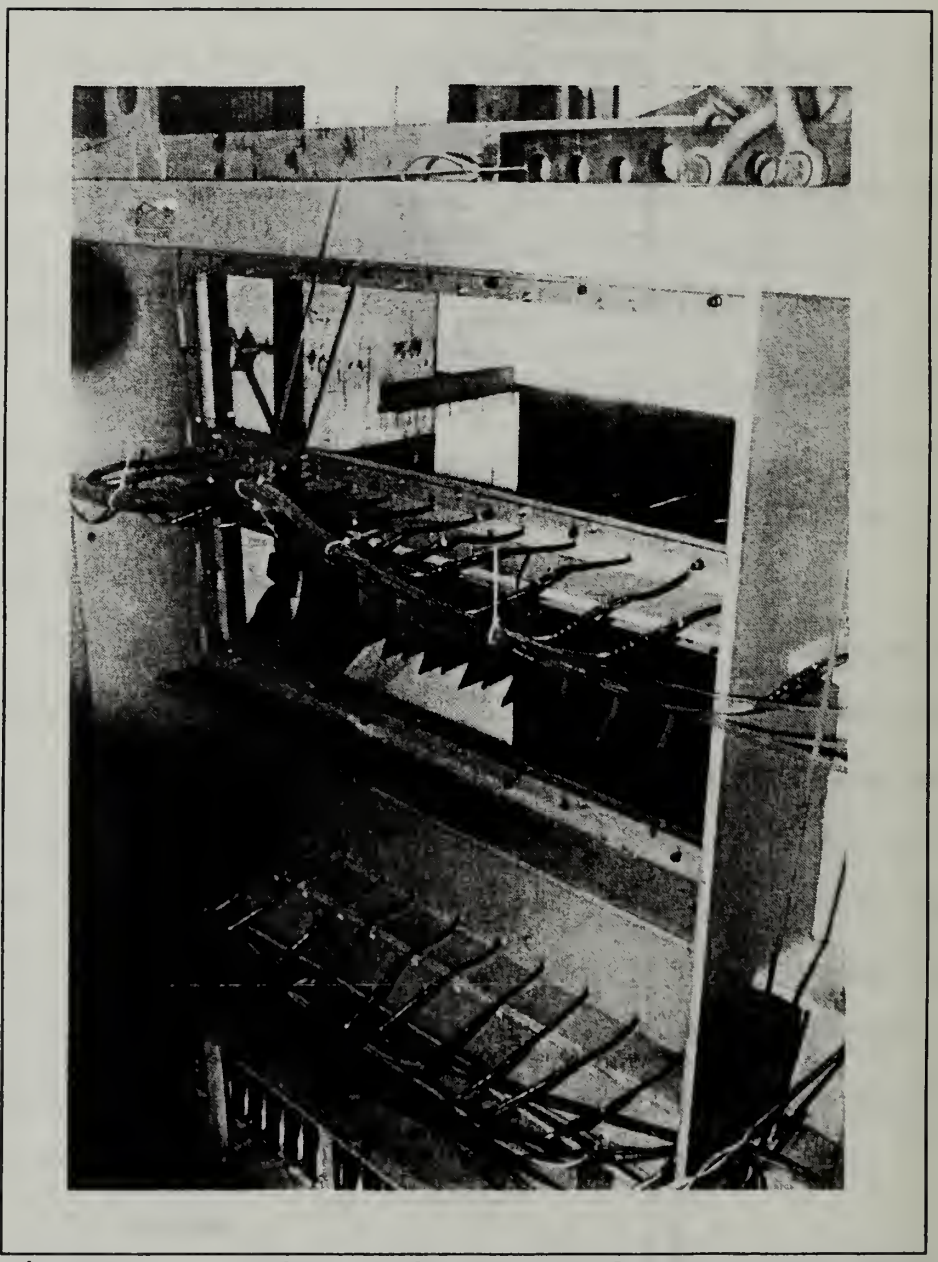

Figure 7. Rake Probe Mounted to Downstream Traverse

For the modified tunnel tests, a different LDV system was used to measure the flow under the influence of high suction. The new system used a similar laser light source, however, the rest of the optical system was primarily fiber optics. A complete description of the system is given by Dober. [Ref. 15] Figure 8 shows the test passage bounded by blade numbers 7 and 8 as seen through the optical window. Coordinates for each survey station are also given.

3. INSTRUMENTED CD BLADE

Blade pressure measurements were taken with a fully instrumented blade, located at mid-pitch, that contained 39 static pressure taps, 19 on each surface and one at the leading edge. Figure 9 shows the tap locations.

4. STATIC PRESSURES

Endwall static pressure measurements for both the north and south walls, upstream and downstream as shown in Figure 1, were measured with two banks of water manometers. The manometers were also used to monitor the pressures at the suction manifolds, gate valves, as shown in Figures 2 and 3, and plenum and Prandtl total pressures. (A Prandtl probe was used to monitor inlet dynamic pressure near to blade 15). Each manometer consisted of 50 tubes and the arrangement of pressure taps for each is given in Figures 10 and 11.

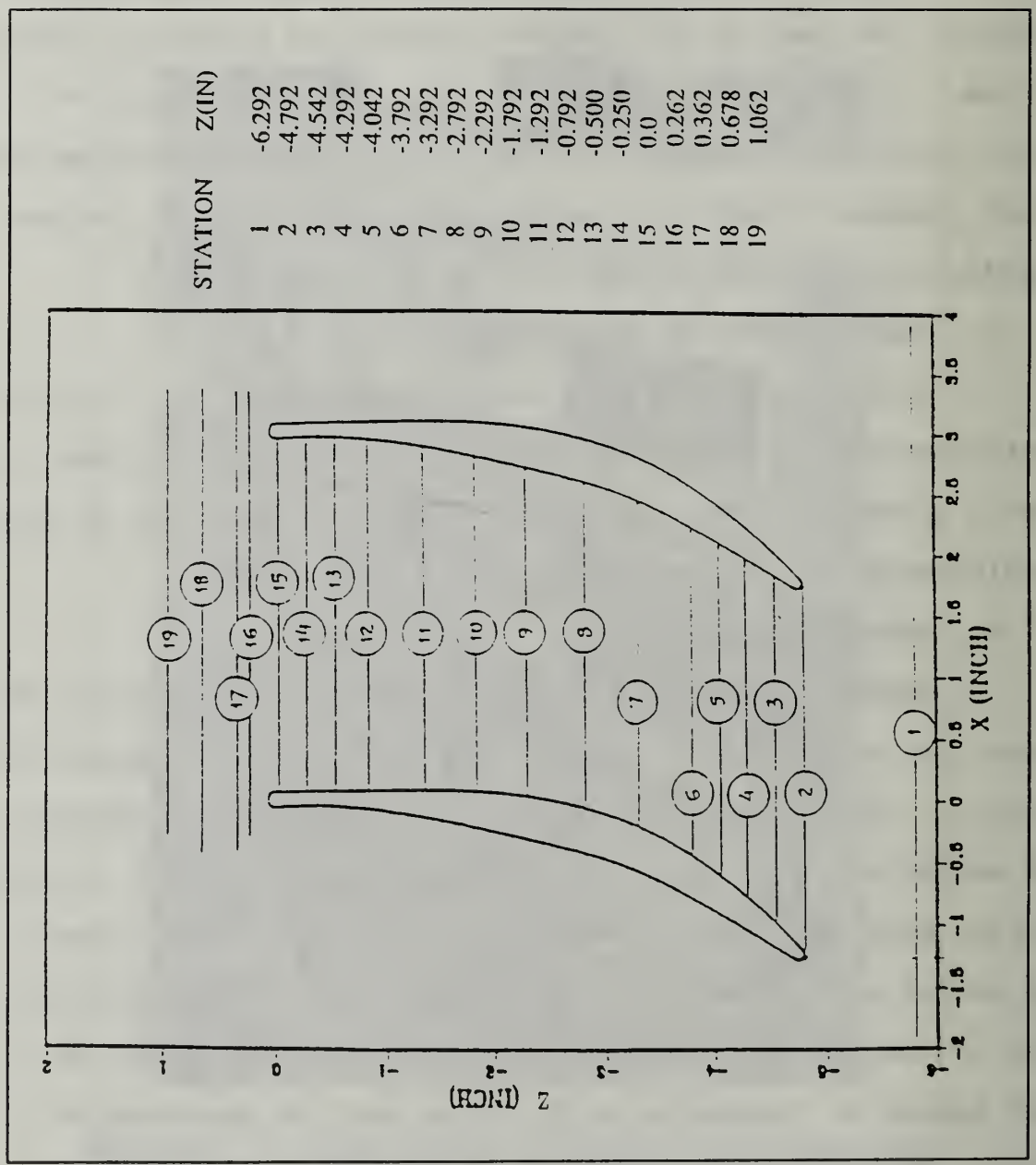

Figure 8. LDV Test Section Geometry

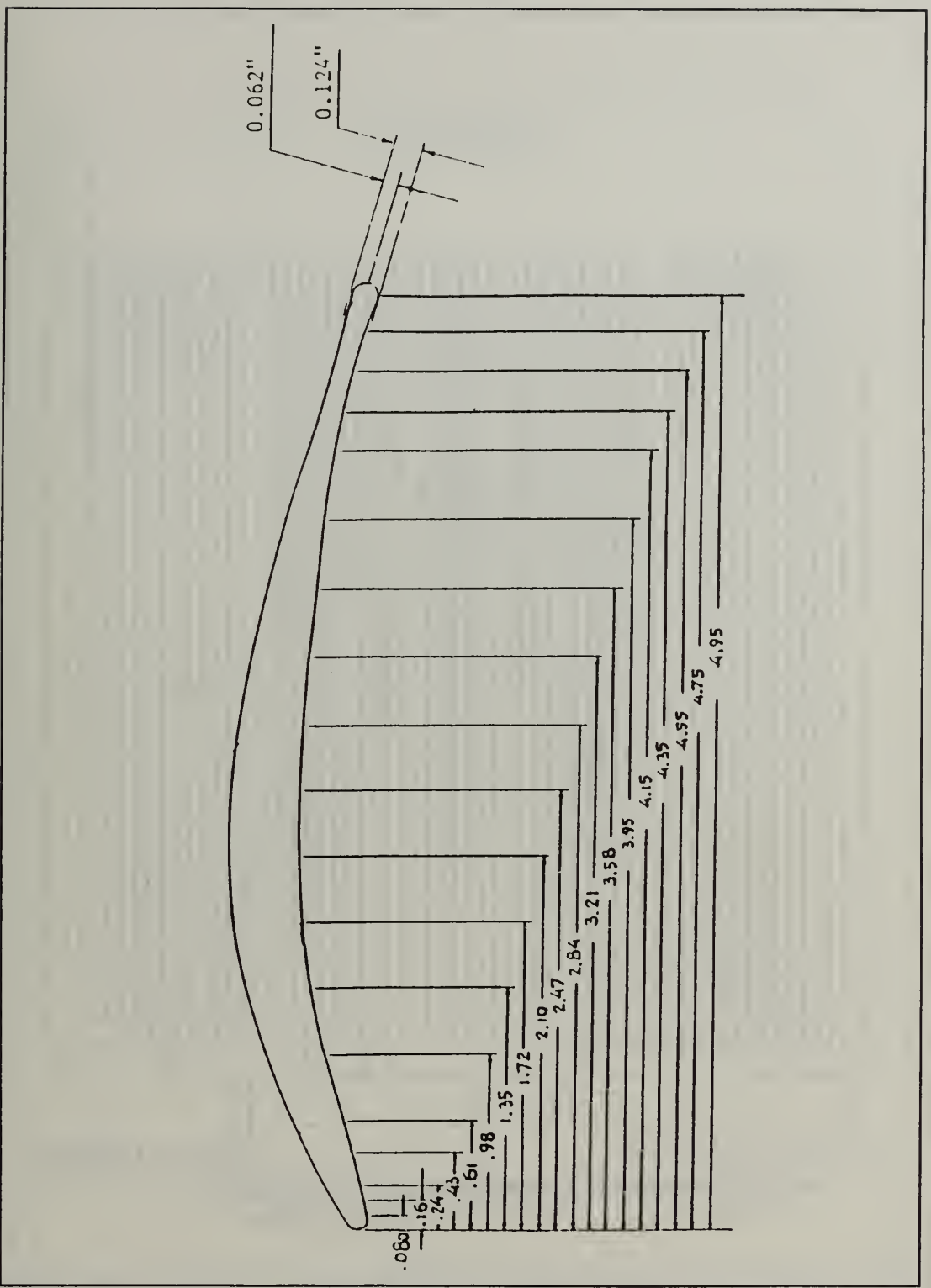

Figure 9. Instrumented Blade Pressure Tap Location

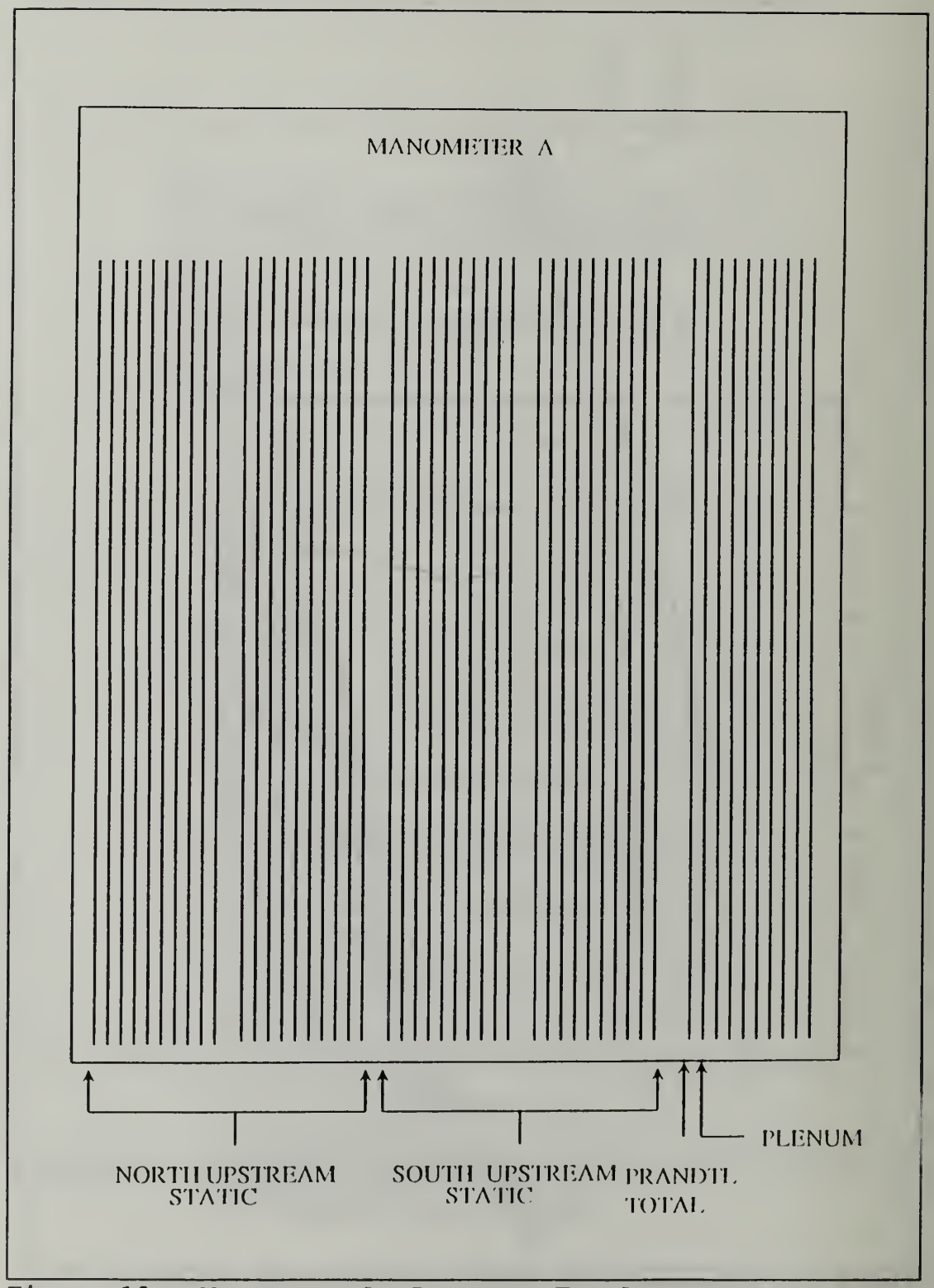

Figure 10. Manometer A. Pressure Tap Arrangement

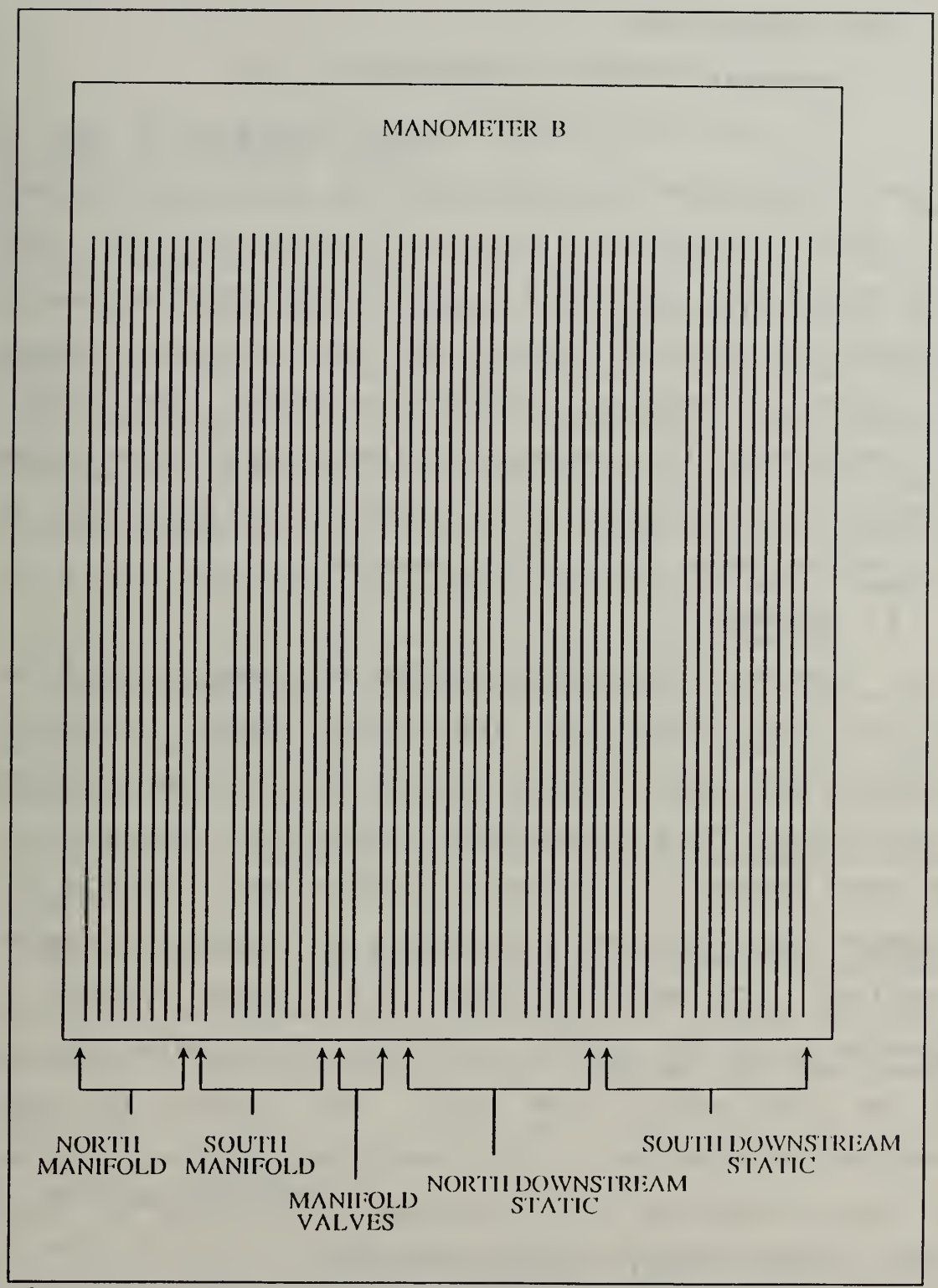

Figure 11. Manometer B. Pressure Tap Arrangement

D. DATA ACQUISITION

1. HARDWARE

The data acquisition system consisted of two 48 channel scanivalves that were connected through an interface to a Hewlett Packard Data Acquisition System (HP-3052). The scanivalves were controlled by the HG-78k controller and is discussed in detail by Classick [Ref. 10]. A Hewlett Packard 900 series 300 computer controlled the system. Scanivalve 0 was connected to the instrumented blade along with the plenum pressure. Scanivalve 1 was connected to the rake probe as well as the plenum and Prandtl pressures.

2. SOFTWARE

Two data acquisition programs were used to record the various tunnel pressures. The program ACQUIRE written by Classick [Ref. 10] was used to take the instrumented blade measurements. The program ACQUIRE4 was a fourth adaptation to the same program and its basic function was to obtain the spanwise rake pressure distribution at various pitchwise locations. In post-processing, the program produced a spanwise C_p plot and finally plotted a C_p surface distribution of the test section flow field. The program is fully described in Reference 15. The fourth modification consisted of adding equations to the program to calculate air flow angle, total velocity and axial velocity.

III. EXPERIMENTAL PROCEDURE

A. BASE LINE CONFIGURATION

The procedure used to adjust the inlet flow angle of the cascade using the LDV system is well documented by Murray [Ref. 14]. Using this procedure, the inlet flow angle was measured to be 44.4° with the sidewalls set at 43.4° and inlet guide vane position at 50mm. LDV measurements were taken at stations 1, 2, 7, 15 and 18 to compare with earlier data [Ref. 9] and to produce a basis for later comparison with results with endwall suction. The plenum pressure was maintained at 12.0 inches of water with a deviation of ±0.1 inches.

Inlet surveys were taken by mounting the rake probe to the upstream traverse position, as shown in Figure 1, and traversing the entire pitch-wise distance referenced from the east sidewall. Appendix A. contains the data taken at each location.

The AVR was obtained by surveying across one blade passage starting at 20 inches and terminating at 23 inches in ¼ in. increments. This was done at both upstream and downstream locations.

B. SUCTION PROCEDURE

Three levels of suction were used to compare with the base line configuration. The levels were measured by the static

pressure taps located at the gate valves at each end of the suction manifolds. The blower was always operated at full speed with its downstream throttle valve in the full open position. When the blower was turned on, the plenum pressure dropped as much as one inch of water in the case of high suction. Therefore, the Prandtl total pressure was used as P_{ref} for all suction tests. This was kept at 10.5 inches of water, the same as the base line tests.

The procedure to set up suction was as follows: (a) start the tunnel and stabilize at 10.5 inches of total pressure on the Prandtl probe. (b) Fully open the gate valves and switch on the blower. (c) Close the valves to obtain equal and stable static pressure at the valves. (d) Adjust the plenum back to 10.5 inches on the Prandtl probe. All four valve static pressures measured -32.0 inches of water for high suction, -20.0 inches for medium suction and -10.0 inches for low suction. The maximum deviation allowed was .5 inches of water for any of the valves. Polaroid photographs were taken of the manometers for documentation purposes at each suction level. Example photographs are given in Appendix A.

The same measurements were taken for suction as for the base line. The instrumented blade measurements were taken only with suction. The LDV measurements were taken only at the inlet and outlet planes and referenced with respect to the Prandtl total pressure, ambient pressure and plenum pressure to calculate V_{REF} as described by Elazar [Ref. 9].

IV. RESULTS AND DISCUSSION

All data and equations for the graphs given in this chapter are found in Appendices A and B respectively.

A. INLET SURVEYS

Inlet carpet plots are seen in Figures 12 through 15. These show that the inlet core flow uniformity is the same for the base line and at all levels of suction. Figure 12 is the full survey for the base line configuration. Figure 13 is for low suction, and shows the endwall boundary layers are being removed at the east and west ends of the test section with the minimum reduction at the mid-pitch location. Figures 14 and 15 are for medium and high suction respectively and show the same trend, giving the first indication of non-uniform suction in the pitchwise direction.

Plots for the spanwise pressure distribution are shown in Figures 16 through 20 for different pitch locations. These locations were chosen as a result of the carpet plots and the locations chosen for displacement thickness and AVR calculations. Figure 16, at 11.8 in. pitch, shows the increased boundary layer removal for increased suction at both end walls. However, the north wall boundary layer was not reduced to the same degree as the south wall. The base line showed the north wall boundary layer was thicker than that on

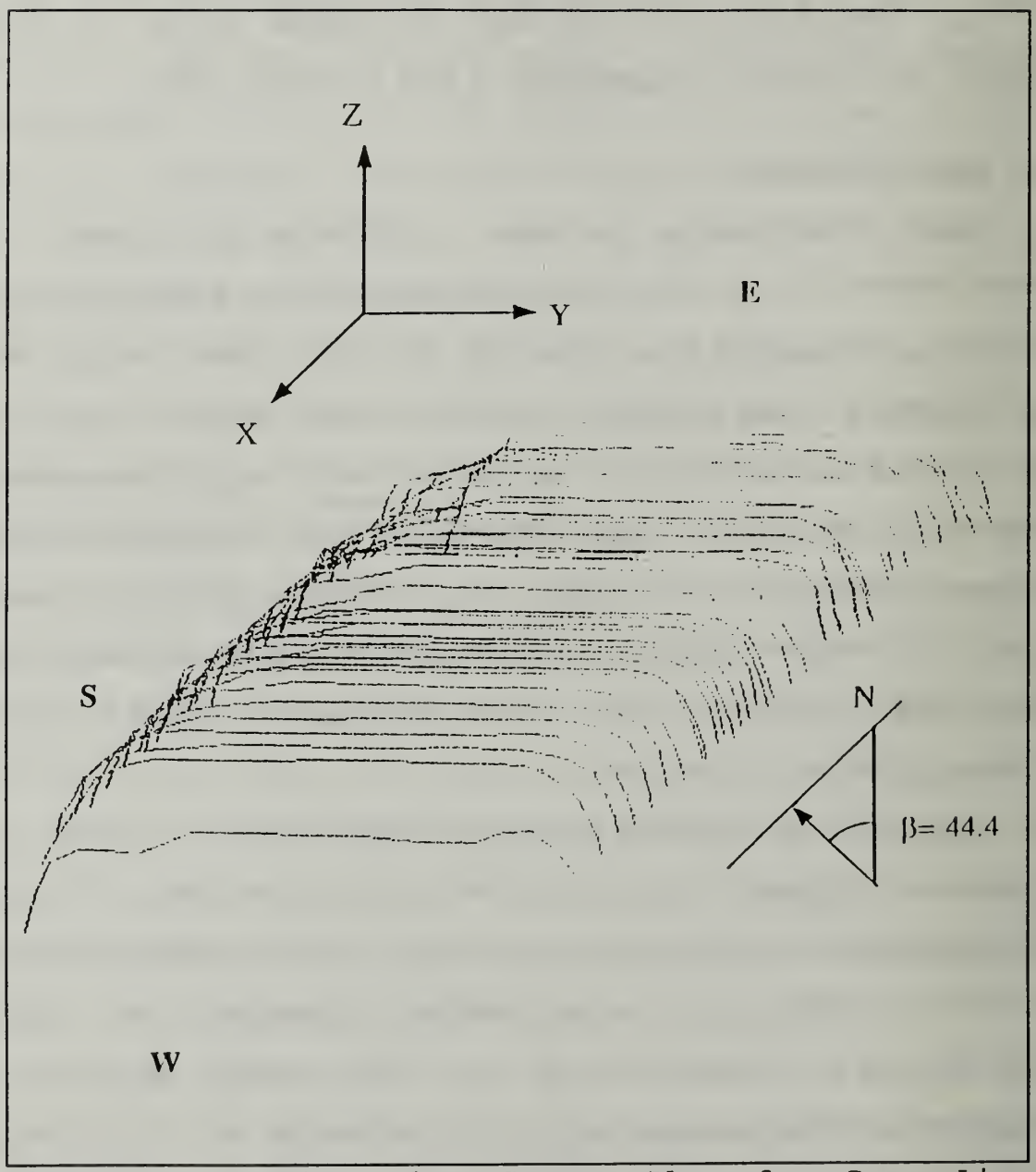

Figure 12. Inlet Flow Carpet Plot for Base Line Configuration

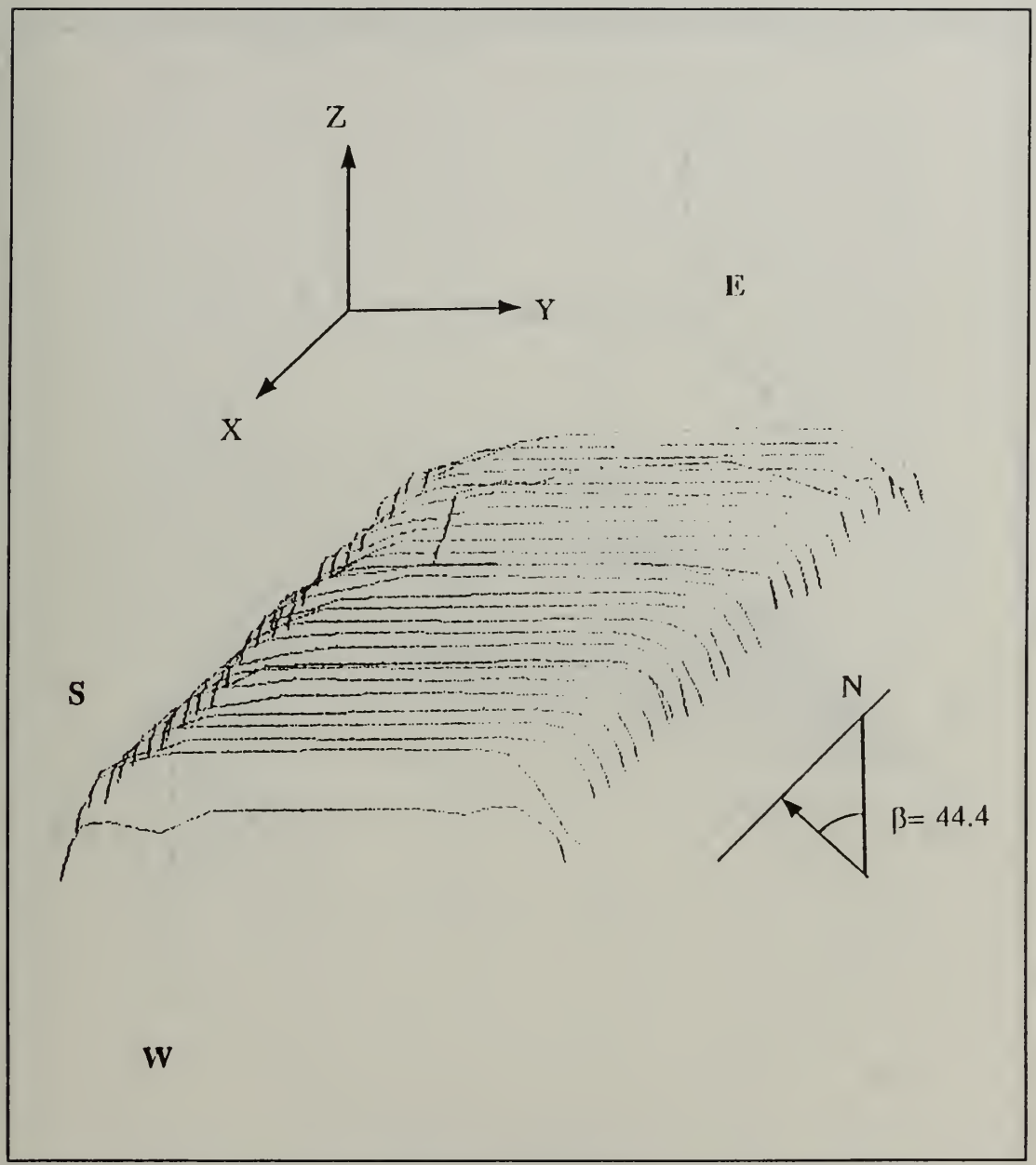

Figure 13. Inlet Flow Carpet Plot for Low Suction

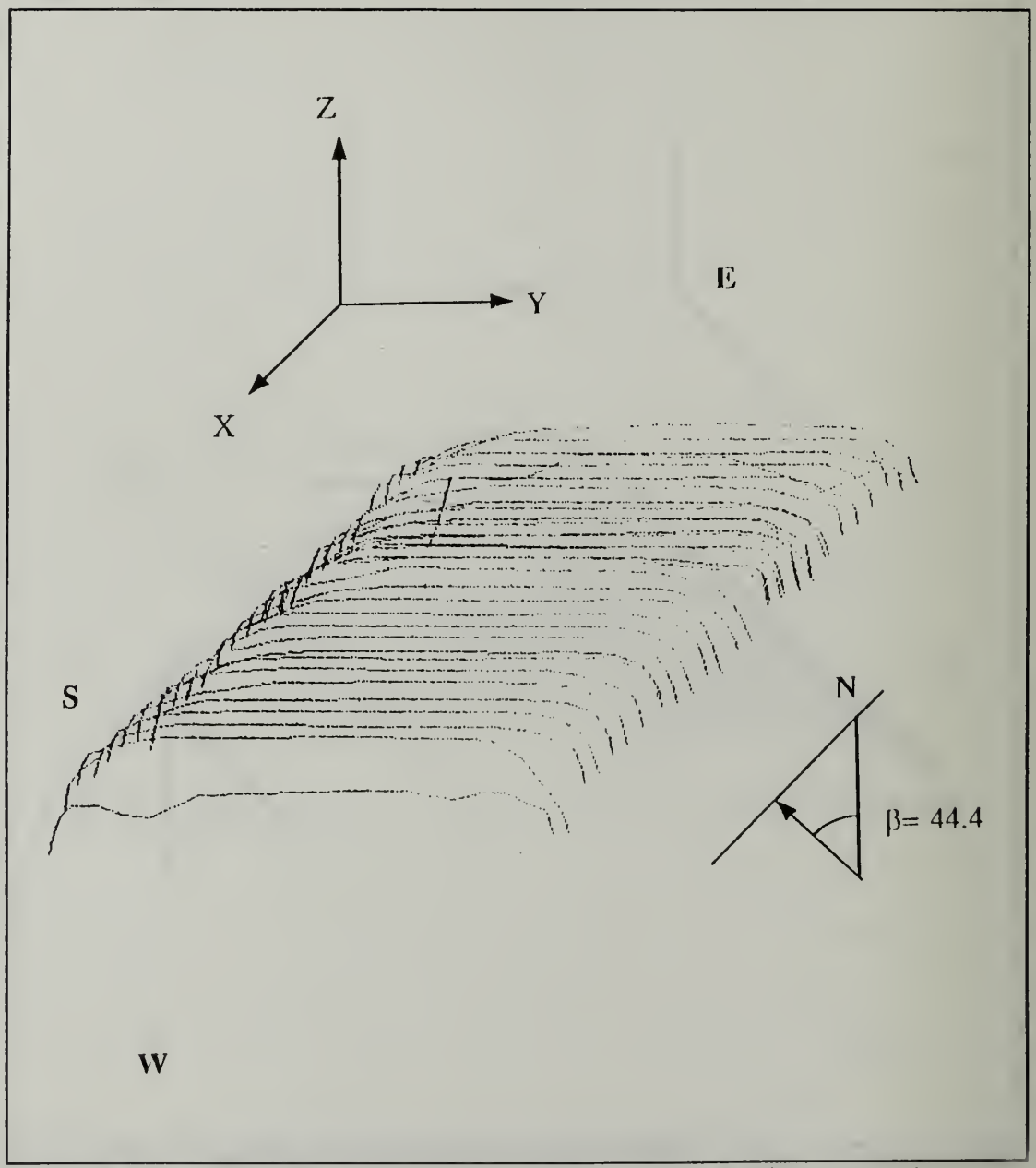

Figure 14. Inlet Flow Carpet Plot for Medium Suction

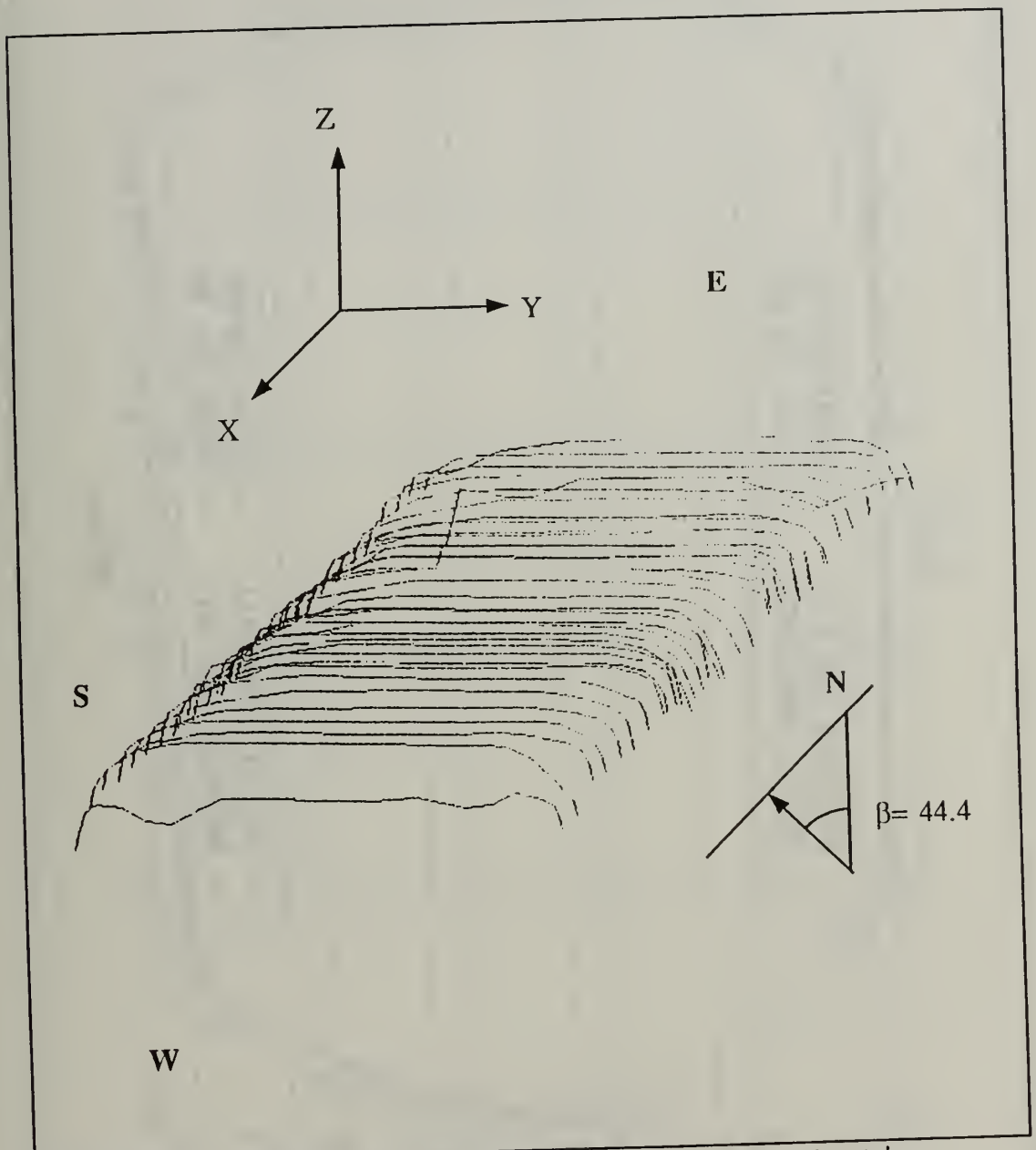

Figure 15. Inlet Flow Carpet Plot for High Suction

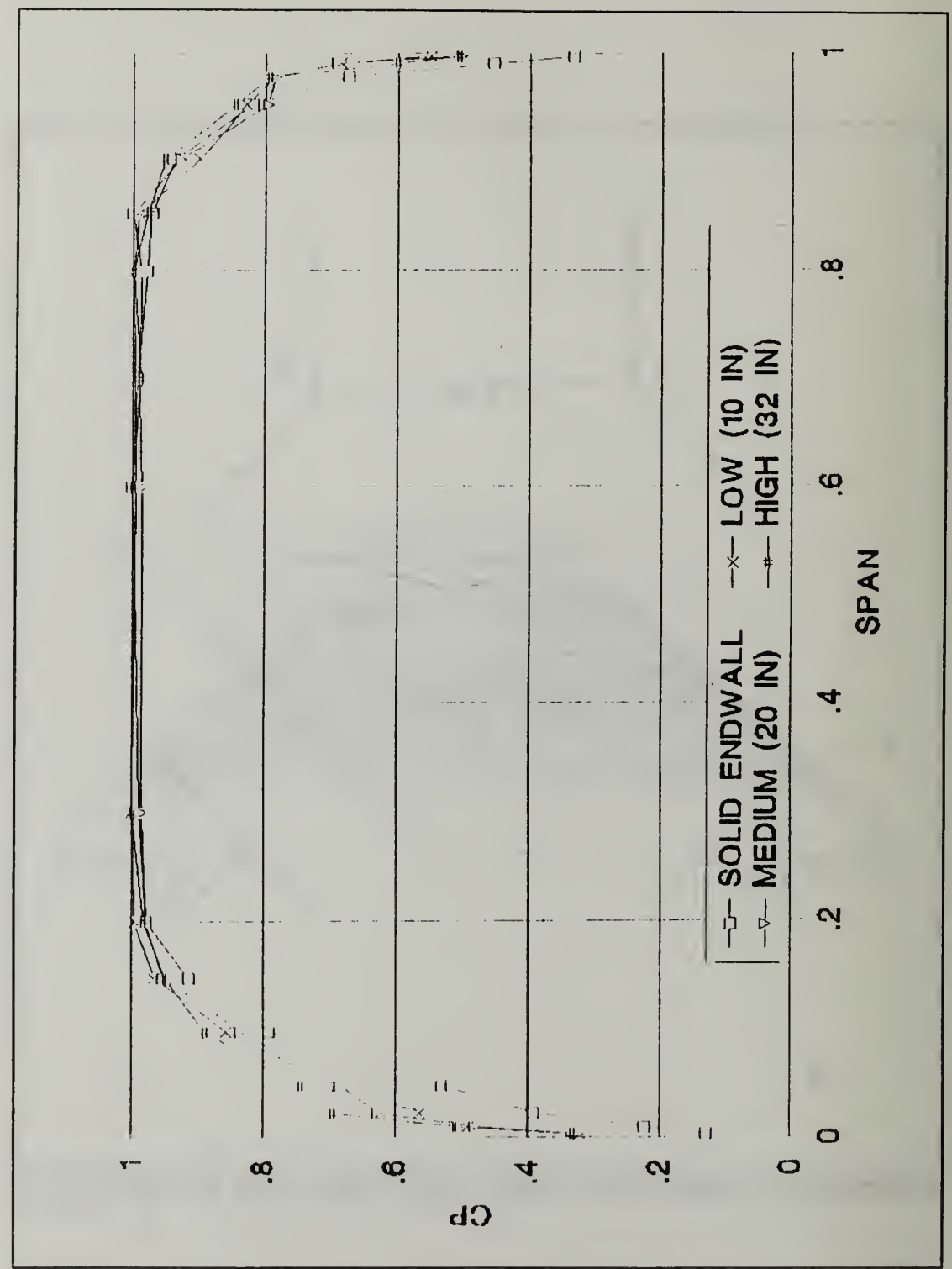

Figure 16. Superimposed Spanwise Pressure Distribution at 11.8 in. Pitch for Increased Suction

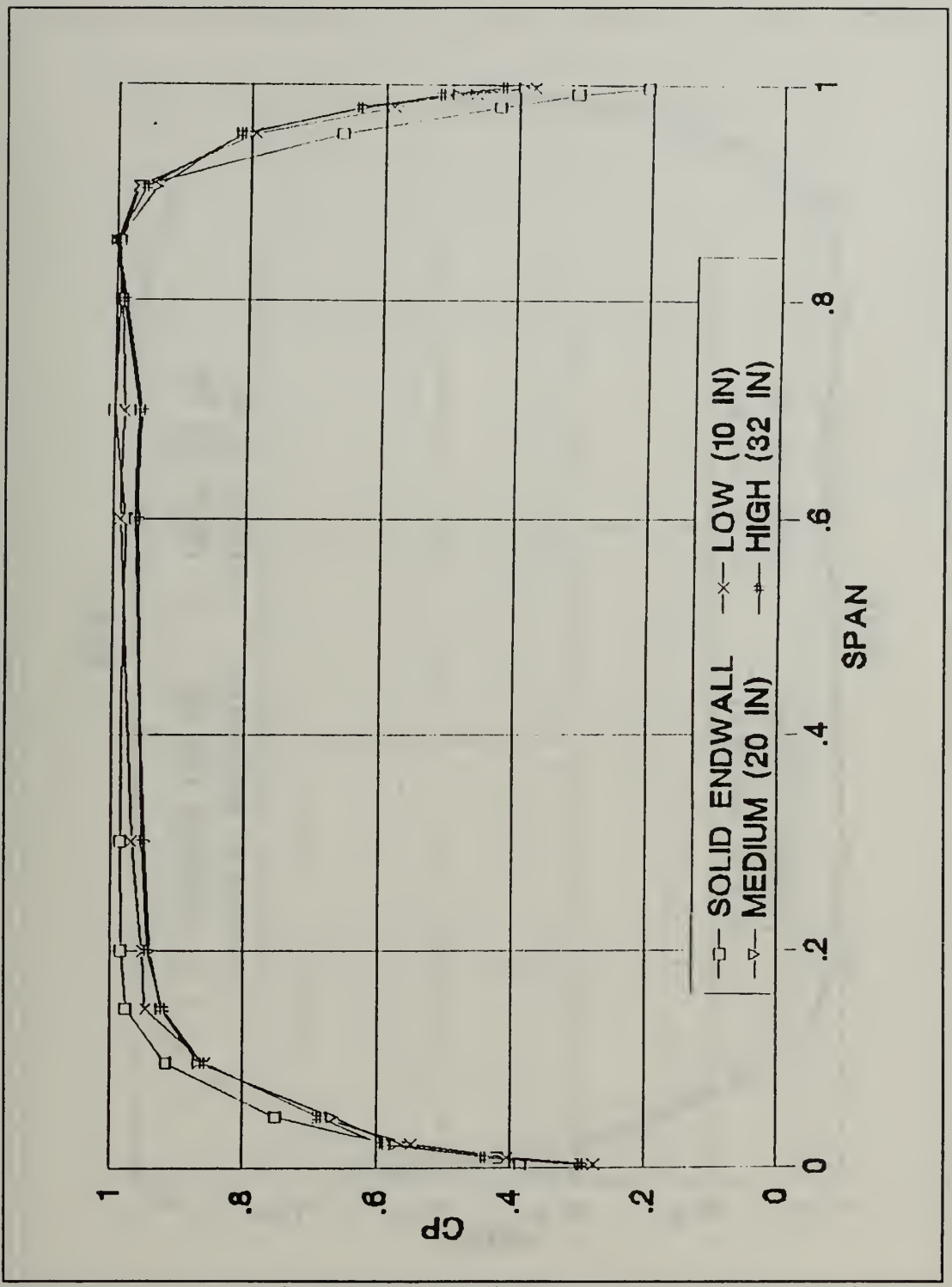

Figure 17. Superimposed Spanwise Pressure Distribution at 20 in. Pitch for Increased Suction

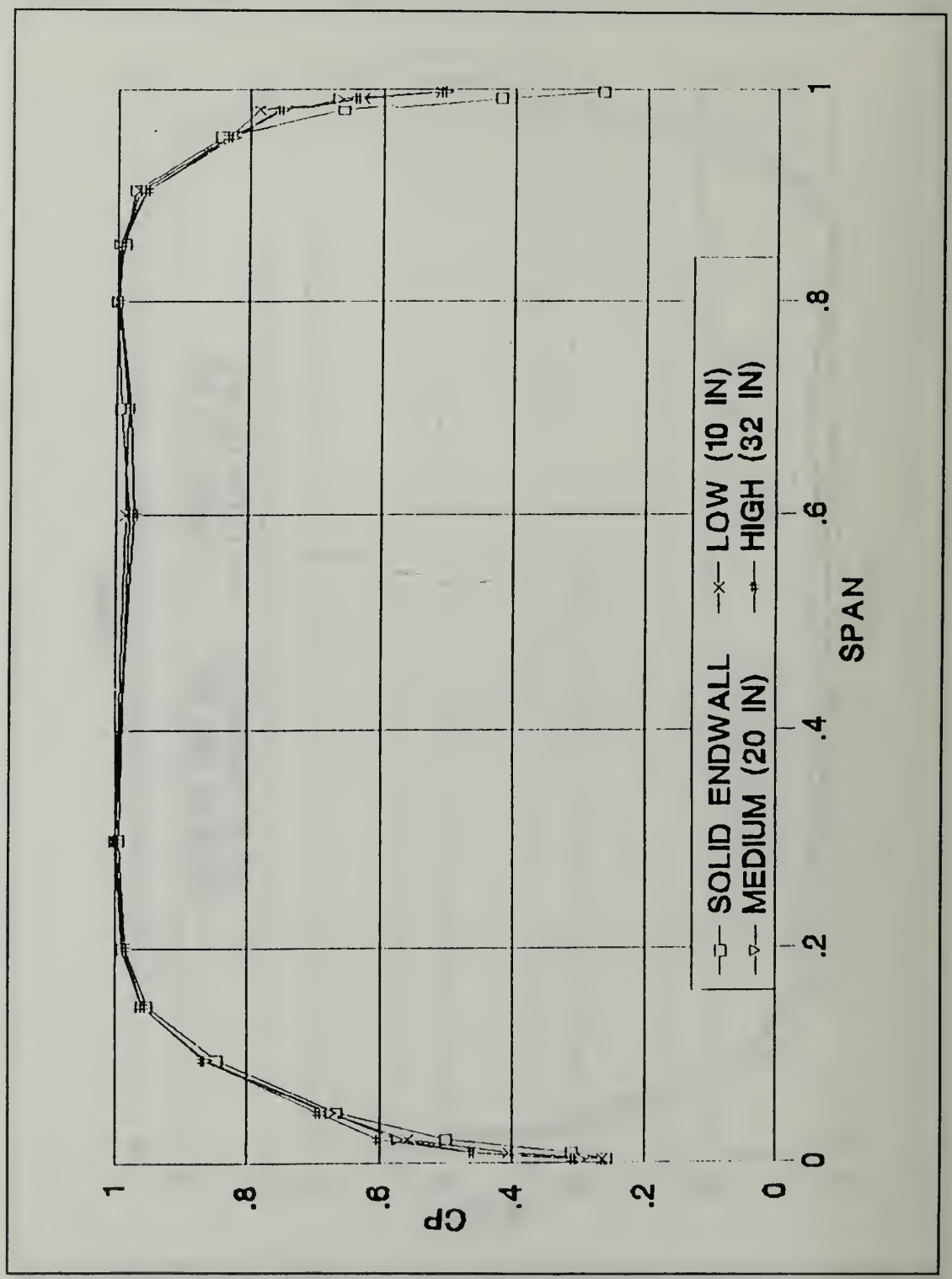

Figure 18. Superimposed Spanwise Pressure Distribution at 22 in. Pitch for Increased Suction

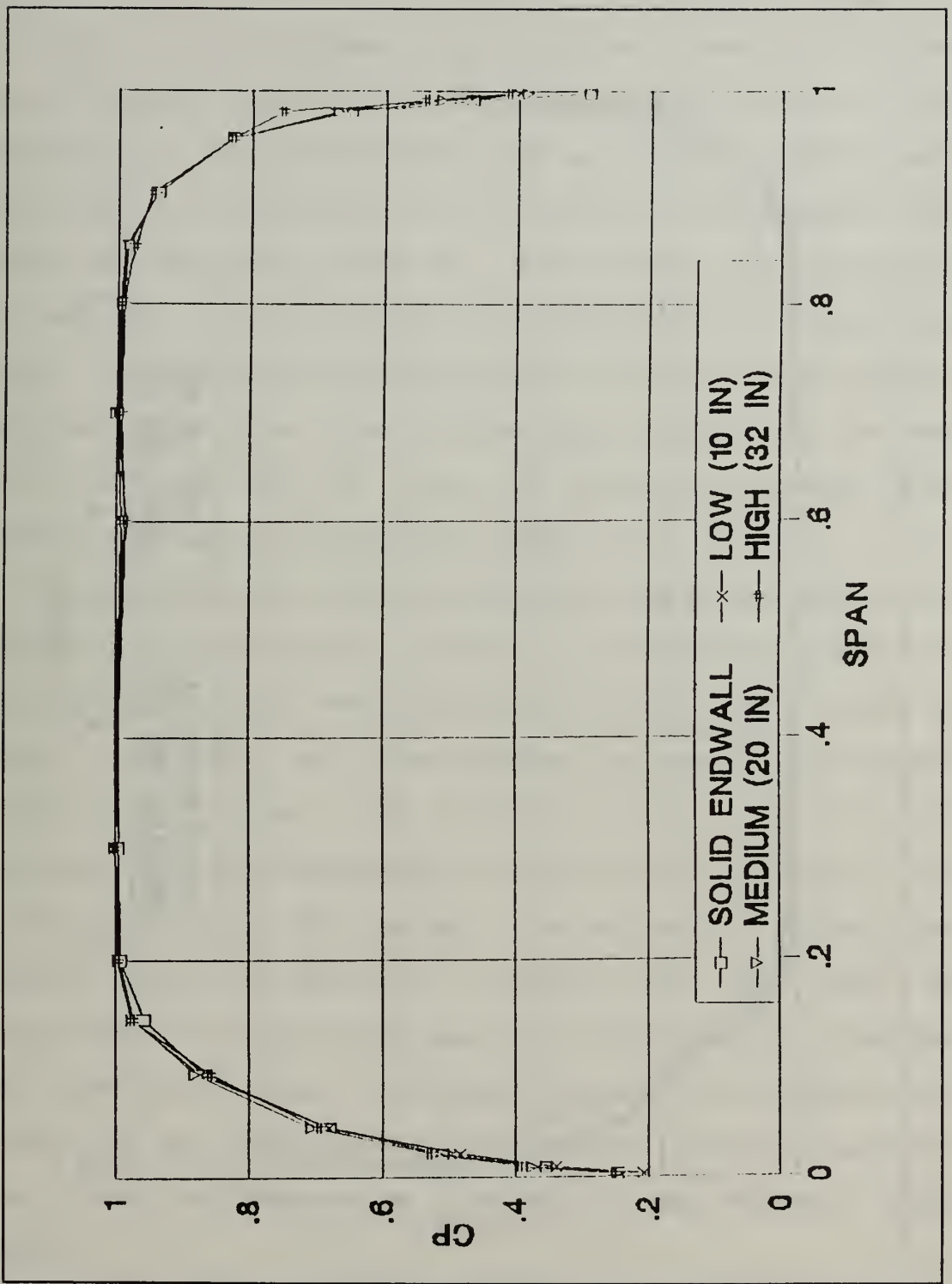

Figure 19. Superimposed Spanwise Pressure Distribution at 35.88 in. Pitch for Increased Suction

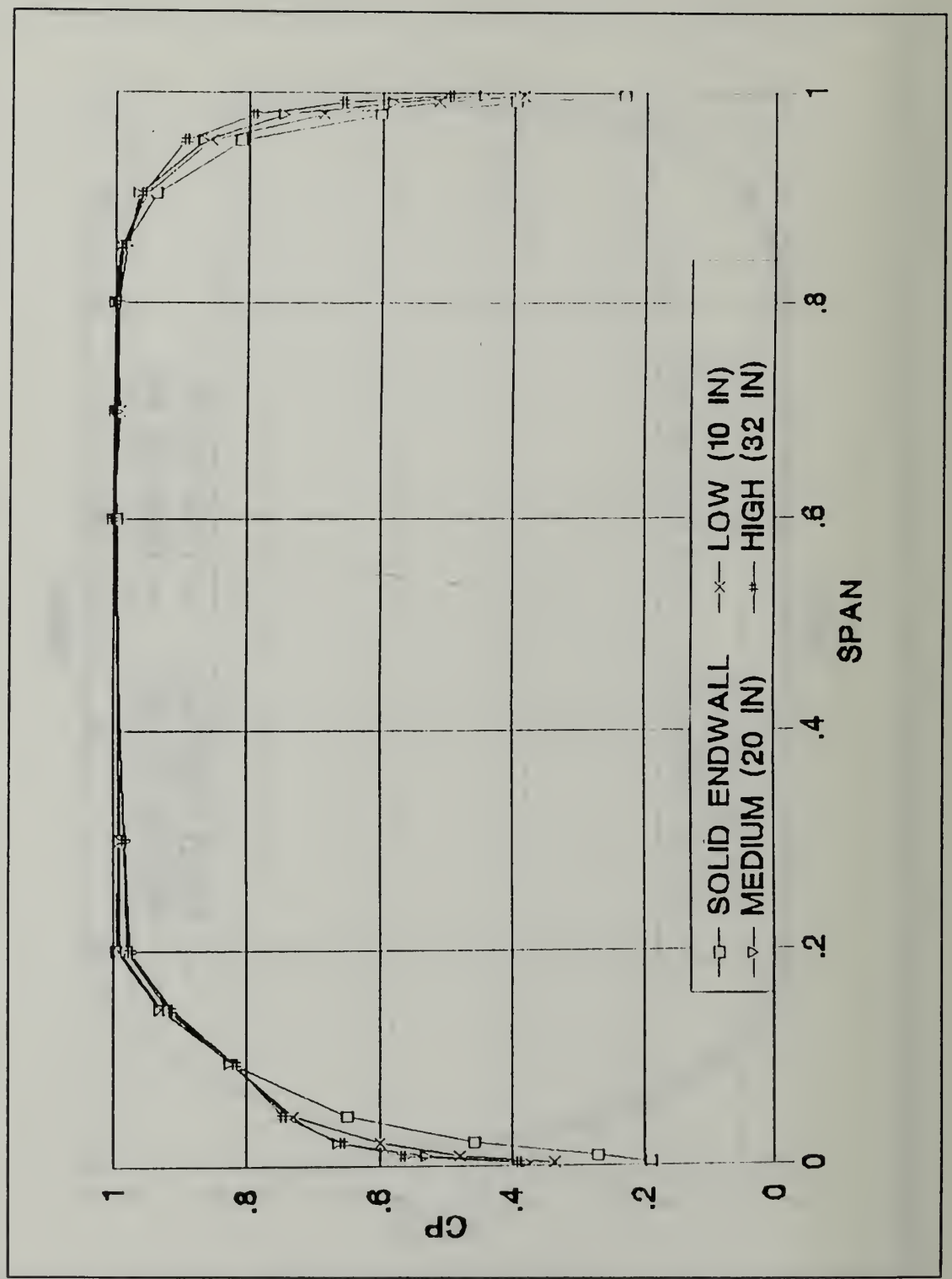

Figure 20. Superimposed Spanwise Pressure Distribution at 50.9 in. Pitch for Increased Suction

the south wall. This characteristic is seen in all the plots. In Figure 17, at 20 inches, the core flow is seen to have been shifted towards the south wall and the boundary layer to have thickened at the north wall from an initial displacement thickness of 0.133 inches to 0.146 inches. This happened only at the 20 inch pitch location. Furthermore, the removal of the boundary layer is seen to decrease moving towards mid-pitch. Figures 18 and 19 show reduced effects to the boundary layer which was also shown in the carpet plots. At the west end of the test section, Figure 20 shows the boundary layer removal again has a noticeable effect.

The displacement thickness was calculated for each level of suction and is shown in Figure 21. The value plotted is the average obtained over three inches from 20 to 23 inches in pitch. The north wall displacement thickness was reduced 0.0255 inches, (13%), from 0.1964 inches to 0.1709 inches. The south wall was decreased by .0591 inches, (39.5%), from 0.1497 inches to 0.0906 inches. The asymmetry of the inlet boundary layer displacement thickness is also seen as characteristic of the tunnel base line configuration. For the base line, there was a difference between the endwalls of 0.0467 in. and this increased to 0.0803 at high suction. Thus, there was a spanwise asymmetry of the boundary layer removal.

After viewing these data, it was evident that equalizing the gate valve pressures might not have been the best method

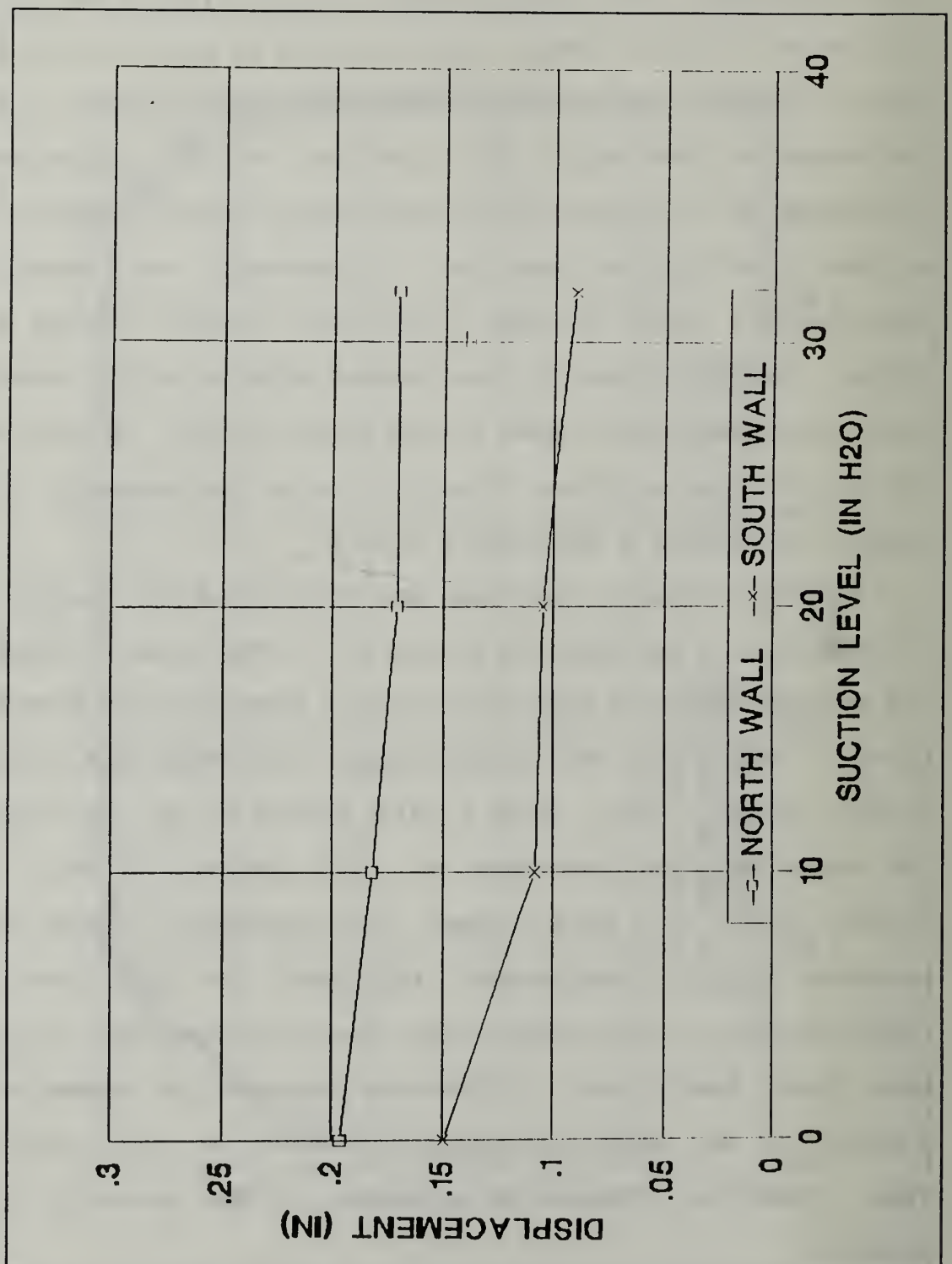

Figure 21. Average Displacement Thickness for the North and South Endwalls, 20 to 23 in. Pitch

of adjusting the suction. An additional test was conducted, but this time the manifold pressures were balanced with each other. This was accomplished by opening the north manifold valves fully and closing the south manifold valves to the medium suction level. This yielded a north endwall displacement thickness of 0.1767 inches and a south endwall displacement thickness of 0.1038 inches. The difference between these is 0.0729 inches, a 0.0074 inch reduction in the endwall boundary layer thickness difference.

Further illustration of the non-uniformity in the suction is seen in Figures 22 through 24. These show the suction manifold static pressures at their pitch locations for each level of suction. Figure 22 shows the manifold pressures were well below the endwall static pressures at the east end of the test section. This is the region where suction showed the most benefit, as seen in Figure 16. It also shows that the pressure differential between manifolds was at a minimum. In the mid-pitch region, the manifold pressure was above the endwall static pressures. This was the region where suction showed the least effect, as seen in Figure 19. The pressure differential between the manifolds is seen also to have increased. In the west end of the test section, the manifold pressures drop below the endwall static pressures but not to the same degree as the east end. This region showed effects of boundary layer removal as seen in Figure 20. The pressure differential between the manifolds also reached a maximum in

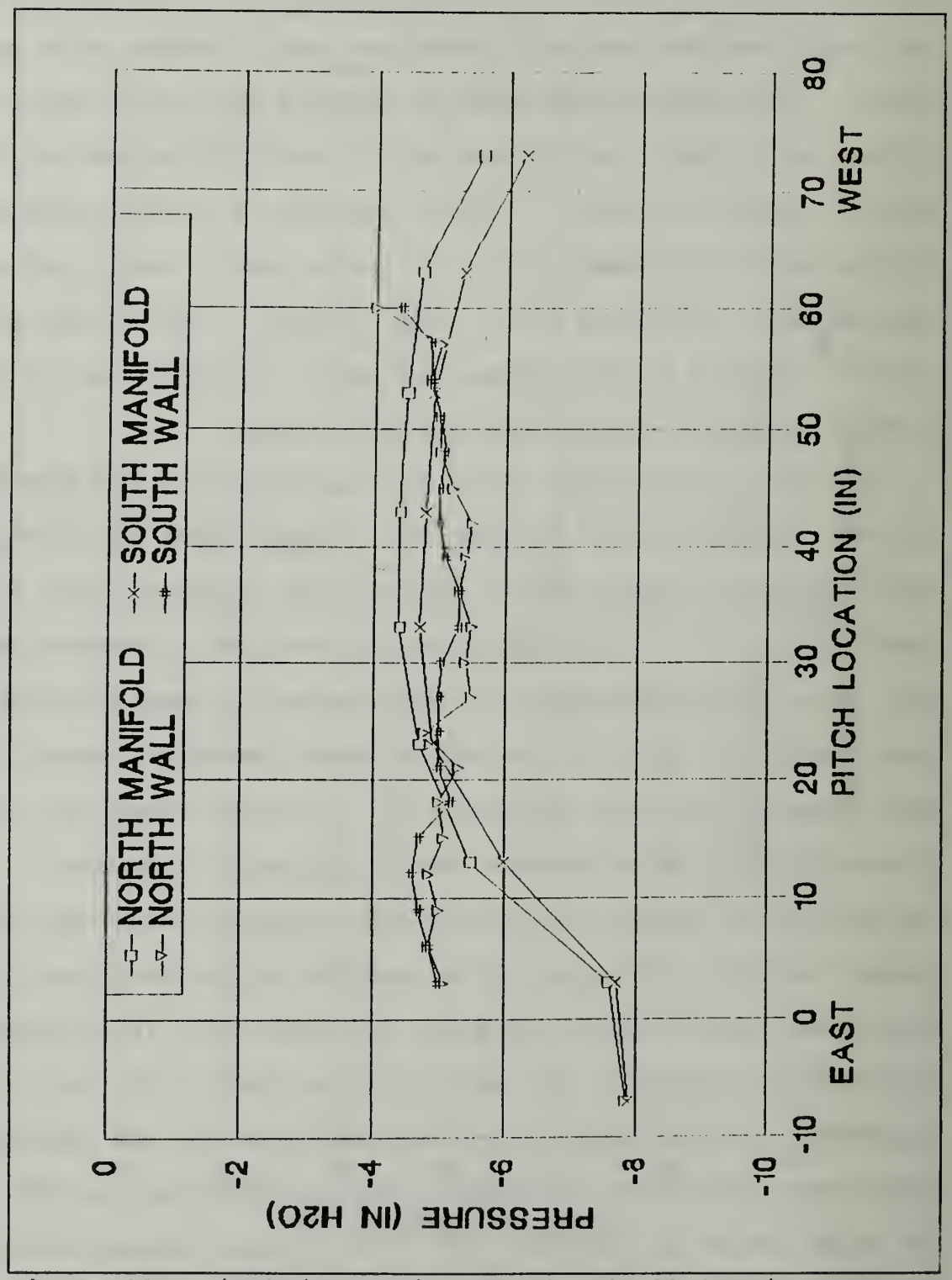

Figure 22. Pitchwise Manifold and Endwall Static Pressure Variations for Low Suction

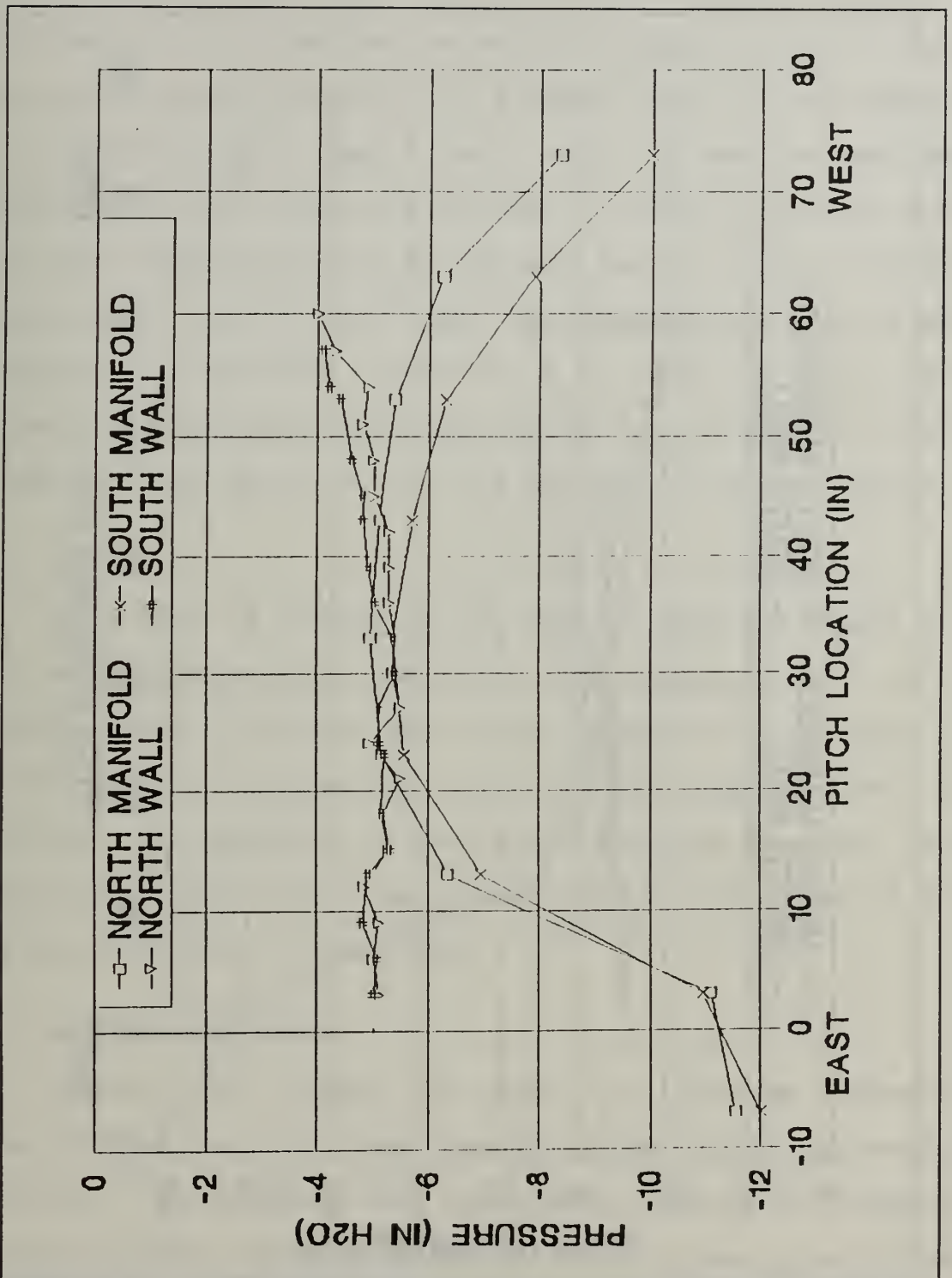

Figure 23. Pitchwise Manifold and Endwall Static Pressure Variation for Medium Suction

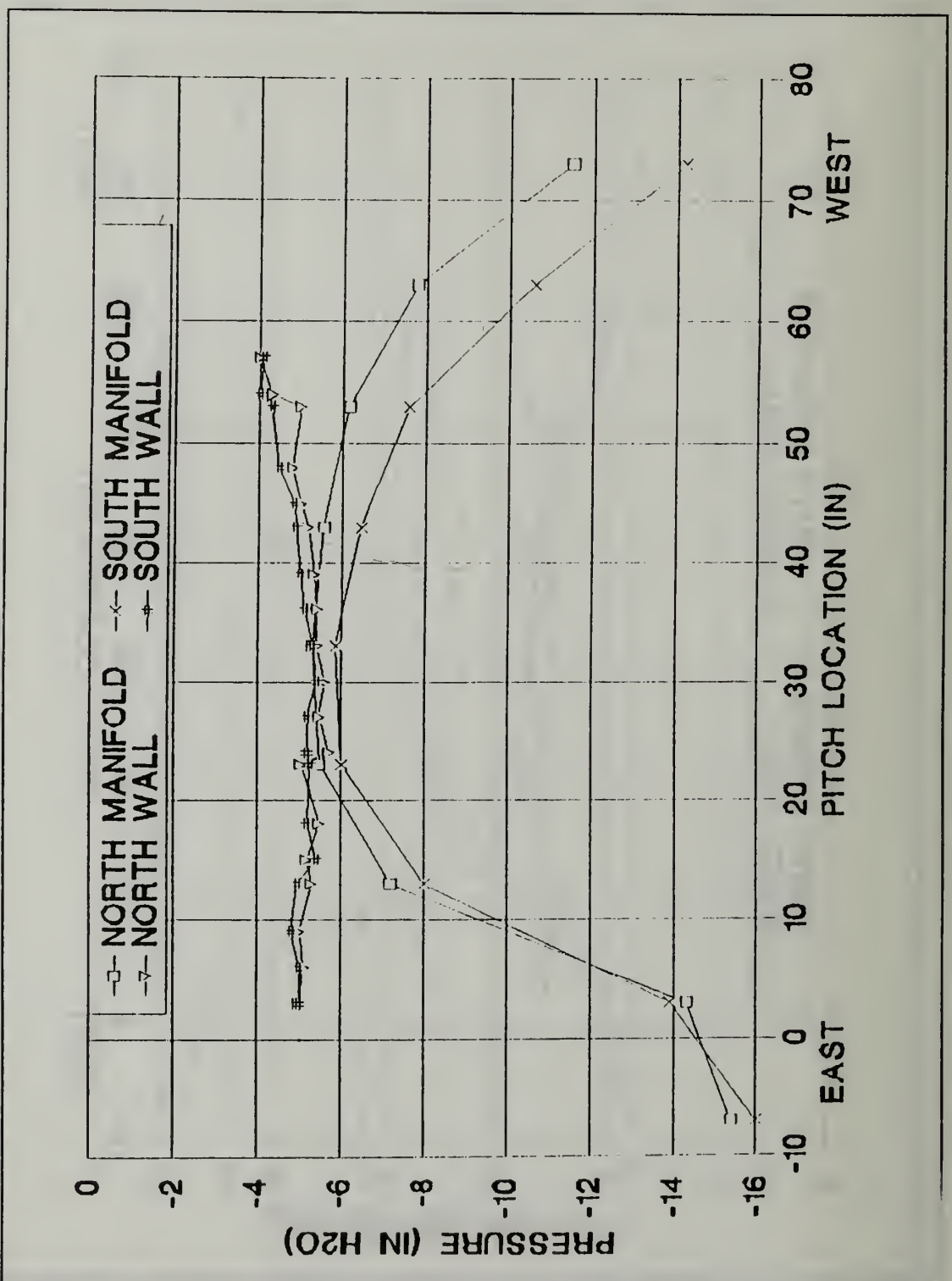

Figure 24. Pitchwise Manifold and Endwall Static Pressure Variation for High Suction

this region. The effect of increased suction, shown in Figures 23 and 24, shifted the manifold pressures down, until at high suction the mid-pitch minimum equalled the endwall static pressures. The endwall static pressures remained unchanged for all levels of suction. It is still unclear as to the relationship between the end wall and the manifold static pressures. It is noted that the boundary layer did not thicken at mid-pitch locations as it would if there were blowing in the region where the end wall static pressures were lower than the manifold, for low and medium suction levels.

B. AVR

The effect of suction on the AVR is shown in Figure 25. The were obtained over the three inch passage from 20 to 23 inches pitch. The base line AVR was computed to be equal to 1.071 and was reduced to 1.052 at the highest level of suction. The reduction of the AVR was expected, however, this value is not expected to be independent of pitch location due to non-uniformity in suction.

C. INSTRUMENTED BLADE

Figures 26 through 28 show the midspan pressure distribution on the instrumented blade with increasing suction. The pressures were non-dimensionalized with respect to the Prandtl dynamic pressure. It is seen that blade loading increased with increased suction. However, it was

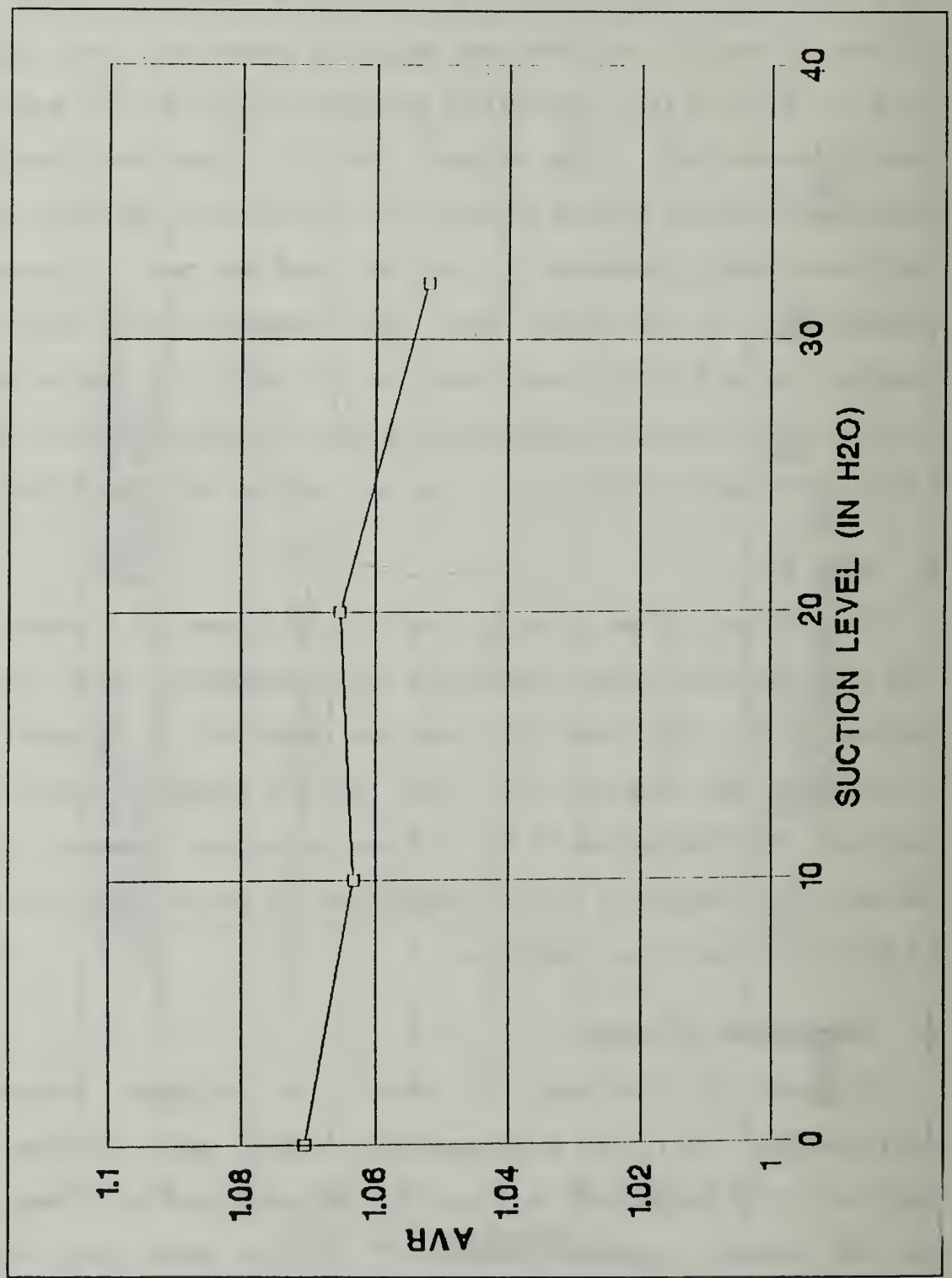

Figure 25. Suction Effects on the Axial Velocity Ratio for the Passage of 20 to 23 in. Pitch

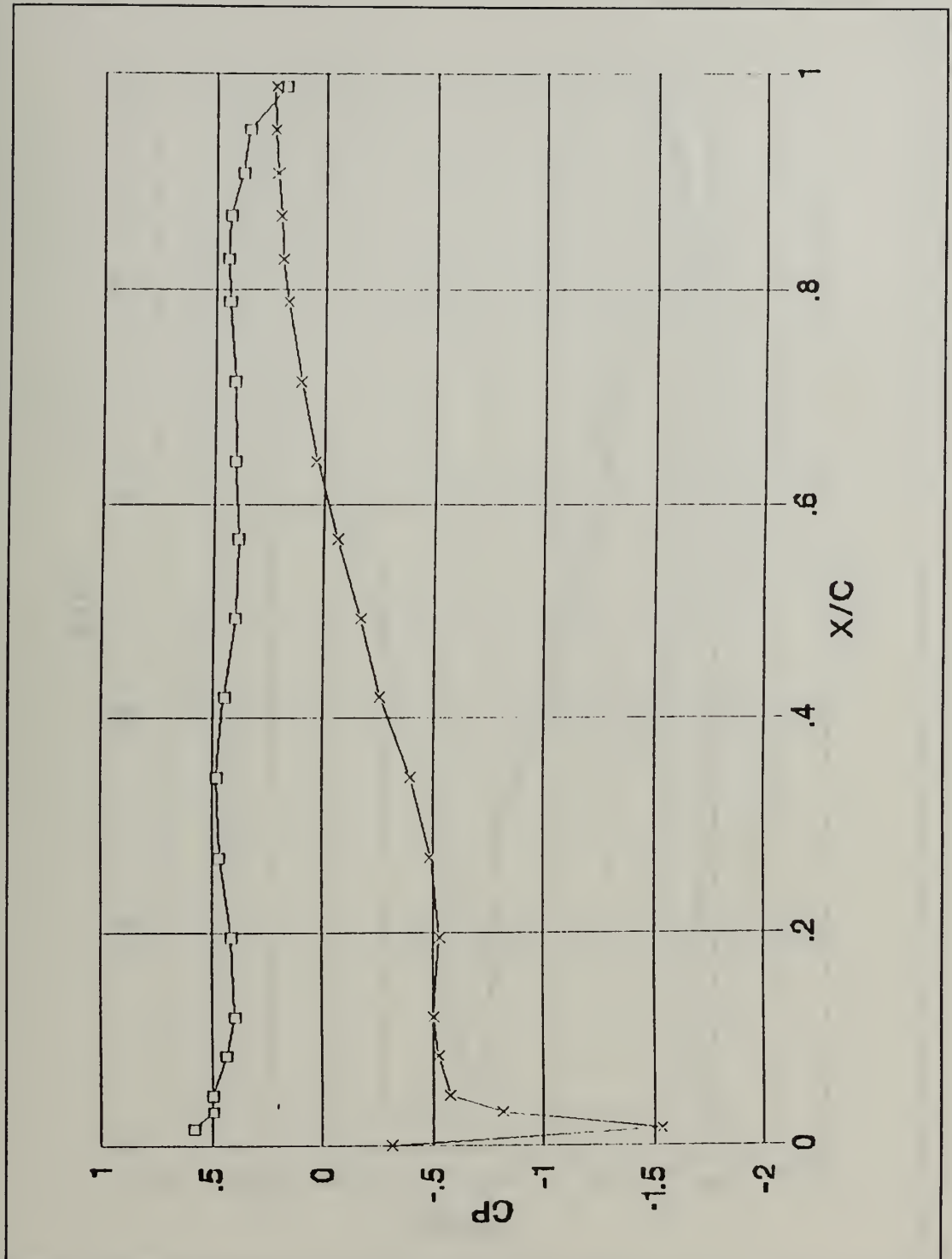

Figure 26. Instrumented Blade Pressure Distribution for Low Suction

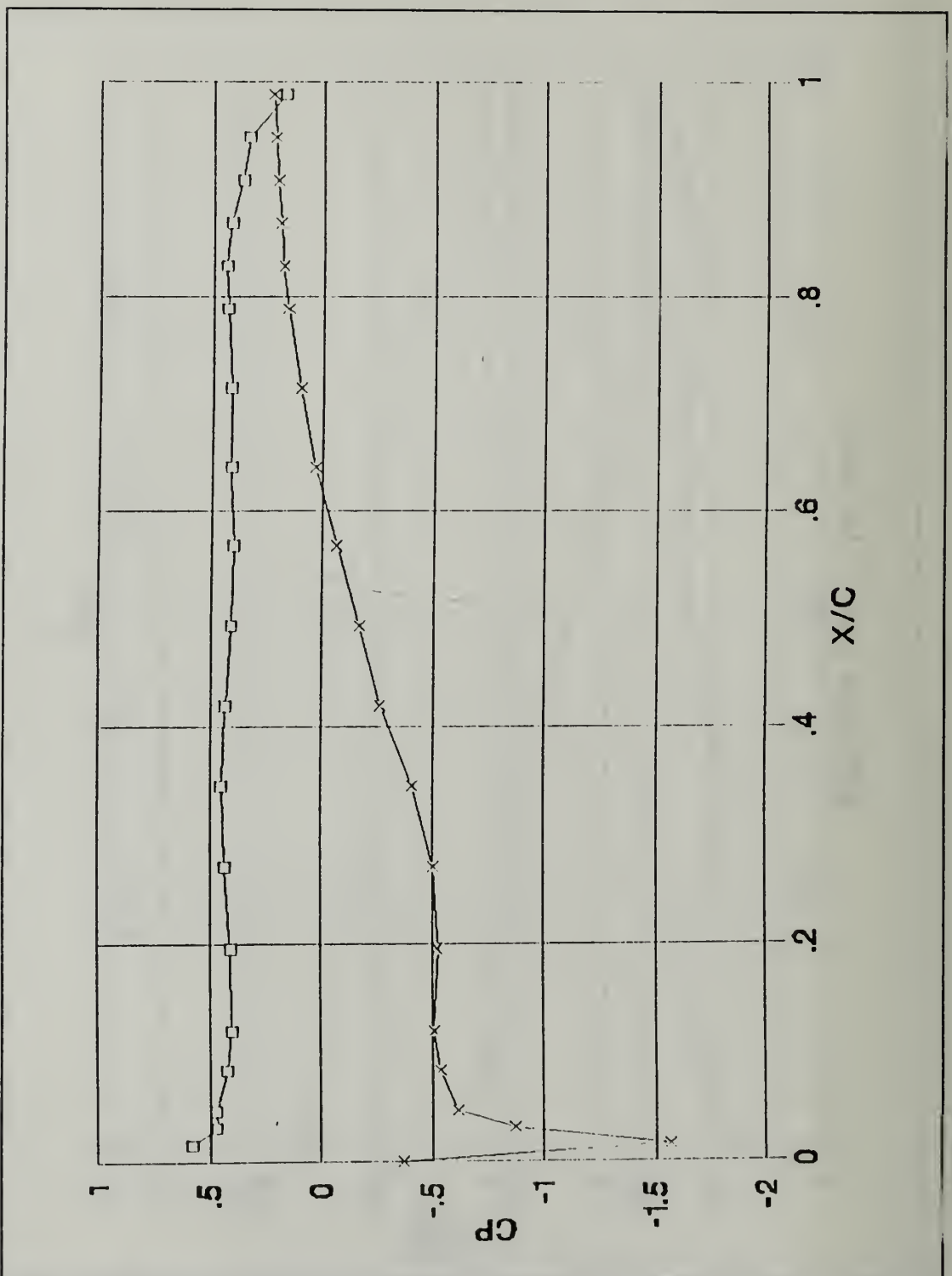

Figure 27. Instrumented Blade Pressure Distribution for Medium Suction

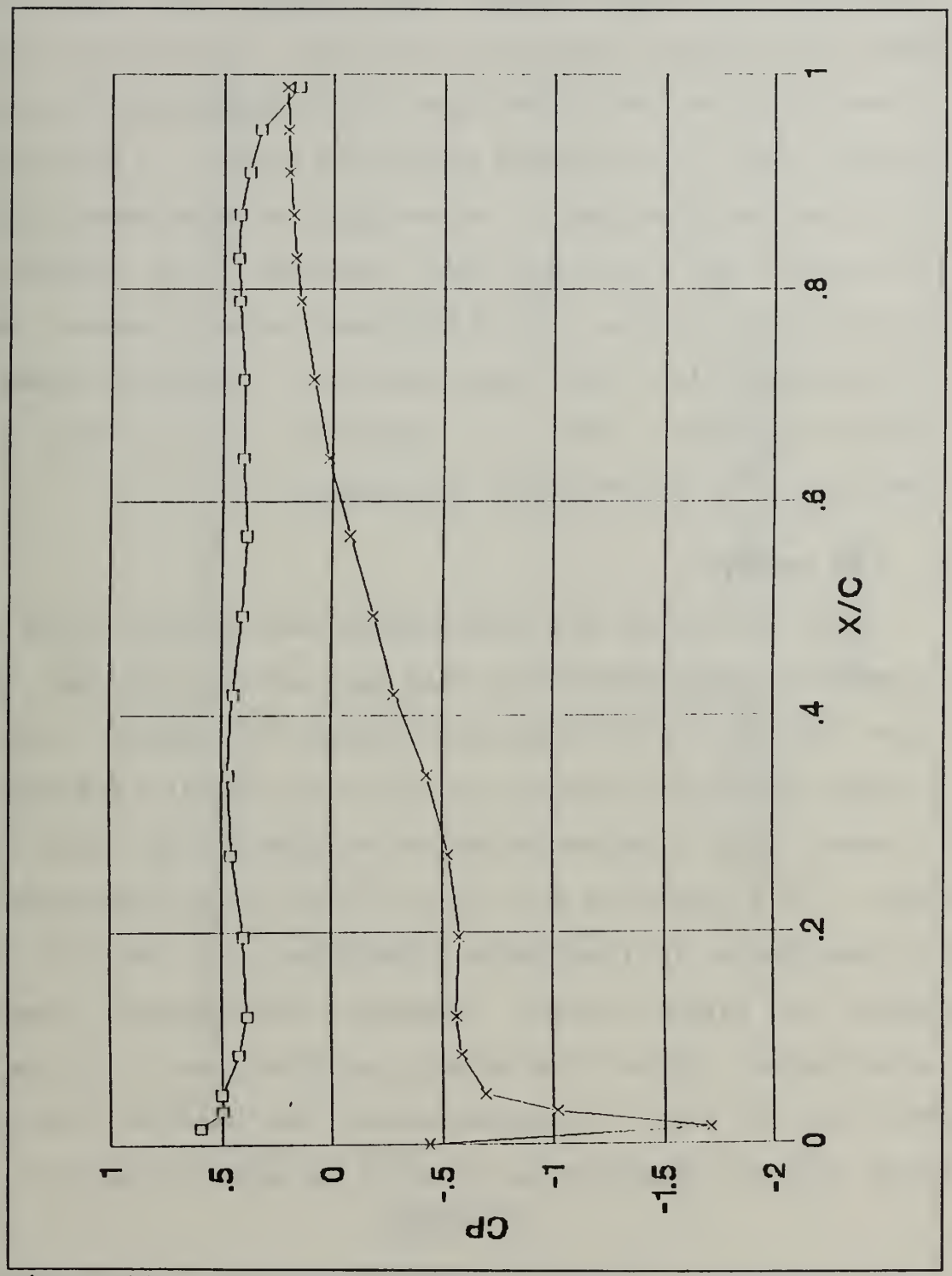

Figure 28. Instrumented Blade Pressure Distribution for High Suction

inconclusive whether boundary layer removal was responsible since the blade was located at mid-pitch. The yaw probe data for each suction level showed that the increased blade loading may be a result of increased inlet flow angle. In the region of the instrumented blade, the average flow angle measured for low suction was 44.02° and this increased to an average of 44.59° at high suction. It is important to note however, that the average inlet flow angle remained relatively constant across the pitch and all deviations were within the uncertainty in the yaw probe measurement.

D. LDV SURVEYS

Inlet and outlet flow measurements were made with the LDV system for comparison between base line and high suction. The inlet flow is seen in Figures 29 through 31. Figure 29 shows a slight reduction occurred in the inlet velocity and Figure 30 shows a half a degree reduction occurred in the inlet flow angle. This conflicts with the rake yaw probe measurements for the change in flow angle, therefore, the cause of the change in blade surface pressure distribution remains inconclusive. Outlet flow velocity profiles seen in Figure 31 show that the point of maximum deficit was shifted, thus the blade wake was displaced as a result of applying suction.

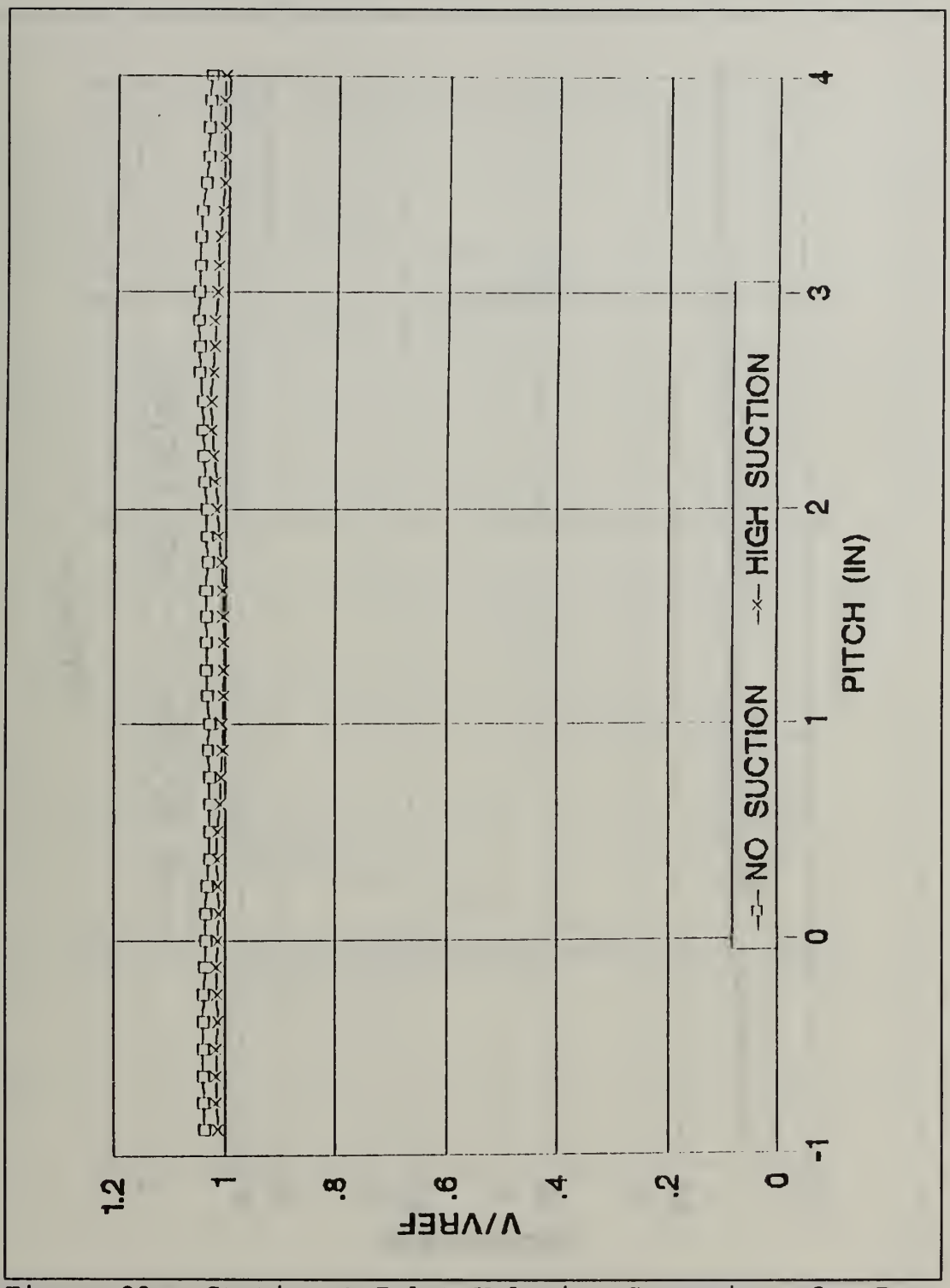

Figure 29. Station 1 Inlet Velocity Comparison for Base Line Configuration and High Suction

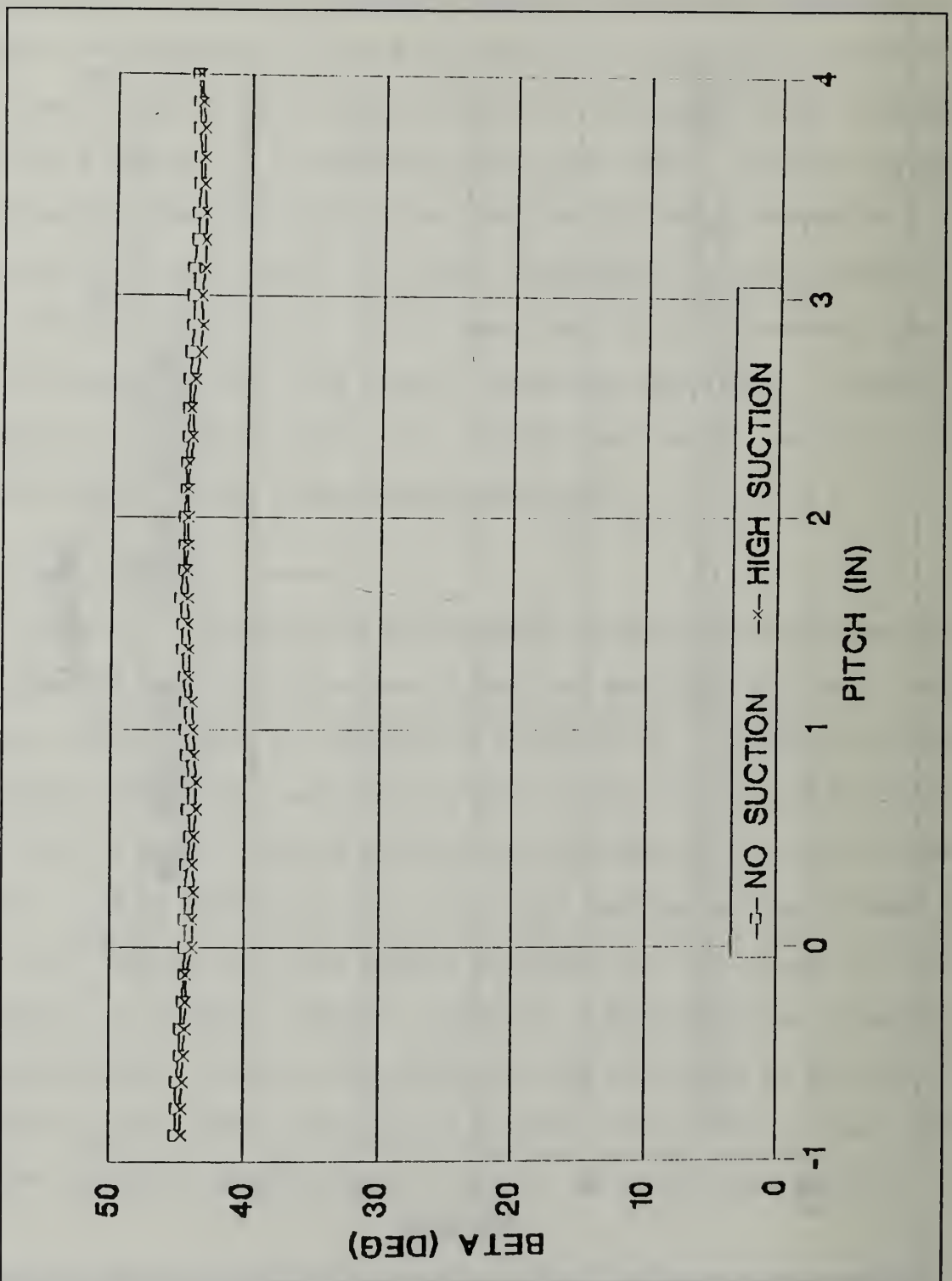

Figure 30. Station 1 Inlet Flow Angle Comparison for Base Line Configuration and High Suction

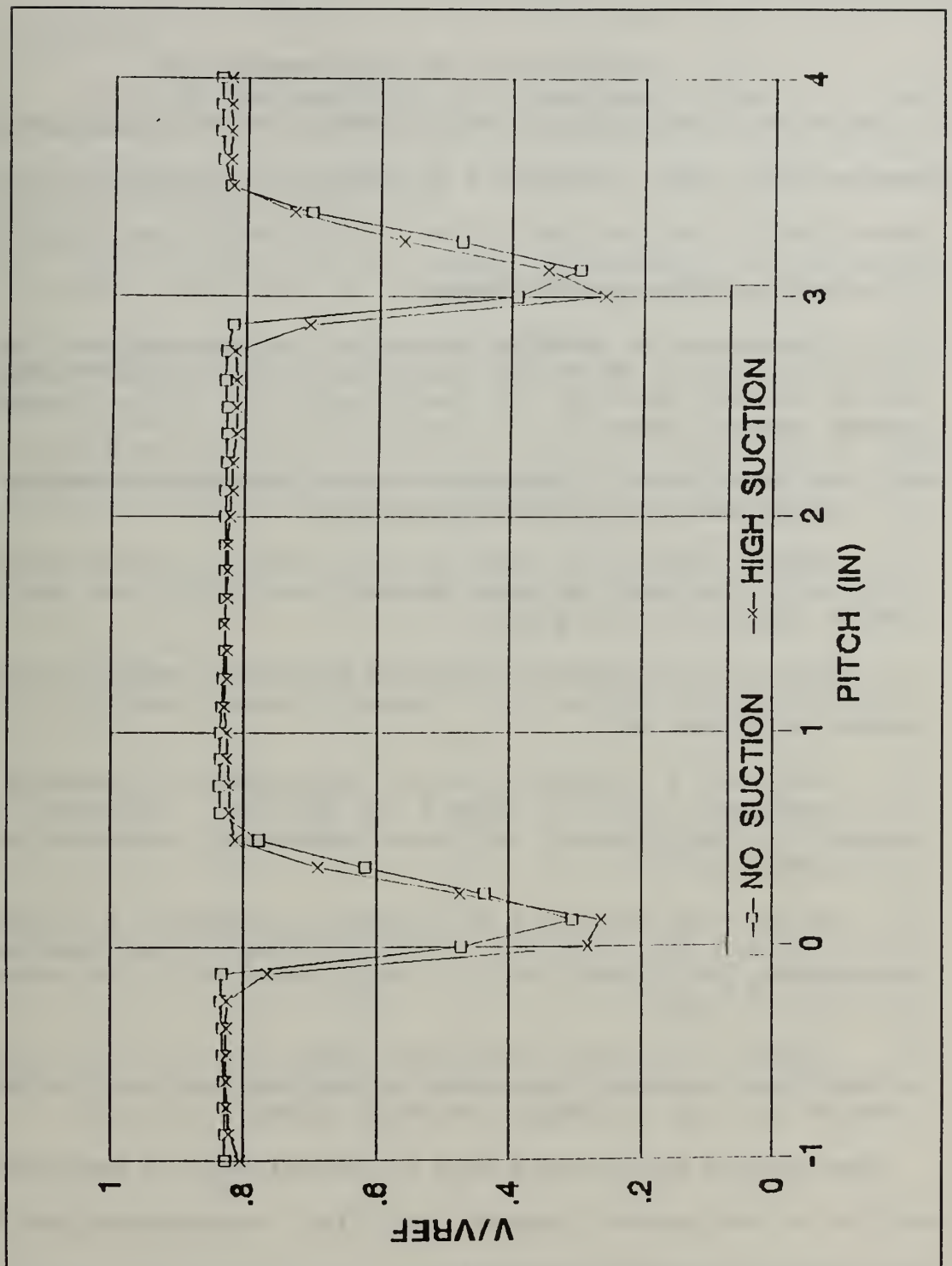

Figure 31. Station 18 Outlet Flow Velocity Comparison for Base line Configuration and High Suction

IV. CONCLUSIONS AND RECOMMENDATIONS

Boundary layer suction was performed 17.25 inches axially ahead of the test section in an effort to improve the two-dimensionality of the inlet flow. The conclusions resulting from these tests are as follows:

1. The base line configuration of the cascade now has a detailed set of data for the inlet flow boundary layers which can be used as the bench mark for future boundary layer removal tests.

2. The base line configuration has an inherent asymmetry in its endwall boundary layer thicknesses.

3. Carpet plots of rake probe surveys showed maximum suction at the east and west extremities of the test section and a minimum at mid-pitch.

4. The suction configuration and procedure used for these tests produced asymmetrical boundary layer removal in the spanwise direction.

5. There was a reduction in the displacement thickness on both endwalls for all levels of suction. However, the amount of displacement thickness reduction decreased with increased suction.

6. The AVR was reduced 1.9% across the passage of blades 7 and 8 from 1.071 to 1.052. For the flow to be considered acceptably two-dimensional, it would have had to be reduced to 1.03 or lower.

7. Endwall balanced manifold pressures did not yield symmetrical boundary layer suction and reduced south endwall suction did not increase the north endwall suction.

The present experiments were a first attempt at performing suction in the present cascade facility. Recommendations for the program to follow include:

1. Investigate the effect of varying the slot width.

2. Make provisions for the addition of another feed pipe to the suction plenum at the mid-pitch location of the manifold.

3. Section the manifold into separate chambers to enable better control of the pitchwise and spanwise suction levels.

4. Place an instrumented orifice at each gate valve to monitor the mass flow rate.

5. Perform tests on the blower to determine the optimum in its mass flow rate vs. pressure ratio characteristic.

6. Investigate the cause of the base line cascade's asymmetric endwall boundary layers.

7. Consider other methods for boundary layer removal, including the use of a porous plate with the present tunnel wall hardware, or, more extensively, rebuilding the tunnel walls to allow suction within the blade passages.

APPENDIX A. RECORDED DATA

This Appendix contains the following:

1. All rake probe data.
2. Instrumented blade data.
3. Manometer data.
4. LDV data.

A1. RAKE PROBE DATA

All rake probe data presented in this appendix was used for the computation of AVR, displacement thickness, spanwise pressure distribution and carpet plots. It is given in the order of the experimental procedure.

BASE LINE CONFIGURATION
UP STREAM LOCATION

PITCH)	0	2.36	4.72	7.08	9.44	11.8	14.16
PROBE PORT	Cp						
1	-.7808	-.0514	.1706	.2995	.4223	.1291	.1851
2	-.4715	-.0116	.2758	.3824	.5617	.2214	.3081
3	-.1837	.064	.4312	.5543	.7183	.3893	.4704
4	.4905	.1587	.5516	.803	.7738	.5304	.6244
5	.7262	.4899	.6617	.7303	.8214	.7908	.8364
6	.8556	.7777	.7818	.8357	.9203	.9142	.9396
7	.749	.8921	.9397	.9602	.9758	.979	.9651
8	.8977	.9214	.972	.9833	.9874	.9891	1
12	1	1	.9946	.9867	.9894	1	.9751
13	.7708	.978	1	.9974	.9998	.993	.9827
14	.4892	.947	.9962	1	1	.979	.9764
15	.6679	.9591	.9928	.994	.9953	.9724	.9697
16	.5538	.879	.9081	.9663	.9489	.9362	.9254
17	.2024	.6425	.5544	.8307	.7494	.8244	.7416
18	.0262	.428	.3012	.5899	.5265	.6744	.4767
19	-.0443	.2782	.1374	.3912	.3918	.4553	.3432
20	-.1924	.1686	.0615	.2619	.2396	.3315	.2087

PITCH)	16.52	18.88	21.24	23.6	26	17	19.36
PROBE PORT							
1	.2276	.3383	.2714	.2231	.2152	.3107	.3847
2	.3558	.4611	.3889	.324	.3739	.4385	.5457
3	.5272	.6017	.5337	.5026	.4826	.6031	.6503
4	.6256	.6568	.6693	.6447	.6835	.675	.7334
5	.8036	.7651	.751	.7867	.8402	.7528	.7978
6	.8691	.8498	.8558	.8866	.9497	.8427	.9056
7	.8997	.9066	.959	.9928	.9978	.9174	.9614
8	1	1	.9842	.9959	1	.9921	.9853
12	.9851	.9592	.9818	.9669	.9863	1	.9808
13	.9824	.9692	.9813	.9702	.9941	.9966	.9839
14	.9758	.9766	.9998	.9862	.9965	.9916	1
15	.9605	.974	1	1	.9867	.9709	.9916
16	.8755	.8838	.9485	.9698	.9473	.8965	.9455
17	.7387	.6077	.8174	.8517	.8964	.6872	.6202
18	.619	.3472	.5588	.5346	.718	.5638	.3622
19	.4818	.1823	.3586	.3659	.454	.3837	.2423
20	.319	.077	.202	.2279	.3157	.2848	.17

CONTINUED
BASE LINE CONFIGURATION RAKE DATA
FULL TRAVERSEUP STREAM LOCATION

PITCH) 21.72	24.08	26.44	28.8	31.16	33.52	35.88
PROBE PORT						
1	.1792	.1874	.291	.2957	.3093	.0758	.246
2	.3126	.3183	.3989	.4273	.4358	.2476	.3531
3	.4547	.4646	.5975	.5698	.5696	.4341	.5084
4	.6244	.6356	.6935	.7018	.6948	.661	.6792
5	.7599	.8184	.8757	.8431	.8042	.8081	.8686
6	.9014	.924	.9319	.8772	.8538	.8721	.9571
7	.9761	1	.9868	.9078	.9077	.9759	.9915
8	.9841	.9895	1	1	1	.9937	.9942
12	.9508	.9738	.9637	.9795	.9696	.9885	.9931
13	.9854	.9878	.9646	.9709	.9645	.9971	1
14	1	.9849	.9495	.9506	.9575	1	.9933
15	.9881	.9973	.915	.8964	.9354	.999	.9871
16	.9615	.9639	.8887	.8417	.8726	.9515	.9406
17	.8699	.8277	.8662	.6103	.711	.7604	.8304
18	.654	.6333	.7455	.398	.5655	.4952	.6519
19	.452	.4319	.5251	.2997	.365	.3127	.4637
20	.2912	.2813	.357	.167	.211	.2264	.2904

PITCH) 38.24	40.6	43	34.4	36.74	39.1	41.45
PROBE PORT						
1	.3627	.2666	.2161	.3336	.2473	.3959	.2175
2	.4811	.3686	.3638	.4632	.3553	.5435	.2983
3	.6522	.5736	.5257	.6099	.5098	.7311	.4698
4	.7146	.6624	.6614	.7012	.6897	.7885	.6954
5	.8567	.809	.7605	.8421	.8442	.8646	.8476
6	.9517	.8643	.8521	.9211	.8895	.9312	.9738
7	.9833	.9082	.95	.9378	.8964	.959	.9944
8	1	1	1	1	1	.9743	.991
12	.984	.9915	.9888	.982	.9791	1	1
13	.9836	.987	.9837	.9772	.9733	.9926	1
14	.9799	.9798	.9917	.9749	.9672	.9804	.999
15	.9539	.965	.9883	.9569	.9582	.9693	.9854
16	.8827	.91678	.946	.8948	.9113	.9088	.9366
17	.7556	.7944	.766	.7461	.7215	.7126	.8357
18	.5948	.5852	.5092	.4953	.5007	.4659	.5981
19	.4179	.421	.324	.3043	.3256	.292	.4183
20	.2341	.2824	.2077	.1896	.1985	.1829	.2675

CONTINUED
BASE LINE CONFIGURATION RAKE DATA
FULL TRAVERSE UP STREAM LOCATION

PITCH >	43.81	46.18	48.54	50.9	53.3	55.61	57.98
PROBE PORT							
1	.2597	.2525	.1948	.1603	.244	.2144	.0667
2	.4014	.348	.3143	.2694	.3696	.3573	.1482
3	.5492	.5165	.4697	.4571	.5444	.4395	.2162
4	.7077	.6835	.6996	.6493	.6996	.6891	.4277
5	.8646	.8301	.8334	.8232	.8892	.8485	.8188
6	.9641	.9073	.9059	.9299	.977	.9299	.9273
7	.9865	.9242	.95	.9955	.9988	.9547	.988
8	1	1	.9994	.9922	.9923	1	.9868
12	.9899	.9693	1	.9942	.9898	.9801	1
13	.9891	.9733	.9882	.9996	.9942	.9885	.9931
14	.9952	.9597	.9697	1	1	.9775	.9943
15	.9838	.9426	.9679	.9872	.9952	.9455	.9689
16	.9388	.8746	.9393	.9396	.9341	.8962	.873
17	.8286	.7017	.8172	.8125	.7464	.7617	.6863
18	.5833	.4981	.608	.6003	.5084	.5538	.4739
19	.4001	.3158	.4	.3965	.3512	.3667	.3377
20	.2567	.2045	.2782	.2321	.2119	.2207	.196

PITCH >	57.98	60.38
PROBE PORT		
1	.0667	-.72
2	.1482	-.4612
3	.2162	-.0524
4	.4277	.3904
5	.8188	.6025
6	.9273	.5396
7	.988	.5345
8	.9868	.9189
12	1	.8736
13	.9931	.806
14	.9943	.8088
15	.9689	.9614
16	.873	1
17	.6863	.6
18	.4739	.2896
19	.3377	.2078
20	.196	.126

BASE LINE CONFIGURATION RAKE DATA
UP STREAM LOCATION 20 TO 23 INCHES

PITCH > PROBE PORT	20 Cp	20.25	20.5	20.75	21	21.25	21.5
1	.3835	.2685	.2171	.2379	.2858	.3487	.3559
2	.4183	.3076	.2875	.3237	.4205	.4512	.457
3	.5804	.4887	.4341	.4586	.5668	.5995	.5776
4	.7522	.6952	.6303	.6211	.6482	.677	.686
5	.9166	.903	.8441	.781	.7452	.7443	.7587
6	.9769	.96	.907	.8692	.8633	.8726	.8848
7	.9842	.9845	.9701	.9552	.9539	.9727	.9765
8	.9861	1	1	.9863	.9847	.9844	.991
12	.9801	.9786	.9581	.9475	.9777	.9953	.9728
13	1	.9836	.9655	.9668	.9836	.9889	.991
14	.9945	.9987	1	1	1	1	1
15	.9957	.9996	.9825	.981	.9946	.9917	.9869
16	.9688	.952	.9253	.9114	.9279	.9516	.9635
17	.6643	.701	.705	.6828	.7277	.7695	.882
18	.4289	.4772	.441	.3947	.4341	.5473	.6227
19	.3111	.2927	.261	.2024	.2146	.32	.385
20	.2046	.2041	.1486	.0962	.1266	.1702	.2787

PITCH > PROBE PORT	21.75	22	22.25	22.5	22.75	23
1	.3086	.2563	.2454	.2426	.3245	.3559
2	.384	.3085	.3186	.3504	.419	.4377
3	.5275	.4977	.4621	.4757	.5515	.5749
4	.6525	.6652	.6447	.6291	.6573	.6787
5	.8027	.8463	.8665	.8531	.8129	.7813
6	.925	.9527	.9142	.9241	.8967	.8594
7	.988	.9864	.9459	.9631	.9461	.9463
8	.9944	.9955	1	1	1	.9845
12	.9751	.9783	.9687	.9542	.9524	.9611
13	.9872	.9938	.9763	.9188	.9206	.9257
14	.9996	1	.987	.9735	.9919	1
15	1	.989	.9868	.9682	.9827	.9839
16	.9711	.9729	.9542	.9312	.9003	.8988
17	.8708	.8445	.8185	.7534	.7186	.7
18	.6497	.6603	.6358	.5635	.5152	.4645
19	.4346	.4208	.4061	.3873	.3323	.3065
20	.2659	.2664	.2706	.2257	.2086	.1721

BASE LINE CONFIGURATION RAKE DATA
DOWN STREAM LOCATION 20 TO 23 INCHES

PITCH > PROBE PORT	20 Cp	20.25	20.5	20.75	21	21.25	21.5
1	.4517	.4278	.4504	.479	.518	.4991	.39
2	.5918	.5617	.5932	.6387	.6441	.6143	.4598
3	.7261	.7118	.716	.7373	.7327	.6747	.5099
4	.6498	.6825	.722	.7743	.7841	.7234	.5977
5	.5897	.5253	.6078	.6994	.8112	.8726	.8461
6	.6082	.5341	.5837	.683	.82	.9022	.9202
7	.5617	.563	.6353	.7658	.8407	.9343	.9552
8	.7085	.8569	.9488	.9961	1	1	1
12	1	1	1	1	.9735	.9765	.9659
13	.742	.8661	.9217	.9742	.9769	.9875	.974
14	.5602	.5278	.5714	.6562	.7611	.8842	.9605
15	.6936	.5722	.5562	.5645	.6508	.7861	.9315
16	.601	.5055	.5266	.5687	.6641	.7998	.9234
17	.586	.5801	.6374	.7105	.7944	.8359	.781
18	.7175	.7171	.7516	.7914	.8304	.835	.7311
19	.7466	.7551	.7929	.8311	.8537	.8283	.701
20	.6834	.7163	.7652	.8051	.8247	.7956	.7016

PITCH > PROBE PORT	21.75	22	22.25	22.5	22.75	23
1	.289	.2882	.3951	.4808	.4503	.4339
2	.3539	.3663	.4627	.5544	.5808	.5256
3	.4164	.4658	.6005	.7268	.7132	.6691
4	.4716	.4817	.5431	.6113	.6447	.6121
5	.8072	.7398	.7023	.7217	.6357	.5066
6	.9296	.9225	.9294	.9551	.7912	.5885
7	.9466	.8933	.82	.7855	.6483	.5337
8	1	.9533	.838	.7871	.6576	.6183
12	.9633	.8478	.7158	.8076	1	1
13	.9916	.9221	.7842	.7755	.7734	.8448
14	.9988	.9555	.8707	.8081	.6335	.5284
15	.9922	1	1	1	.8214	.6016
16	.9685	.9694	.9285	.9248	.7635	.5615
17	.6821	.5733	.5979	.6491	.5889	.5351
18	.6152	.5322	.6194	.7075	.7407	.6854
19	.5902	.4865	.5893	.6923	.7535	.6951
20	.5738	.4376	.5184	.6479	.702	.6782

LOW SUCTION RAKE DATA
FULL TRAVERSE UP STREAM LOCATION

PITCH >	0	2.36	4.72	7.08	9.44	11.8	14.16
PROBE PORT	Cp						
1	-.9632	.3665	.5075	.4171	.5128	.3205	.3328
2	-.7206	.4172	.6626	.5621	.6475	.4896	.4729
3	-.4396	.61	.7382	.6987	.7441	.5624	.6122
4	.4427	.6431	.7334	.7689	.7862	.6863	.6775
5	.5687	.6794	.8199	.8337	.8803	.8577	.7897
6	.6648	.7663	.9472	.9656	.961	.966	.6975
7	.5778	.8817	.9831	.9629	.989	.9951	.94
8	.8907	.9447	.9815	.9909	1	1	1
12	1	1	.9936	.8851	.9926	.9943	.9725
13	.683	.9916	1	.9948	.9927	.9974	.968
14	.366	.9712	.9974	.9946	.9959	.998	.9708
15	.604	.9669	.9968	1	.998	.9919	.9471
16	.6541	.8844	.9089	.9771	.9581	.9006	.9119
17	.3967	.6311	.6522	.9312	.836	.8294	.873
18	.3588	.5114	.5029	.8366	.8007	.7885	.7695
19	.2817	.3573	.3669	.6696	.65	.6854	.5881
20	.1048	.2924	.255	.5266	.4968	.549	.4727
Ptot	5.268	10.226	9.97	10.064	10.206	10.164	10.692
Ppr	10.712	10.632	10.558	10.49	10.588	10.514	10.574
Ppl	12.25	12.174	12.146	12.022	12.146	12.042	12.116
Tpl	533.62	534.01	534.38	534.58	534.64	535.11	535.06
RAKE Q	7.834	13.56	13.118	13.118	13.296	13.328	13.63
BETA	44.3	43.11	44.1	43.66	43.62	43.77	43.76

PITCH >	16.52	18.88	21.24	23.6	26	26.44	28.8
PROBE PORT							
1	.3344	.3863	.3364	.2382	.3081	.3447	.3381
2	.4697	.5532	.4584	.3741	.4319	.4684	.4631
3	.6156	.665	.5686	.5197	.557	.6456	.6089
4	.6752	.694	.664	.655	.7083	.7199	.6942
5	.8052	.7619	.751	.7928	.8551	.8473	.8
6	.8592	.8697	.8847	.9375	.9595	.9036	.8402
7	.8967	.9332	.9785	.9949	.994	.9204	.8889
8	1	.9788	.9774	1	1	1	1
12	.7958	1	.9843	.9825	.9957	.994	.9722
13	.9916	.9907	.9921	.9836	.9918	.9835	.9563
14	.9846	.9802	.9998	.9935	.9858	.9331	.9311
15	.9511	.9708	1	.9951	.9518	.8854	.9014
16	.88971	.9348	.9813	.9901	.9243	.864	.8741
17	.7771	.8096	.926	.9439	.8884	.7915	.6916
18	.6879	.6362	.7323	.7654	.837	.7883	.5119
19	.5904	.446	.5363	.6107	.6667	.6846	.3677
20	.4632	.2881	.368	.4862	.5179	.5259	.2689
Ptot	10.67	10.484	10.162	10.152	10.284	10.648	10.948
Ppr	10.552	10.514	10.47	10.478	10.508	10.518	10.448
Ppl	12.07	12.084	12.03	12.028	12.084	12.076	12.056
Tpl	535.14	535.03	535.15	535.7	535.72	535.51	535.67
RAKE Q	13.856	13.944	13.522	13.478	13.72	14.032	14.08
BETA	43.69	43.36	43.71	44.07	44.1	44.05	43.85

CONTINUED

LOW SUCTION RAKE DATA

FULL TRAVERSE UP STREAM LOCATION

PITCH >	31.16	33.52	35.88	38.24	40.6	43	43.81
PROBE PORT							
1	.3382	.2334	.2066	.26	.2771	.2827	.2648
2	.4722	.3792	.3378	.4001	.3914	.4307	.4351
3	.6251	.4817	.4824	.5218	.5614	.5769	.5782
4	.721	.682	.6801	.671	.6881	.6825	.6995
5	.8087	.7968	.8718	.8469	.8187	.7506	.8367
6	.8739	.916	.9769	.9423	.8696	.847	.9677
7	.9598	.9854	.9983	.979	.953	.9707	.9991
8	.9847	.9983	1	1	.9978	.9957	1
12	.9992	.9913	.9939	.9829	.9891	.9951	.9881
13	.9959	.9918	.9992	.9885	1	1	.994
14	1	1	.995	.9718	.9928	.9968	.9898
15	.9884	.9996	.9878	.9536	.985	.9951	.9896
16	.9334	.9683	.9401	.8803	.9468	.9762	.9783
17	.7618	.7367	.8293	.7135	.8202	.8425	.9081
18	.5566	.4861	.6611	.50377	.6564	.665	.721
19	.445	.3398	.4719	.3693	.4399	.5177	.5479
20	.3728	.2772	.3977	.2715	.308	.4281	.429
Ptot	10.36	10.542	10.486	10.778	10.798	10.578	10.582
Ppr	10.404	10.548	10.478	10.44	10.464	10.36	10.362
Ppl	12.04	12.066	12.038	12.064	12.034	12.014	12.038
Tpl	535.73	535.68	535.67	535.74	536.02	536.03	536.21
RAKE Q	13.792	13.858	13.806	13.892	13.916	13.71	13.584
BETA	44.16	44.61	44.77	44.78	44.96	44.61	44.88

PITCH >	46.18	48.54	50.9	53.3	55.61	57.98	60.38
PROBE PORT							
1	.2967	.3473	.3344	.2809	.3811	.2693	-.0789
2	.4333	.5092	.4795	.4237	.5413	.4373	.1632
3	.5927	.6297	.5983	.5883	.691	.5192	.5
4	.7168	.7133	.729	.7475	.7605	.7461	.7969
5	.8501	.8144	.8236	.9069	.8578	.8771	.852
6	.9168	.8732	.9285	.9791	.911	.9503	.7443
7	.9405	.9109	.9907	.991	1	.991	.6579
8	1	.9871	.991	.9938	.9977	.9846	.9851
12	.9745	1	.9977	.9955	.9861	1	1
13	.9829	.9912	.992	1	.9932	.9923	.9997
14	.971	.97	1	.9929	.991	.9828	.9037
15	.9411	.9502	.9912	.9929	.9669	.9478	.9957
16	.8915	.9281	.9521	.9563	.9258	.7063	.8858
17	.7762	.7964	.857	.79	.8026	.3335	.6929
18	.6661	.5917	.6885	.6222	.6424	.1599	.5158
19	.5285	.4546	.5136	.4715	.4949	.1303	.3065
20	.3874	.3366	.3837	.3686	.3721	.0819	.1093
Ptot	10.966	10.884	10.486	10.63	10.648	10.916	6.46
Ppr	10.388	10.37	10.358	10.32	10.396	10.384	10.32
Ppl	12.05	12.052	12.064	12.048	12.07	12.094	12.076
Tpl	536.33	536.1	536.06	536.17	536.06	536.09	535.99
RAKE Q	13.718	13.968	13.508	13.54	13.384	13.642	9.824
BETA	44.49	44.34	44.71	45.07	45.2	45.52	47.08

LOW SUCTION SETTING RAKE DATA
UP STREAM LOCATION 20 TO 23 INCHES

PITCH >	20	20.25	20.5	20.75	21	21.25	21.5
PROBE PORT	Cp						
1	.2738	.2876	.3022	.3496	.378	.3437	.2989
2	.4036	.4325	.4481	.5005	.5215	.4459	.4052
3	.5485	.5709	.5823	.6275	.6425	.5822	.5597
4	.6843	.6618	.6571	.6734	.6822	.6704	.6686
5	.857	.854	.8202	.7951	.7821	.7759	.7942
6	.9465	.9265	.9006	.8923	.8914	.9007	.918
7	.9503	.9473	.9417	.9647	.9718	.968	.9695
8	.958	.9696	.9736	1	.9861	.9783	.9685
12	.9899	.973	.9551	.9783	.9978	.9897	.9754
13	.986	.9653	.9585	.9847	.9936	.9819	.9834
14	.9905	1	.9858	.9957	.994	1	1
15	1	.9979	1	.9884	1	.9885	.9978
16	.9691	.964	.9185	.9465	.9601	.9762	.9725
17	.7942	.817	.8058	.8638	.8924	.9317	.8877
18	.5874	.6177	.5932	.578	.6632	.7163	.8051
19	.4642	.4604	.4588	.4325	.4216	.5015	.591
20	.3759	.3937	.3676	.3546	.2983	.3525	.429
Ptot	10.534	10.668	10.702	10.326	10.07	10.066	10.098
Ppr	10.604	10.612	10.62	10.62	10.42	10.398	10.474
Ppl	12.096	12.15	12.08	12.054	11.98	11.936	11.882
Tpl	535.58	535.71	535.77	535.81	535.89	536.01	535.95
RAKE Q	13.942	13.844	13.71	13.614	13.538	13.438	13.348
BETA	43.32	43.55	43.56	43.35	43.14	43.28	43.26

PITCH >	21.75	22	22.25	22.5	22.75	23
PROBE PORT						
1	.2379	.2605	.3127	.3335	.3571	.2874
2	.3697	.4041	.4498	.48	.4873	.4387
3	.5188	.5565	.5826	.5948	.5862	.5752
4	.6631	.6785	.6672	.6678	.6733	.6819
5	.8465	.8565	.8424	.8232	.7933	.7847
6	.9404	.9578	.9432	.9029	.893	.8768
7	.9732	.9912	.9867	.9539	.9307	.9419
8	.9814	1	1	.9841	.9824	.9875
12	.984	.9851	.96	.9383	.9552	.9591
13	.9855	.9825	.9694	.9545	.9663	.9496
14	1	.9969	.9963	1	.9987	.9802
15	.9969	.9974	.8858	.988	1	1
16	.9691	.9674	.9367	.9262	.9296	.9273
17	.8573	.8344	.7821	.7566	.7797	.8112
18	.7892	.7852	.6977	.6304	.5822	.6273
19	.6213	.6291	.5624	.4781	.4467	.4498
20	.4972	.512	.4598	.358	.3238	.3397
Ptot	10.23	10.196	10.392	10.542	10.45	10.404
Ppr	10.44	10.548	10.494	10.596	10.47	10.5
Ppl	12.03	12.002	12.006	12.002	11.984	12
Tpl	536	535.91	535.96	536.08	536.01	535.96
RAKE Q	13.57	13.558	13.474	13.398	13.45	13.434
BETA	43.41	43.42	43.57	43.47	43.5	43.68

LOW SUCTION SETTING RAKE DATA
DOWN STREAM LOCATION 20 TO 23 INCHES

PITCH >	20	20.25	20.5	20.75	21	21.25	21.5
PROBE PORT	Cp						
1	.4873	.4219	.4949	.5199	.5178	.4299	.3262
2	.6341	.5944	.6472	.6555	.5989	.5254	.3974
3	.7029	.6938	.7207	.7235	.6553	.5457	.4548
4	.6163	.6678	.7134	.7546	.7188	.5882	.5166
5	.5621	.5334	.6024	.7335	.818	.8324	.7934
6	.6251	.546	.5915	.7	.8275	.8887	.9073
7	.5108	.532	.6482	.7726	.9043	.9321	.9435
8	.6847	.8139	.9274	.9884	.967	.9981	.9906
12	1	1	1	.9939	.9878	.9994	.9873
13	.8605	.9447	.9939	1	1	1	.999
14	.5742	.597	.7083	.8327	.9464	.9968	1
15	.6524	.5824	.6193	.7235	.8933	.9732	.9992
16	.6307	.5537	.5937	.7197	.9027	.9551	.9778
17	.5899	.6131	.7169	.8291	.8929	.8909	.8512
18	.7273	.7375	.7998	.839	.8878	.8655	.7467
19	.736	37612	.8049	.8362	.8705	.8525	.7485
20	.681	.7037	.7246	.7676	.8	.7848	.6989
Ptot	9.592	10.158	10.16	10.148	10.178	10.156	10.202
Ppr	10.582	10.486	10.482	10.576	10.574	10.514	10.508
Ppl	12.054	11.982	11.986	12.042	12.048	11.988	11.982
Tpl	534.88	535.14	535.23	535.34	535.35	535.58	535.67
RAKE Q	8.604	8.854	8.76	8.678	8.636	8.69	8.698
BETA	-2.75	-1.69	-1.94	-2.32	-3.58	-2.28	-2.84

PITCH >	21.75	22	22.25	22.5	22.75	23
PROBE PORT						
1	.2993	.3922	.4837	.5835	.5638	.5294
2	.4117	.4841	.5984	.7281	.7018	.6556
3	.4653	.5361	.6395	.7536	.7532	.688
4	.4915	.4978	.5363	.6252	.6203	.6297
5	.7471	.7414	.7616	.8327	.6894	.5856
6	.8986	.9216	.9455	.9725	.7882	.6164
7	.9428	.9165	.8786	.7865	.6274	.5248
8	.9678	.9059	.8447	.7448	.6681	.7155
12	.9739	.8731	.7582	.8779	1	1
13	.9829	.9328	.8229	.8135	.8171	.8773
14	.9943	.9802	.9315	.8522	.6583	.5737
15	1	1	1	1	.8108	.663
16	.9635	.9544	.9486	.9171	.7611	.5979
17	.6819	.5862	.6204	.6567	.5924	.5766
18	.628	.5426	.6395	.764	.7463	.7188
19	.6862	.4912	.6029	.7476	.759	.7352
20	.5477	.4342	.5455	.6794	.6947	.6632
Ptot	10.178	9.622	8.91	8.01	8.68	9.744
Ppr	10.49	10.478	10.504	10.586	10.514	10.486
Ppl	11.978	11.988	11.998	12.028	11.984	11.996
Tpl	535.51	535.51	535.69	535.59	535.66	535.593
RAKE Q	8.766	7.862	5.962	6.236	7.842	8.724
BETA	-2.86	-2.73	-2.3	-1.79	-2.15	-3.27

BASE LINE STATION 1
Velocity in M/SEC
Data is from the following files:
ST1A1209.1.41
STATION 1

X(in)	Z(in)	U-Mean VEL	U-Standard DEV	V-Mean Velocity	V Standard Deviation	UV-Angle Mean
-1	-6.29	0	0	0	0	0
-.875	-6.29	60.7	1.21	60.5	1.23	44.9
-.75	-6.29	60.7	1.24	60.6	1.28	45
-.625	-6.29	60.7	1.22	60.8	1.17	45
-.5	-6.29	60.6	1.23	60.9	1.23	45.2
-.375	-6.29	60.5	1.88	61	1.17	45.2
-.25	-6.29	60.3	1.28	61.1	1.19	45.4
-.125	-6.29	60	1.23	61	1.27	45.5
0	-6.29	59.7	1.25	61	1.2	45.6
.125	-6.29	59.7	1.2	61	1.16	45.6
.25	-6.29	59.6	1.2	60.9	1.2	45.6
.375	-6.29	59.3	1.48	60.9	1.28	45.7
.5	-6.29	59.1	1.48	61	1.26	45.9
.625	-6.29	59.2	1.13	61	1.38	45.8
.75	-6.29	59.3	1.27	60.9	1.29	45.8
.875	-6.29	59.4	1.19	60.8	1.25	45.7
1	-6.29	59.5	1.3	60.7	1.31	45.6
1.13	-6.29	59.8	1.23	60.7	1.28	45.5
1.25	-6.29	59.9	1.3	60.7	1.26	45.4
1.38	-6.29	60.1	1.34	60.6	1.3	45.2
1.5	-6.29	60.1	1.69	60.6	1.13	45.2
1.62	-6.29	60.3	1.4	60.6	1.21	45.1
1.75	-6.29	59.9	1.23	60.6	1.22	45.3
1.87	-6.29	60.1	1.24	60.6	1.28	45.3
2	-6.29	60	1.26	60.7	1.27	45.3
2.13	-6.29	60.3	1.14	61.1	1.21	45.4
2.25	-6.29	60.3	1.18	61.2	1.38	45.4
2.37	-6.29	60.4	1.19	61.4	1.25	45.5
2.5	-6.29	60.4	1.18	61.6	1.31	45.6
2.63	-6.29	60.6	1.19	61.9	1.29	45.6
2.75	-6.29	60.5	1.22	62	1.32	45.7
2.87	-6.29	60.7	1.21	62.3	1.3	45.8
3	-6.29	60.6	1.28	62.3	1.41	45.8
3.12	-6.29	60.5	1.32	62.2	2.29	45.8
3.25	-6.29	60.2	1.37	62.3	1.25	46
3.37	-6.29	60.1	1.43	62.3	1.25	46
3.5	-6.29	59.7	1.49	62	1.18	46.1
3.62	-6.29	59.4	1.44	61.8	1.21	46.1
3.75	-6.29	59.4	1.38	61.6	1.18	46
3.87	-6.29	59.4	1.32	61.4	1.17	46
4	-6.29	59.3	1.26	61.1	1.2	45.9

Velocity in M/SEC
Data is from the following files:
ST1SUCK,1,41
STATION 1 HIGH SUCTION

X(mm)	Z(mm)	U-Mean Velocity	U-Standard Deviation	V-Mean Velocity	V-Standard Deviation	UV-Ar Mea
-25.4	-160	58	1.35	58.6	1.89	
-22.2	-160	58	1.28	58.5	2.1	
-19	-160	58.2	1.31	58.8	2.01	
-15.9	-160	58.1	1.38	58.9	2.03	
-12.7	-160	57.9	1.16	59	1.73	
-9.52	-160	57.7	1.17	58.9	2.03	
-6.35	-160	57.6	1.09	59	1.94	
-3.17	-160	57.7	1.13	59.2	2.35	
0	-160	57.1	1.17	59.3	1.84	
3.17	-160	57.1	1.17	59.2	2.91	
6.35	-160	57	1.2	59.4	2.29	
9.52	-160	57.2	1.14	59.5	2.38	
12.7	-160	57.1	1.2	59.6	2.15	
15.9	-160	56.7	1.36	59.5	2.05	
19	-160	56.7	1.34	59.4	1.93	
22.2	-160	56.6	1.33	59	2.2	
25.4	-160	56.7	1.32	59	1.86	
28.6	-160	56.6	1.29	58.7	1.93	
31.7	-160	56.9	1.24	58.4	2.59	
34.9	-160	56.8	1.16	58.4	2.45	
38.1	-160	57.1	1.13	58.5	2.18	
41.3	-160	57.2	1.19	58.5	2.12	
44.5	-160	57.6	1.04	58.6	2.38	
47.6	-160	57.7	1.08	58.9	2.29	
50.8	-160	57.8	1.01	59.1	2.28	
54	-160	58	1.04	59.3	2.47	
57.2	-160	58.2	1.11	59.6	2.21	
60.3	-160	58.1	1.08	59.9	1.61	
63.5	-160	58.3	1.15	60	3.01	
66.7	-160	57.9	1.19	60.1	2.57	
69.8	-160	57.4	1.39	60.3	2.46	
73	-160	57.4	1.39	60.3	2.08	
76.2	-160	57.1	1.37	60.1	2.72	
79.4	-160	56.8	1.33	60.2	2.18	
82.6	-160	56.7	1.37	60	3.02	
85.7	-160	56.6	1.2	59.8	2.75	
88.9	-160	56.5	1.17	59.6	2.77	
92.1	-160	56.5	1.16	59.6	1.99	
95.2	-160	56.5	1.12	59.6	2.54	
98.4	-160	56.8	1.2	59.4	2.55	
102	-160	56.9	1.12	59.2	2.89	

STATION 1

U TURBULENCE INTENSITY

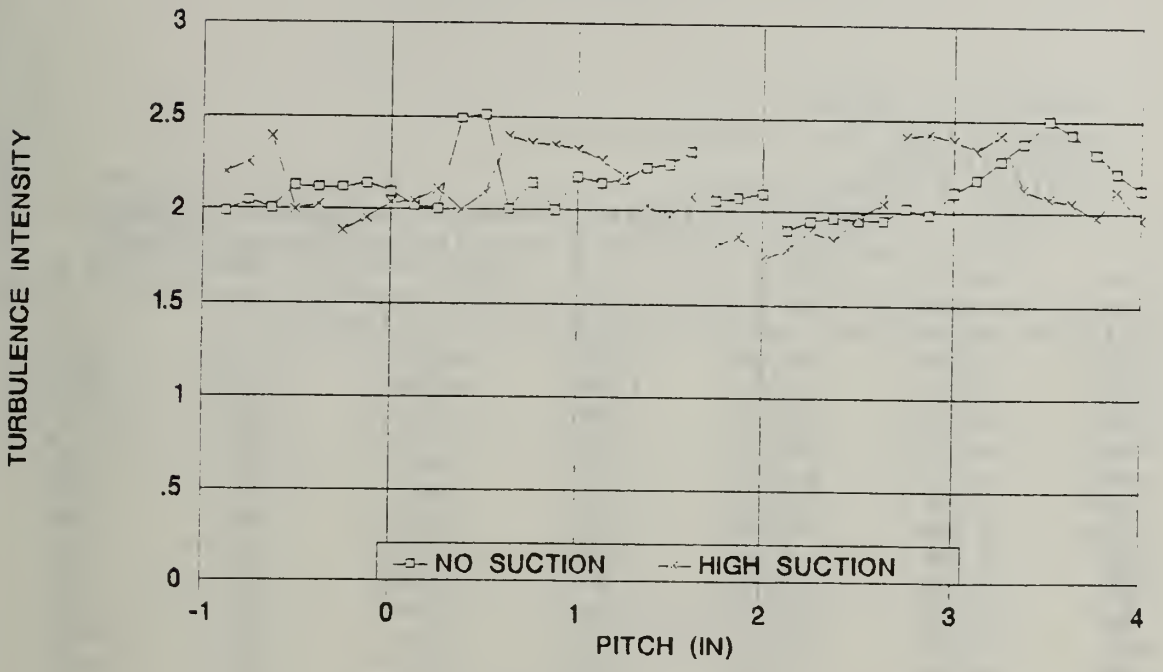

STATION 1

V TURBULENCE INTENSITY

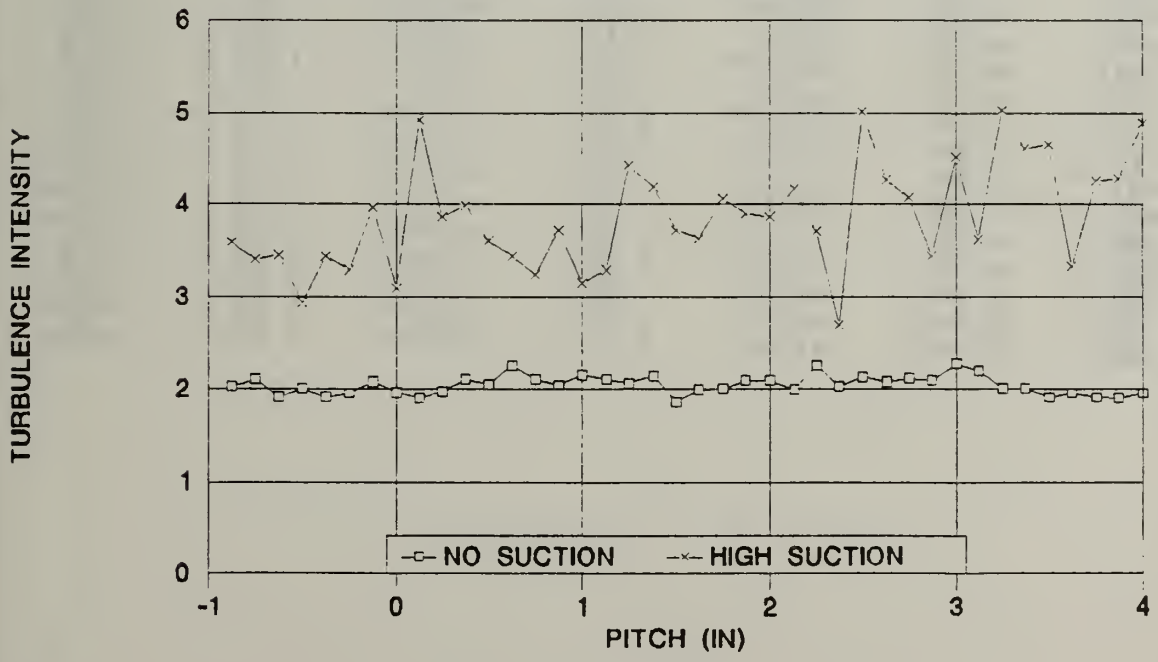

Velocity in M/SEC
Data is from the following files:
ST2A1118,1,33
STATION 2 SUCTION SIDE

X(in)	Z(in)	U-Mean Velocity	U-Standard Deviation	V-Mean Velocity	V-Standard Deviation	UV-Angle Mean
-1.08	-4.79	78.3	3.75	39.1	1.35	26.5
-1.02	-4.79	89.6	2.53	67.4	4.74	36.9
-1.01	-4.79	89	1.61	68	4.53	37.4
-1	-4.79	88.3	1.65	69.2	4	38.1
-.992	-4.79	87	1.75	69.8	3.76	38.7
-.979	-4.79	85.2	1.88	70	3.94	39.4
-.964	-4.79	83.5	1.8	70.9	3.49	40.3
-.948	-4.79	81.3	1.79	71.5	3.24	41.3
-.93	-4.79	79.1	1.89	72	3.05	42.3
-.911	-4.79	76.6	1.72	72.2	2.96	43.3
-.889	-4.79	75.3	1.78	72.7	2.59	44
-.866	-4.79	73.3	1.57	72.6	2.37	44.7
-.84	-4.79	71.2	1.54	72.5	2.42	45.5
-.811	-4.79	69.4	1.6	72.5	2.41	46.3
-.78	-4.79	67.5	1.52	72.2	1.87	46.9
-.745	-4.79	66	1.45	72.4	1.74	47.7
-.707	-4.79	64.2	1.34	71.8	1.66	48.2
-.665	-4.79	62.8	1.27	71.4	1.48	48.6
-.619	-4.79	61	1.25	70.7	1.61	49.2
-.569	-4.79	59.7	1.25	70.4	1.41	49.7
-.513	-4.79	58.4	1.23	69.8	1.32	50.1
-.452	-4.79	57.1	1.19	69.1	1.33	50.5
-.384	-4.79	55.9	1.14	68.9	1.33	50.9
-.31	-4.79	54.7	1.1	68.4	1.2	51.3
-.229	-4.79	53.5	1.07	67.7	1.16	51.7
-.14	-4.79	52.3	1.06	67.3	1.14	52.1
-.041	-4.79	51.2	1.07	66.7	1.17	52.5
.0672	-4.79	50.1	1.09	65.9	1.16	52.7
.186	-4.79	49	1.03	64.9	1.14	52.9
.317	-4.79	47.9	1.03	63.8	1.19	53.1
.462	-4.79	46.6	1.05	62.4	1.21	53.2
.62	-4.79	45.6	1.13	60.8	1.23	53.1
.795	-4.79	44.4	1.22	58.7	1.24	52.9

Velocity in M/SEC
Data is from the following files:
ST2B1209.1,30
STATION 2B PRESSURE SIDE

X(in)	Z(in)	U-Mean Velocity	U-Standard Deviation	V-Mean Velocity	V-Standard Deviation	UV-Angle Mean
1.72	-4.79	33.9	5.91	22.6	7.21	33.7
1.72	-4.79	31.6	4.22	21.5	3.68	34.3
1.72	-4.79	31.3	3.46	20.6	3.62	33.4
1.71	-4.79	34.9	1.95	20.8	2.27	30.7
1.69	-4.79	38	1.89	23.4	1.87	31.6
1.68	-4.79	40.5	1.74	26.2	1.73	32.9
1.67	-4.79	42.3	1.57	28.6	1.74	34.1
1.65	-4.79	43.9	1.42	30.7	1.48	35
1.63	-4.79	45.2	1.3	32.8	1.51	36
1.61	-4.79	46.1	1.17	34.9	1.56	37.1
1.59	-4.79	47	1.15	36.8	1.39	38
1.57	-4.79	47.6	1.05	38.5	1.38	39
1.54	-4.79	48.1	1.05	40.1	1.44	39.8
1.51	-4.79	48.5	1.05	41.6	1.24	40.6
1.48	-4.79	49	.969	43	1.25	41.2
1.45	-4.79	49.3	.98	44.2	1.35	41.9
1.41	-4.79	49.7	.978	45.6	1.21	42.5
1.37	-4.79	50.2	1	46.8	1.19	43
1.32	-4.79	50.5	.961	48	1.3	43.6
1.27	-4.79	50.7	.948	49.3	1.23	44.2
1.22	-4.79	51	.977	50.6	1.18	44.8
1.16	-4.79	51.4	1	51.8	1.19	45.3
1.09	-4.79	51.6	1.01	52.9	1.18	45.7
1.03	-4.79	51.9	1.07	54.1	1.29	46.1
.953	-4.79	52.3	1.13	55.2	1.23	46.5
.872	-4.79	52.7	1.32	56.3	1.17	46.9
.782	-4.79	53.2	1.22	57.4	1.25	47.2
.683	-4.79	53.9	1.54	58.7	1.1	47.5
.585	-4.79	54.5	1.69	60	1.2	47.8
.485	-4.79	56.2	2.35	60.5	.981	47.1

STATION 2

TOTAL VELOCITY

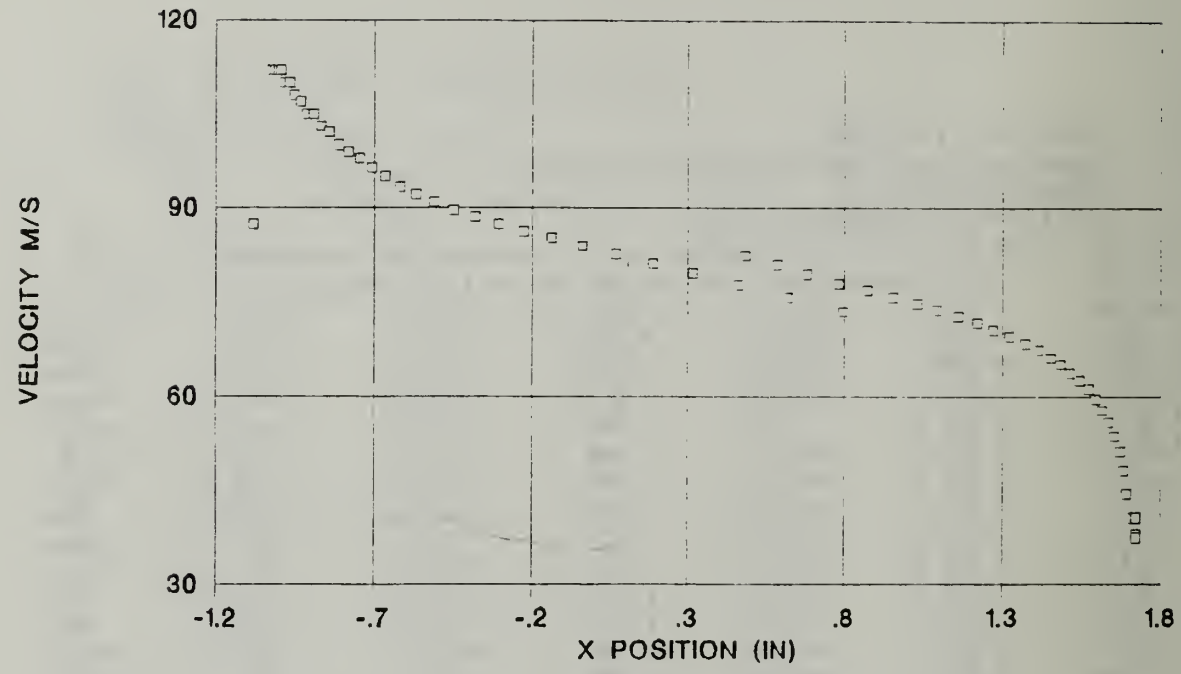

STATION 2

FLOW ANGLE

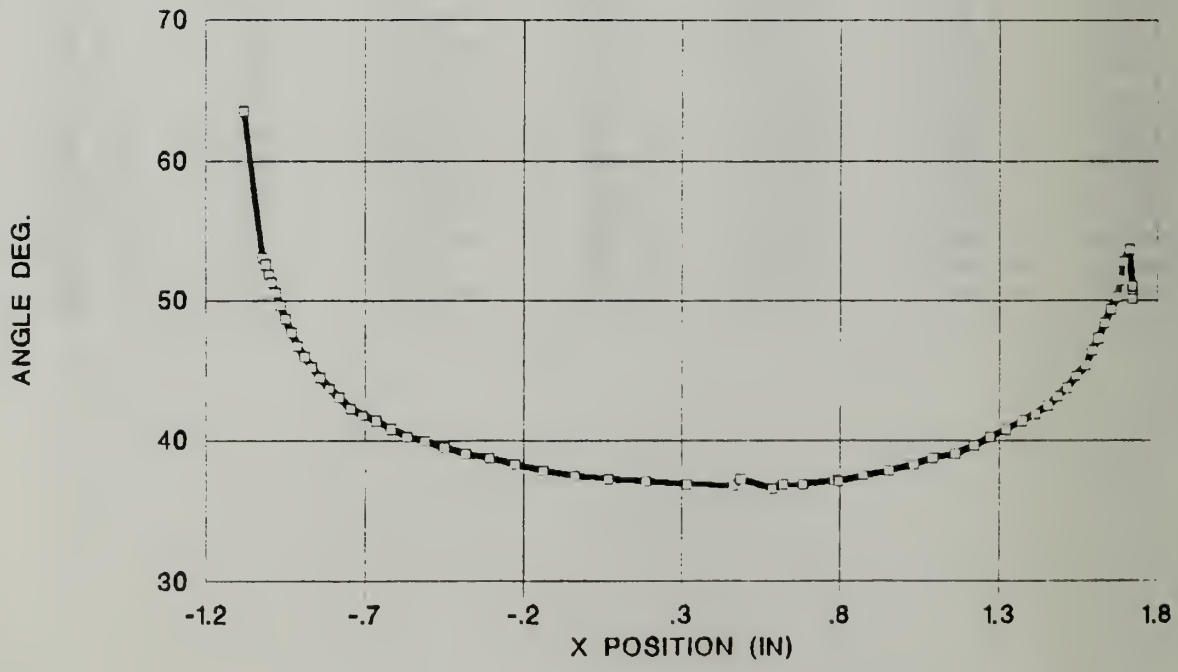

STATION 2

U TURBULENCE INTENSITY

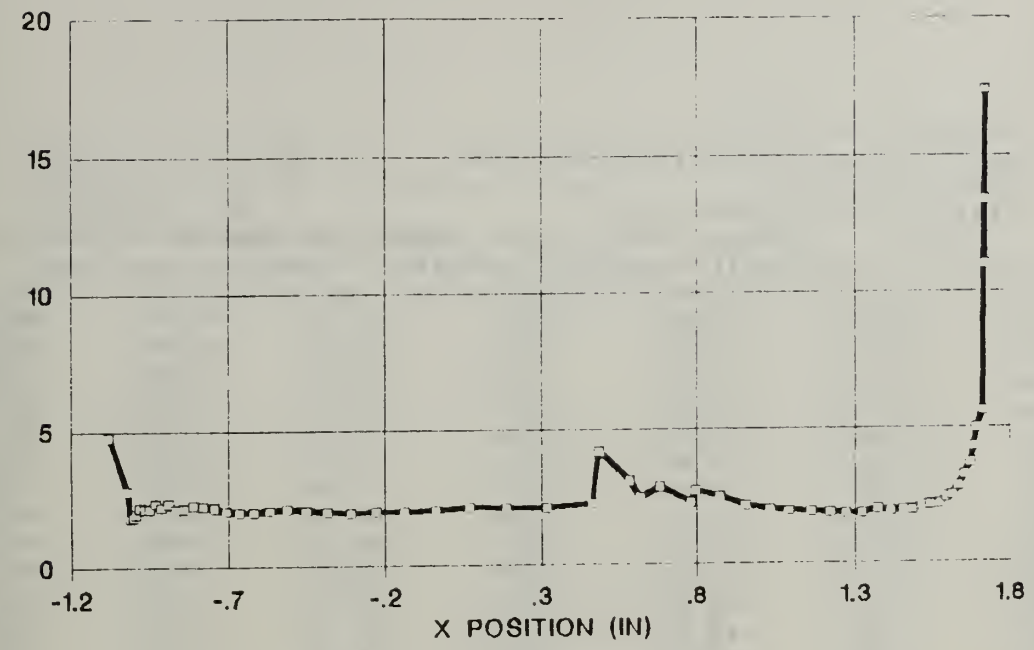

STATION 2

V TURBULENCE INTENSITY

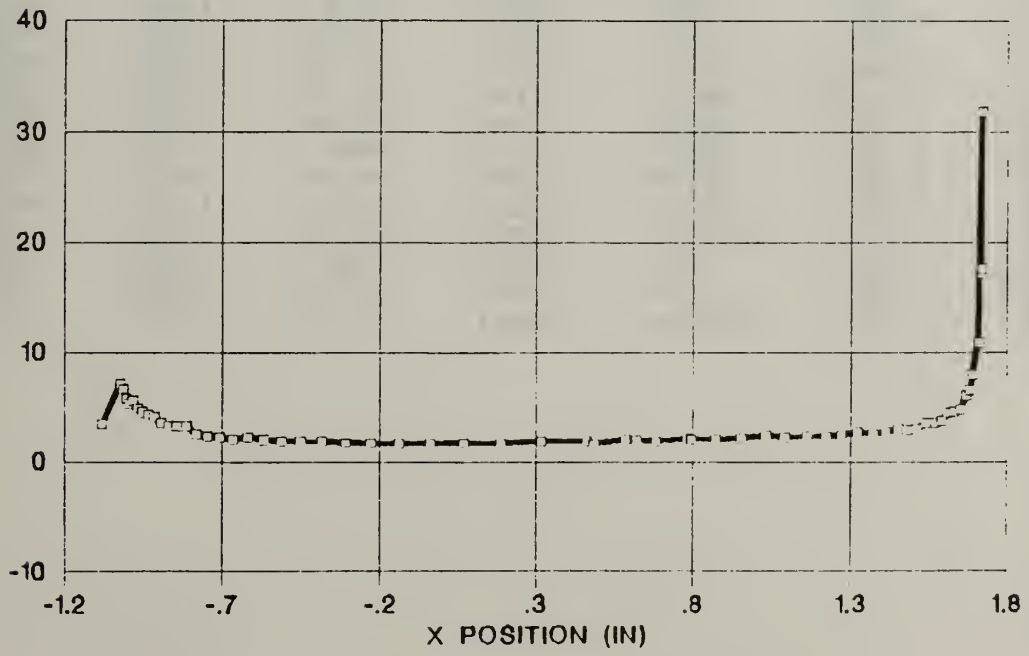

Velocity in M/SEC
Data is from the following files:
ST7A0126,1,31
STATION 7A SUCTION SIDE

X(in)	Z(in)	U-Mean Velocity	U-Standard Deviation	V-Mean Velocity	V-Standard Deviation	UV-Angle Mean
-.169	-3.29	41.8	10.6	58	9.3	54.2
-.164	-3.29	35.7	7.85	60.6	8.14	59.5
-.16	-3.29	43.6	9.57	60.5	8.35	54.2
-.15	-3.29	34.3	4.1	64	8.37	61.8
-.125	-3.29	36.1	4.07	67.7	8.8	61.9
-.101	-3.29	37.5	4.05	71.6	9.03	62.4
-.0837	-3.29	38.5	3.95	73.4	9.35	62.3
-.0642	-3.29	39.8	3.72	76.8	8.75	62.6
-.0428	-3.29	40.1	3.27	79.4	7.84	63.2
-.0192	-3.29	40.7	3.17	81.5	5.89	63.5
.0067	-3.29	40.9	2.47	82.7	4.1	63.7
.0352	-3.29	40.8	2.05	82.9	3.17	63.8
.0667	-3.29	40.5	1.71	82.3	2.66	63.8
.101	-3.29	40.2	1.45	81.9	1.93	63.9
.139	-3.29	39.8	1.39	81.1	2.16	63.8
.181	-3.29	39.3	1.4	80	2.45	63.9
.227	-3.29	38.9	1.35	79	2.97	63.8
.277	-3.29	38.4	1.24	78.2	1.61	63.9
.333	-3.29	38	1.25	77.2	1.39	63.8
.394	-3.29	37.6	1.54	76.2	1.54	63.7
.461	-3.29	37	1.36	75.2	1.66	63.8
.535	-3.29	36.4	1.36	73.9	1.65	63.8
.617	-3.29	35.9	1.16	72.9	1.74	63.8
.706	-3.29	35.2	1.26	71.7	1.44	63.8
.805	-3.29	34.6	1.33	70.4	1.3	63.8
.913	-3.29	33.9	1.08	69.2	1.1	63.9
1.03	-3.29	33.2	1.22	67.9	1.16	63.9
1.16	-3.29	32.4	1.22	66.3	1.2	64
1.24	-3.29	32	1.25	65.4	1.18	64
1.34	-3.29	31.4	1.75	64.3	1.21	64
1.44	-3.29	30.7	1.24	63.3	1.24	64.1

Velocity in M/SEC
Data is from the following files:
ST7B0121.1,30
STATION 7B PRESSURE SIDE

X(in)	Z(in)	U-Mean Velocity	U-Standard Deviation	V-Mean Velocity	V-Standard Deviation	UV-Angle Mean
2.42	-3.29	20.1	1.7	35.4	4.98	60.5
2.41	-3.29	23.6	2.68	40.7	8.56	59.9
2.41	-3.29	24.8	1.29	52.2	4.89	64.6
2.4	-3.29	25	.911	53.5	3.06	64.9
2.4	-3.29	25.2	.833	53.9	1.57	65
2.39	-3.29	25.2	.84	54.1	1.25	65
2.37	-3.29	25.3	.871	54.2	1.24	65
2.36	-3.29	25.4	.882	54.3	1.22	65
2.34	-3.29	25.5	.94	54.5	1.17	64.9
2.33	-3.29	25.7	.945	54.6	1.31	64.8
2.31	-3.29	25.8	.97	54.9	1.19	64.8
2.28	-3.29	25.9	.992	55.1	1.21	64.8
2.26	-3.29	26.1	1.04	55.4	1.16	64.7
2.23	-3.29	26.2	1.02	55.5	1.17	64.7
2.21	-3.29	26.4	1.01	55.8	1.22	64.6
2.17	-3.29	26.6	1.04	56	1.2	64.6
2.14	-3.29	26.8	1.08	56.4	1.14	64.6
2.1	-3.29	27	1.04	56.8	1.15	64.5
2.06	-3.29	27.3	1.07	57.1	1.21	64.5
2.01	-3.29	27.6	1.13	57.4	1.28	64.4
1.96	-3.29	27.9	1.13	58	1.2	64.3
1.91	-3.29	28.2	1.1	58.5	1.22	64.3
1.85	-3.29	28.6	1.16	59	1.19	64.1
1.78	-3.29	29	1.21	59.7	1.15	64.1
1.71	-3.29	29.3	1.17	60.3	1.31	64.1
1.62	-3.29	29.8	1.17	61.1	1.24	64
1.53	-3.29	30.4	1.28	62	1.27	63.9
1.44	-3.29	31	1.22	63	1.21	63.8
1.34	-3.29	31.7	1.26	64.1	1.25	63.7
1.24	-3.29	32.3	1.28	65.2	1.33	63.6

STATION 7

FLOW ANGLE

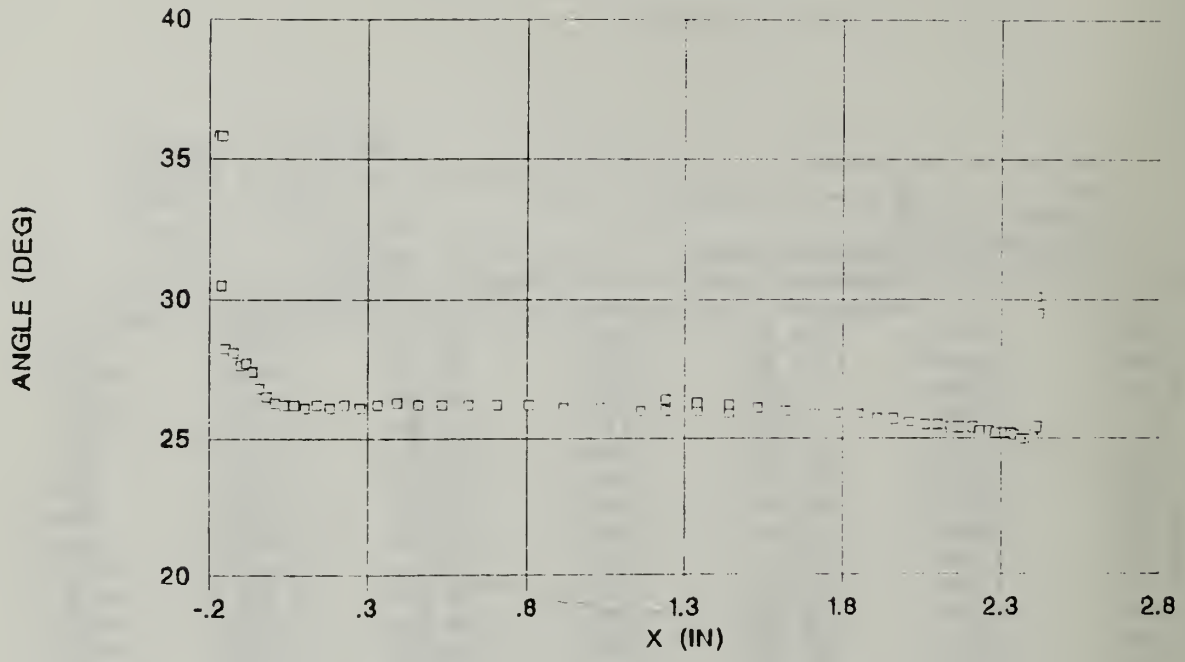

STATION 7

TOTAL VELOCITY

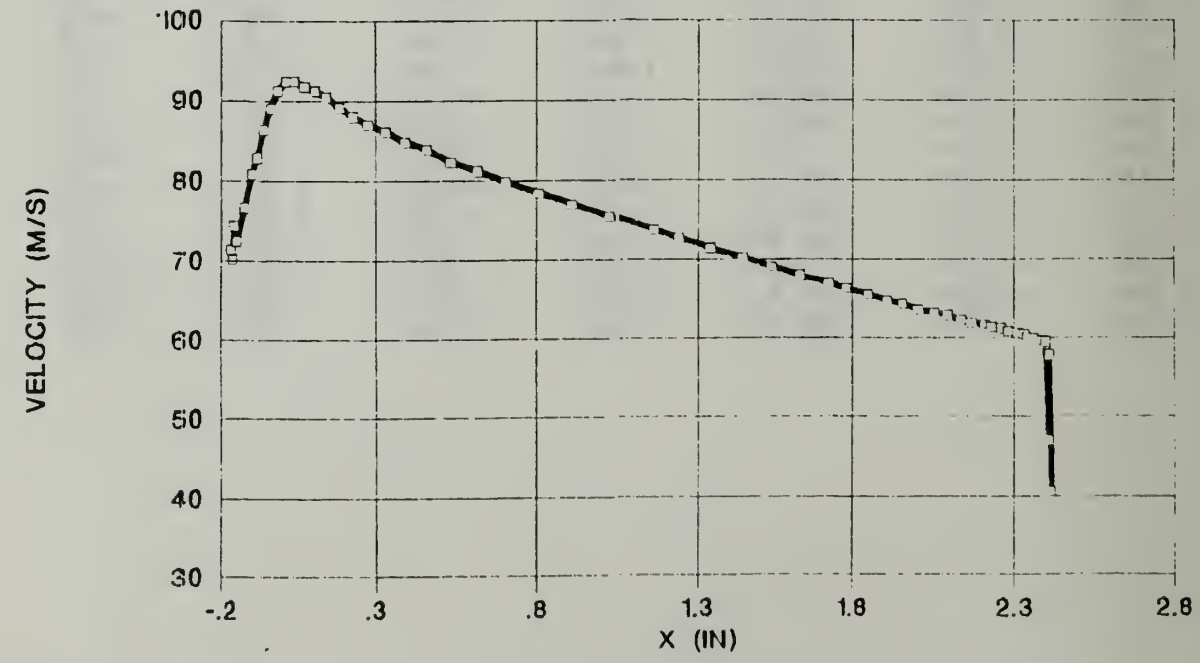

STATION 7

U TURBULENCE INTENSITY

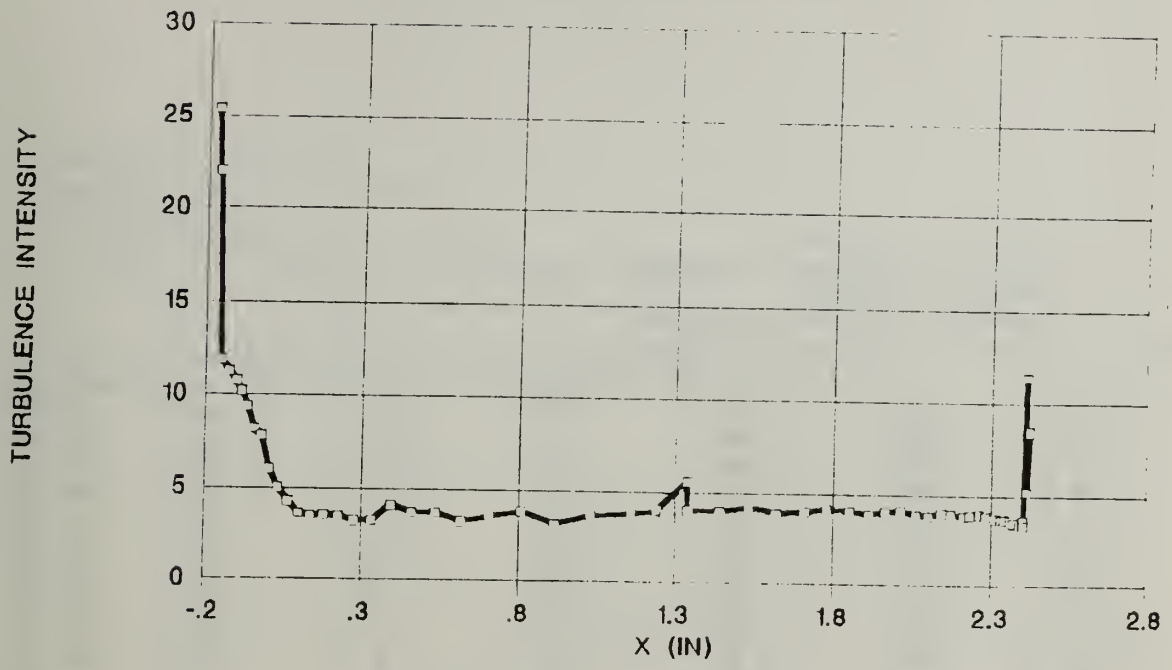

STATION 7

V TURBULENCE INTENSITY

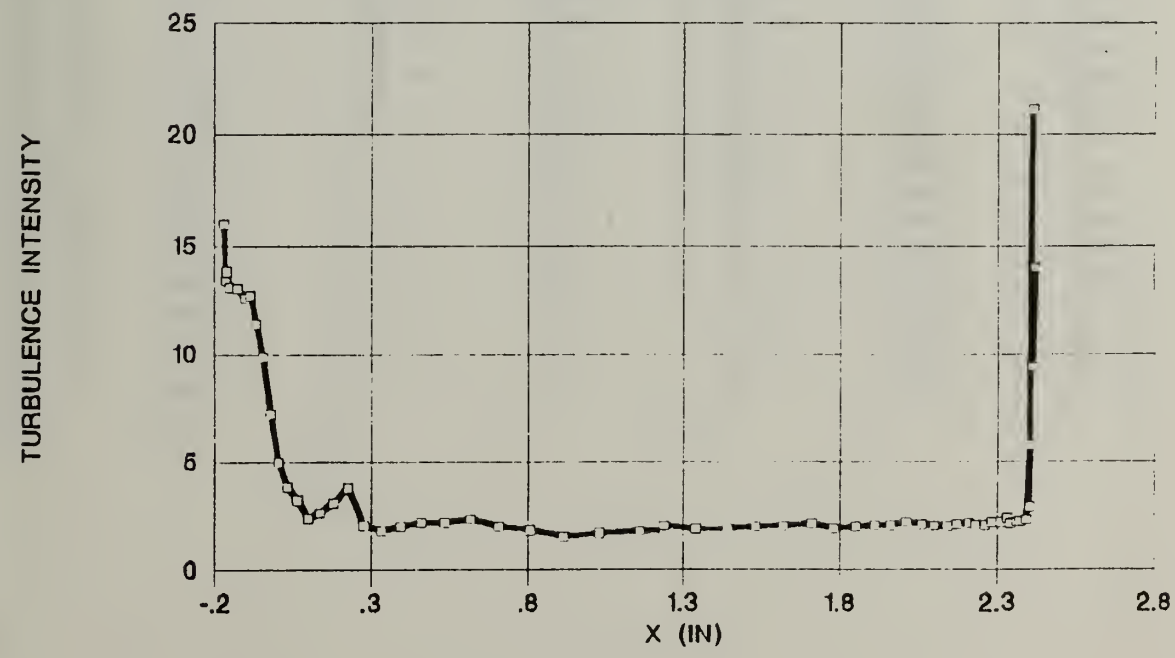

Velocity in M/SEC
Data is from the following files:
S15A1202,1,30
STATION 15 A SUCTION SIDE

X(in)	Z(in)	U-Mean Velocity	U-Standard Deviation	V-Mean Velocity	V-Standard Deviation	UV-Angle Mean
.119	.036	-2.04	.904	24.1	2.66	94.8
.123	.036	-3.04	4	24.2	6.18	97.2
.129	.036	-3.08	4.15	24.6	6.51	97.1
.138	.036	-3.27	4.55	25.6	6.58	97.3
.149	.036	-3.48	4.74	26	6.7	97.6
.162	.036	-3.49	4.92	27.8	7.11	97.2
.175	.036	-3.19	4.96	27.9	6.97	96.5
.19	.036	-3.26	5.16	30.2	7.74	96.2
.206	.036	-3.48	5.21	32	7.97	96.2
.223	.036	-3.8	5.35	34.7	8.58	96.2
.243	.036	-3.67	5.25	37.1	8.9	95.7
.264	.036	-4.01	5.64	40.2	9.04	95.7
.288	.036	-4.13	5.25	44.1	8.68	95.3
.314	.036	-4.1	5.14	47.2	8.06	95
.342	.036	-4.3	5.09	51	7.79	94.8
.374	.036	-4.28	4.51	54.6	7.45	94.5
.408	.036	-4.32	4.59	58.7	7.21	94.2
.446	.036	-4.31	4.08	62.8	6.7	93.9
.488	.036	-4.38	3.49	66.9	4.97	93.7
.534	.036	-4.41	2.83	69.5	3.35	93.6
.584	.036	-4.22	2.19	70.9	2.05	93.4
.64	.036	-3.99	1.73	71.2	1.64	93.2
.701	.036	-3.68	1.36	71.2	1.48	93
.768	.036	-3.43	1.22	71.1	1.42	92.8
.842	.036	-3.17	1.18	70.9	1.4	92.6
.932	.036	-2.86	1.18	70.6	1.34	92.3
1.03	.036	-2.59	1.17	70.4	1.31	92.1
1.13	.036	-2.3	1.2	70.3	1.28	91.9
1.23	.036	-2.11	1.15	69.9	1.53	91.7
1.33	.036	-1.94	1.14	69.7	1.28	91.6

Velocity in M/SEC
Data is from the following files:
S15B1202,1,35
STATION 15B PRESSURE SIDE

X(in)	Z(in)	U-Mean Velocity	U-Standard Deviation	V-Mean Velocity	V-Standard Deviation	UV-Angle Mean
2.92	.0359	6.05	2.71	38.7	8.33	81.1
2.92	.036	7.54	2.91	54.3	7.26	82.1
2.91	.036	7.79	3.05	57.2	6.22	82.2
2.9	.036	8.32	3.13	60.7	5.81	82.2
2.89	.036	8.42	2.91	62.9	5.43	82.4
2.88	.036	8.51	2.66	65.3	4.74	82.6
2.87	.036	8.7	2.2	67.8	4.15	82.7
2.85	.036	8.73	1.8	69.3	2.95	82.8
2.83	.036	8.72	1.4	70.2	1.86	82.9
2.81	.036	8.67	1.16	70.3	1.61	83
2.79	.036	8.78	1.08	70.2	1.4	82.9
2.77	.036	8.77	1.06	70.1	1.23	82.9
2.75	.036	8.8	1.12	69.7	1.34	82.8
2.72	.036	8.79	1.09	69.5	1.19	82.8
2.69	.036	8.93	1.11	69.3	1.23	82.7
2.66	.036	9.02	1.19	69.1	1.37	82.6
2.63	.036	9.11	1.23	68.9	1.44	82.5
2.59	.0359	9.27	1.22	68.8	1.21	82.3
2.55	.036	9.41	1.19	68.5	1.41	82.2
2.5	.036	9.48	1.26	68.4	1.33	82.1
2.45	.0359	9.56	1.28	68.4	1.29	82
2.4	.036	9.8	1.26	68.4	1.24	81.8
2.34	.036	9.88	1.29	68.3	1.27	81.8
2.27	.036	10.1	1.26	68.4	1.32	81.6
2.19	.036	10.1	1.28	68.2	1.23	81.6
2.11	.036	10.2	1.27	68.3	1.26	81.5
2.02	.036	10.4	1.23	68.5	1.25	81.4
1.92	.036	10.4	1.21	68.7	1.35	81.4
1.82	.036	10.3	1.22	68.7	1.34	81.5
1.72	.036	10.4	1.18	68.9	1.19	81.4
1.62	.036	10.3	1.14	69	1.16	81.5
1.52	.036	10.2	1.09	69.1	1.15	81.6
1.42	.036	10.2	1.14	69.3	1.16	81.6
1.32	.036	10.1	1.1	69.5	1.2	81.7
1.22	.036	9.85	1.07	69.6	1.34	81.9

STATION 15

TOTAL VELOCITY

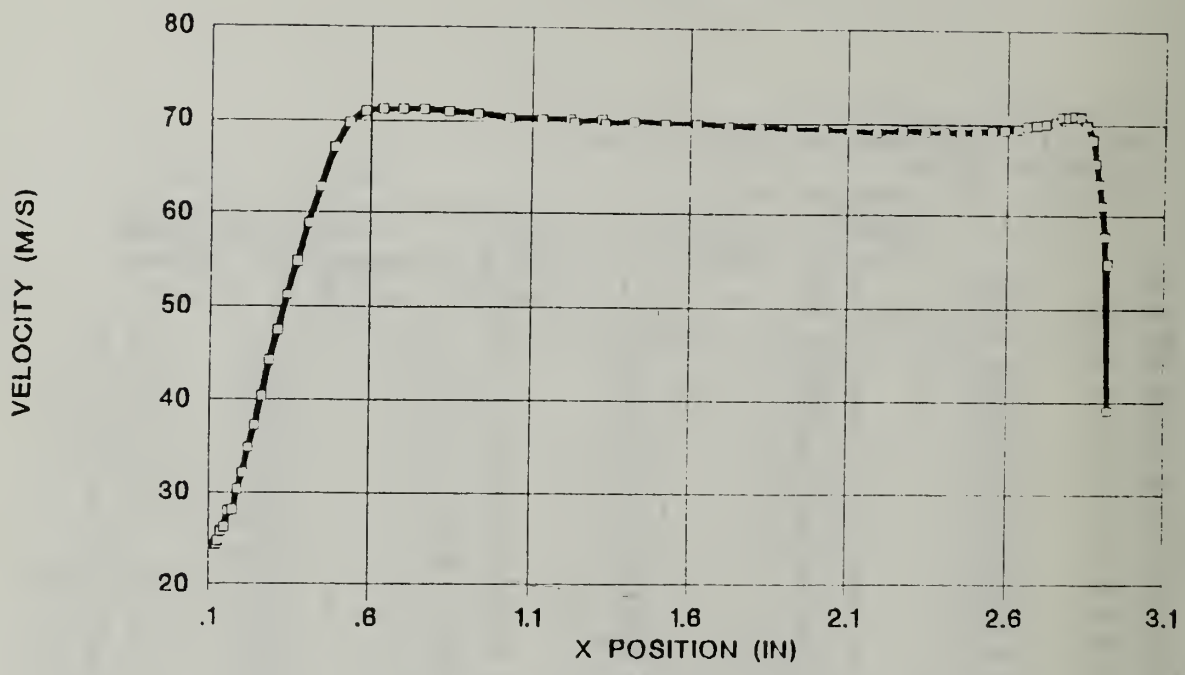

STATION 15

FLOW ANGLE

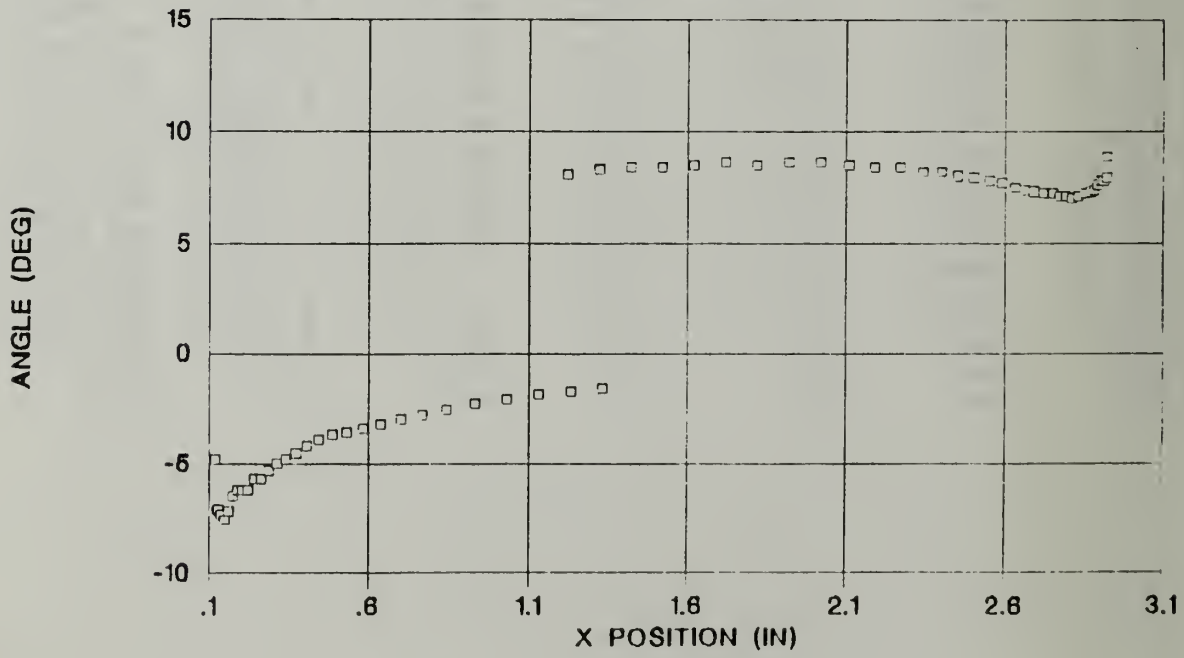

STATION 15

U TURBULENCE INTENSITY

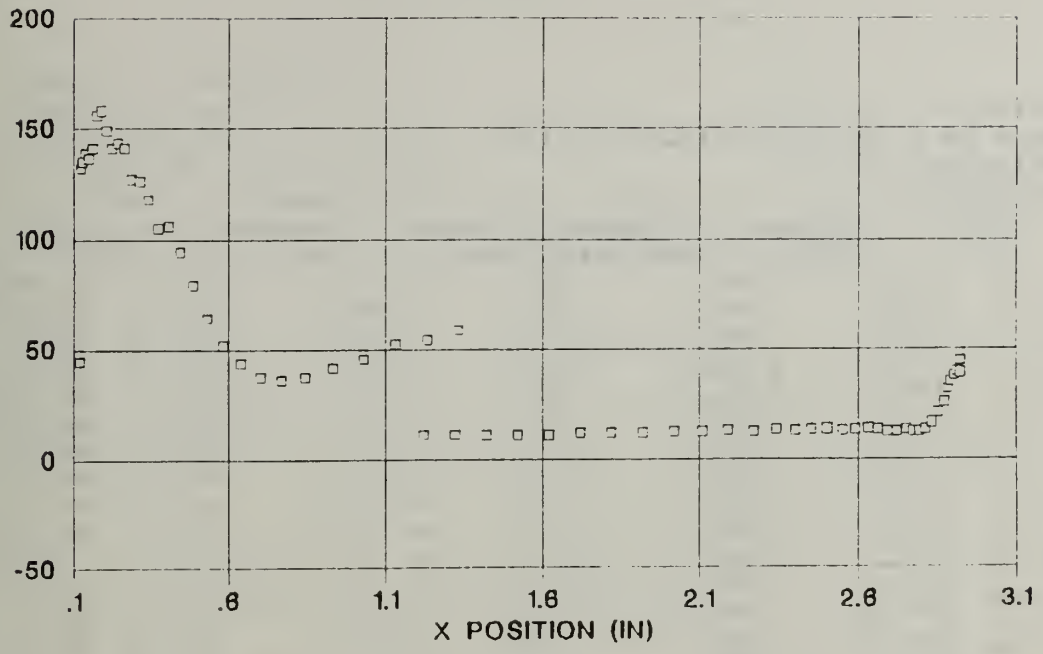

STATION 15

V TURBULENCE INTENSITY

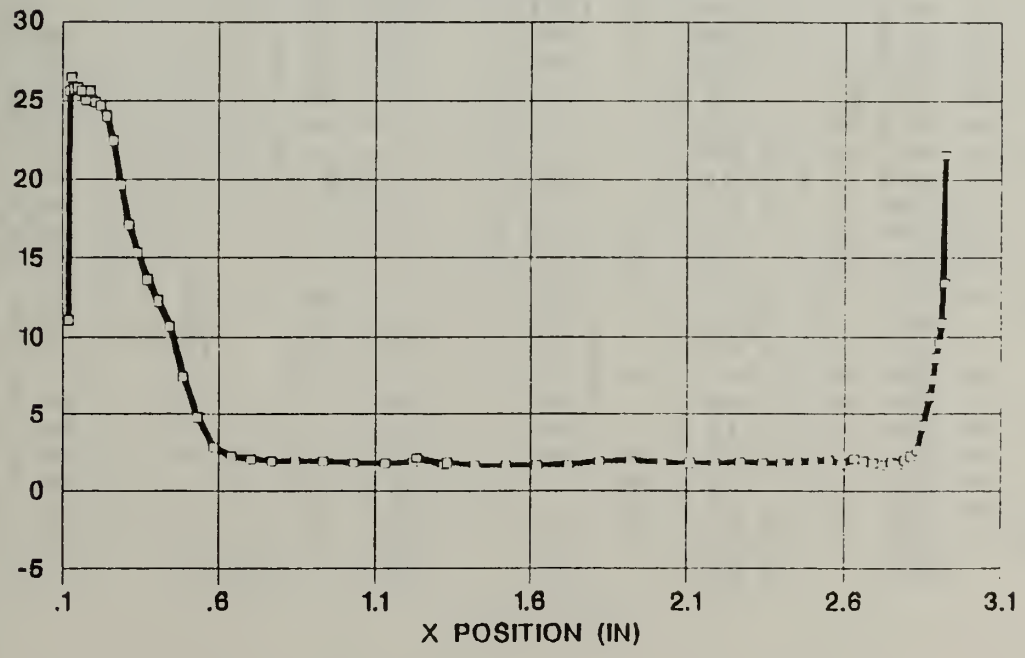

Velocity in M/SEC
Data is from the following files:
ST181207.1,41
STATION 18

X(in)	Z(in)	U-Mean Velocity	U-Standard Deviation	V-Mean Velocity	V-Standard Deviation	UV-Angle Mean
-1	.678	3.64	1.17	67.5	1.31	86.9
-.875	.678	3.66	1.06	67.5	1.4	86.9
-.75	.678	3.78	1.09	67.6	1.37	86.8
-.625	.678	3.82	1.11	67.6	1.56	86.8
-.5	.678	4.01	1.16	67.7	1.43	86.6
-.375	.678	4.14	1.17	67.8	1.26	86.5
-.25	.678	4.28	1.25	67.9	1.36	86.4
-.125	.678	4.68	2.09	67.8	2.56	86.1
.0001	.678	4.64	7.69	38.1	10	83.1
.125	.678	-.398	5.45	24.6	6.5	90.9
.25	.678	-.0235	5.07	35.6	8.03	90
.375	.678	.95	4.37	50.4	7.23	88.9
.5	.678	1.68	3.3	63.4	5.3	88.5
.625	.678	1.87	1.76	68.1	2	88.4
.75	.678	2.09	1.16	68.3	1.77	88.3
.875	.678	2.38	1.09	68.2	1.38	88
1	.678	2.81	1.09	68	1.6	87.6
1.12	.678	3.03	1.08	67.9	1.5	87.4
1.25	.678	3.2	1.03	67.7	1.24	87.3
1.38	.678	3.38	1.02	67.6	1.39	87.1
1.5	.678	3.49	1.01	67.6	1.23	87
1.62	.678	3.68	.992	67.6	1.64	86.9
1.75	.678	3.88	.995	67.6	1.61	86.7
1.87	.678	4.1	1.03	67.6	1.38	86.5
2	.678	4.15	1.06	67.6	1.21	86.5
2.12	.678	3.84	1.17	67.6	1.58	86.7
2.25	.678	3.91	1.22	67.4	1.34	86.7
2.38	.678	4.16	1.19	67.5	1.45	86.5
2.5	.678	4.2	1.13	67.3	1.71	86.4
2.62	.678	4.43	1.18	67.6	1.77	86.3
2.75	.678	4.59	1.16	67.5	1.8	86.1
2.87	.678	5.34	2.57	66.8	3.17	85.4
3	.678	4.67	8.03	31.5	9.13	81.6
3.12	.678	-.476	5.47	24.1	6.5	91.1
3.25	.678	.436	5.05	38.8	9	89.4
3.38	.678	1.45	3.65	57.3	6.65	88.6
3.5	.678	1.64	1.96	67.4	2.28	88.6
3.62	.678	1.8	1	68.3	1.71	88.5
3.75	.678	2.23	.976	68.6	1.36	88.1
3.87	.678	2.54	1.03	68.6	1.52	87.9
4	.678	2.62	1.1	68.5	1.47	87.8

Velocity in M/SEC
Data is from the following files:
ST18SUCK,1,41
STATION 18 HIGH SUCTION

X(mm)	Z(mm)	U-Mean Velocity	U-Standard Deviation	V-Mean Velocity	V-Standard Deviation	UV-Angle Mean
-25.4	17.2	3.6	1.16	66.3	2.96	86.9
-22.2	17.2	3.87	1.19	67.7	2.62	86.7
-19	17.2	3.95	1.26	68	2.79	86.7
-15.9	17.2	4.08	1.34	68.1	2.82	86.6
-12.7	17.2	4.16	1.49	68	2.92	86.5
-9.52	17.2	4.15	1.47	68	3.17	86.5
-6.35	17.2	4.4	1.47	67.9	3.11	86.3
-3.17	17.2	6.53	3.06	62.7	7.15	84.1
0	17.2	4.69	9.07	22.7	7.24	78.3
3.17	17.2	-.586	4.81	21.4	6.95	91.6
6.35	17.2	1.95	4.38	39	9.06	87.1
9.52	17.2	3.39	3.64	56.5	7.16	86.6
12.7	17.2	1.78	1.92	67	3.35	88.5
15.9	17.2	1.3	1.26	67.8	2.57	88.9
19	17.2	1.61	.963	67.7	3.62	88.6
22.2	17.2	1.96	.941	68	2.81	88.3
25.4	17.2	2.19	.954	68	3.29	88.2
28.6	17.2	2.65	1.24	68.3	2.67	87.8
31.7	17.2	2.91	1.03	68.1	3.49	87.6
34.9	17.2	3.27	1.11	68.1	3.3	87.3
38.1	17.2	3.39	1.21	68.3	3.04	87.2
41.3	17.2	3.63	1.29	68.1	3.04	86.9
44.5	17.2	3.77	1.3	67.9	3.78	86.8
47.6	17.2	3.95	1.38	67.9	3.52	86.7
50.8	17.2	4.02	1.36	67.8	3.3	86.6
54	17.2	3.96	1.33	67.5	3.47	86.6
57.2	17.2	4.03	1.33	67.5	3.35	86.6
60.3	17.2	3.8	1.22	67	3.77	86.8
63.5	17.2	3.69	1.21	67.1	3.32	86.9
66.7	17.2	3.8	1.18	67.1	2.93	86.8
69.8	17.2	4.36	1.36	67.2	3.13	86.3
73	17.2	7.56	4.11	57.5	8.55	82.5
76.2	17.2	2.96	8.44	21	6.3	82
79.4	17.2	.362	4.56	28.4	7.98	89.3
82.6	17.2	2.3	3.81	46.3	7.31	87.2
85.7	17.2	3.91	3.33	59.9	6.65	86.3
88.9	17.2	1.76	1.89	67.9	3.36	88.5
92.1	17.2	1.58	1.1	68.2	3.7	88.7
95.2	17.2	1.8	1.16	68.1	3.62	88.5
98.4	17.2	2.19	1.19	68.2	3.58	88.2
102	17.2	2.43	1.14	68.2	2.8	88

STATION 18

FLOW ANGLE

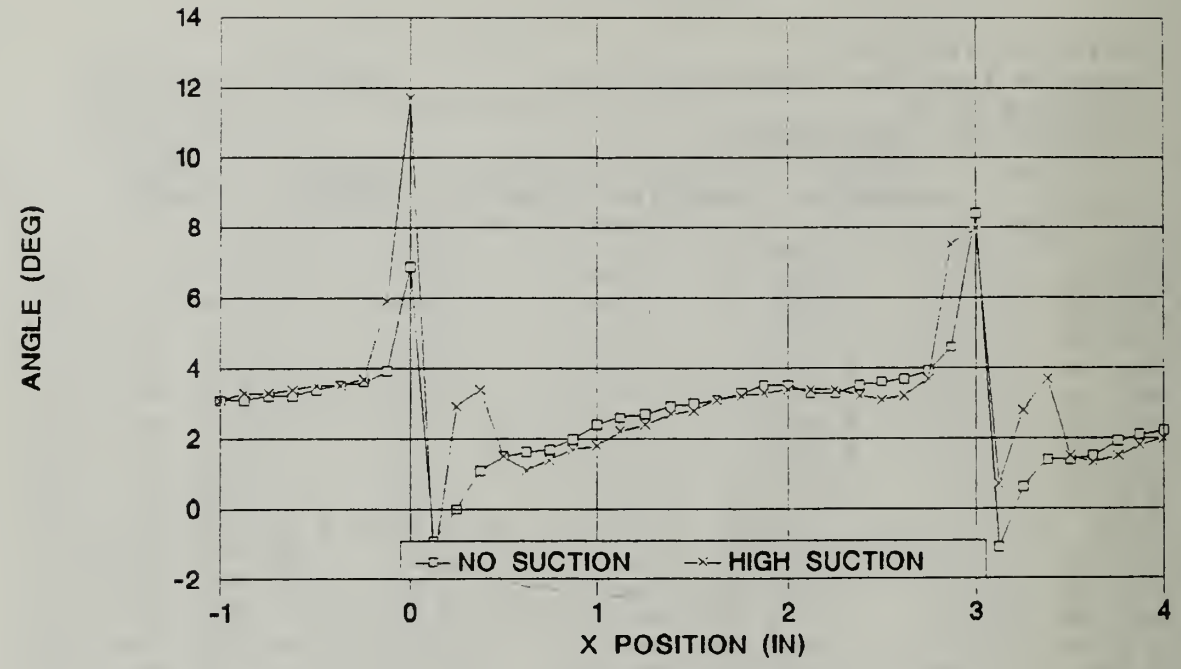

STATION 18

U TURBULENCE INTENSITY

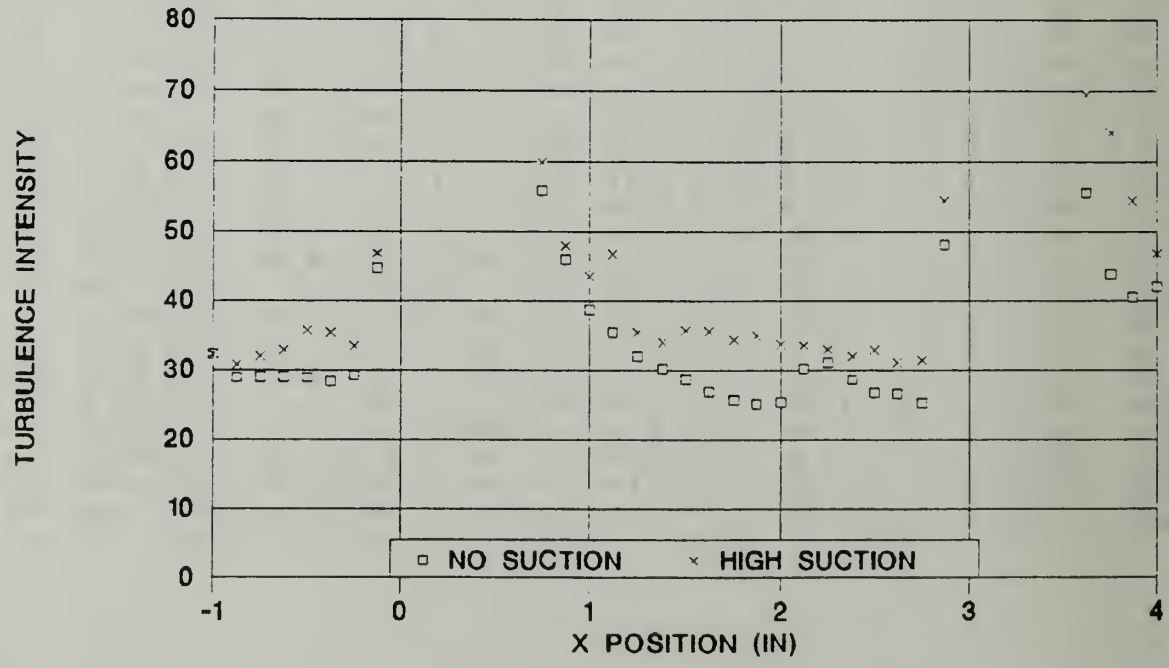

STATION 18

V TURBULENCE INTENSITY

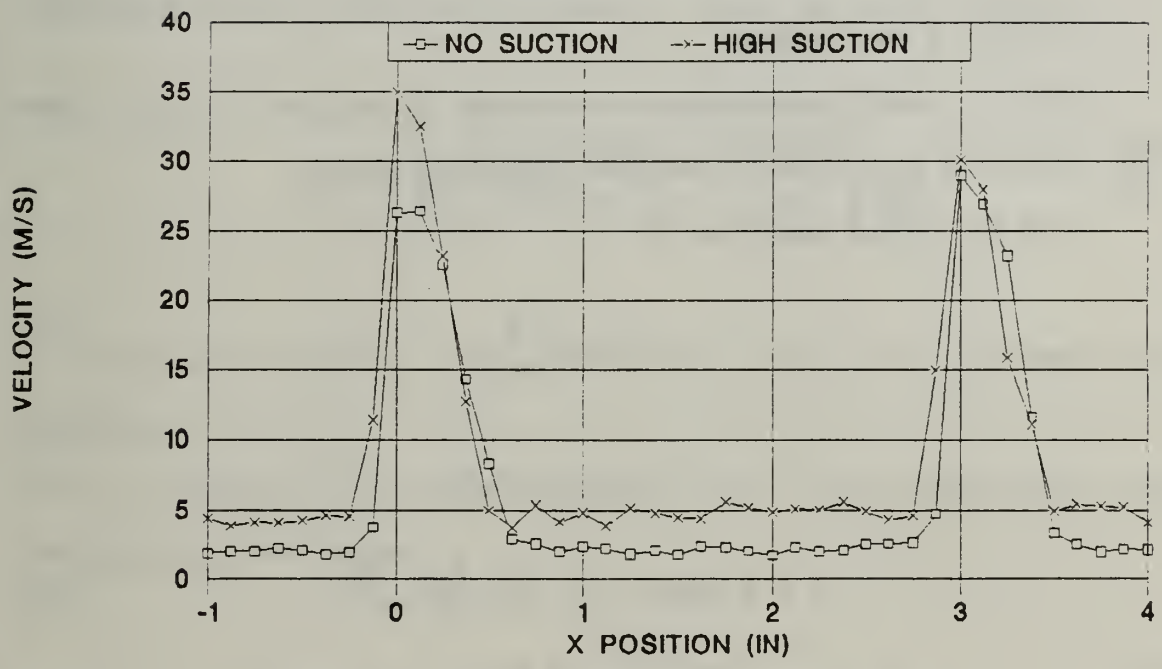

APPENDIX B. DATA REDUCTION

This Appendix contains the following:

1. All equations used for the calculations in this document.

2. The output of V_{ref} calculations for the LDV data and program.

B1. LIST OF EQUATIONS

The following equations were used to reduce all data taken by the rake probe and the instrumented blade.

For all rake surveys:

$$C_p = \frac{P_{T\,i}}{P_{T\,\max}} \tag{1}$$

$$Q = P_{T\,12} - P_{s\,9} \tag{2}$$

$$\alpha = 0.0805 + 31.575\frac{P_{10} - P_{11}}{Q} \tag{3}$$

$$P_{s\ corrected} = P_s - (0.412 + 0.1817Q) \tag{4}$$

where numbered subscripts indicated probe number of the rake. The α and corrected P_s derivations are described in Appendix C.

The computation of the displacement thickness comes from the definition:

$$\delta^* = \int \left(1 - \frac{u}{U} \right) dy \qquad (5)$$

For the rake probe, the integration interval was taken from the endwall to pressure port 8 for the north and 12 for the south, a total of three inches span for each. This resulted in the following equation for the north endwall:

$$\delta^* = \int \left[1 - \sqrt{\frac{\left[\frac{C_{P\,i}}{C_{P\,8}} * P_{T\,\max} \right] - P_s}{Q}} \right] dy \qquad (6)$$

The integration was performed using the trapezoidal method.

To compute the axial velocity ratio, the definition from Reference 1 was used:

$$AVR = \int_0^s \frac{C_{z\,2}}{C_{z\,1}}\, dx \qquad (7)$$

where c_z is the axial velocity at the upstream, (1), and downstream, (2), locations and **s** is one blade space, (3 in.). Because of this definition and since the analysis was done for the incompressible case, the local velocity and flow angle measured by the rake probe was used and corrected for by the

Prandtl total pressure to compensate for the run-to-run variations. This yielded the following equation:

$$AVR = \int \frac{\sqrt{((P_{12} - P_s) * \frac{2}{\rho})_2}}{\sqrt{((P_{12} - P_s) * \frac{2}{\rho})_1}} * \sqrt{\frac{P_{T1}}{P_{T2}}} * \frac{Cos(\beta_2)}{Cos(\beta_1)} \, dx \quad (8)$$

where P_T is the corresponding Prandtl total pressure and P_s is from Equation (4). This integration was performed by a summation since the interval was held constant. ß was measured with the following equation:

$$\beta = \beta_{rake} + \alpha \quad (9)$$

where $ß_{rake}$ is the angle the rake probe was mounted in the tunnel, which was 46° for upstream and 90° for downstream, and α is from Equation (3).

The instrumented blade pressure coefficients were computed as follows:

$$C_p = \frac{P_i - P_\infty}{(P_T - P_s)_{Prandtl}} \quad (10)$$

where P_i was the instrumented blade pressure tap number.

B2. V_{ref} COMPUTATION AND PROGRAM

The method for the calculation of V_{ref} came from Elazar [Ref. 9]. The program was written by Garth V. Hobson.

```
CCCCCCCCCCCCCCCCCCCCCCCCCCCCCCCCCCCCCCCCCCCCCCCCCCCCCCCCCCCCCCCCCCCCCCCCC
C                                                                       C
C                    OUTPUT FROM PROGRAM CALIBRATE                      C
C                                                                       C
CCCCCCCCCCCCCCCCCCCCCCCCCCCCCCCCCCCCCCCCCCCCCCCCCCCCCCCCCCCCCCCCCCCCCCCCC

    LEAST SQUARES STRAIGHT LINE CURVE FIT IS USED
    TO DETERMINE TUNNEL CHARACTERISTICS AT DIFFERENT SPEEDS

    NEWTON S METHOD IS USED TO DETERMINE THE REFERENCE VELOCITY
    FROM THE RECORDED AMBIENT PRESSURE AND TUNNEL PLENUM
    PRESSURE AND TEMPERATURE


BEGIN DETERMINING TUNNEL CHARACTERISTICS
FROM THE FOLLOWING MEASURED VALUES

  AXIAL VEL.          TANGENTIAL VEL.    AMBIENT PRESS.    PLENUM PRESS.    PLENUM TEMP
  M PER SEC.            M PER SEC.       INCHES MERCURY    INCHES WATER      DEG. C.

   53.8110              52.7380            29.9720           8.7000          22.2222
   55.3740              54.4480            29.9700           9.2000          21.6667
   58.4540              57.1400            29.8000          10.4000          22.2222
   60.5060              58.5120            29.9720          11.0000          22.2222
   63.4800              61.1880            29.7500          12.0000          22.2222
   68.0540              66.2070            29.7500          13.9000          22.2222

   CALCULATED VALUES FOR THE TUNNEL CONFIGURATION

  TOTAL VALOCITY        MACH NUMBER             MACH NUMBER FUNCT.    PRESSURE RATIO

  0.753453406979E+02    0.977836427162E-01    0.326715018199E-01    0.218408577690E-01
  0.776586413740E+02    0.100880761990E+00    0.347199174350E-01    0.230686291720E-01
  0.817425820240E+02    0.106086021530E+00    0.382707331870E-01    0.261437708500E-01
  0.841702452180E+02    0.109236657630E+00    0.405294780690E-01    0.274563444120E-01
  0.881684849820E+02    0.114425597580E+00    0.443409258440E-01    0.300940438870E-01
  0.949458464860E+02    0.123221298680E+00    0.511479122300E-01    0.346936228630E-01

          CALLING LEAST SQUARES SUBROUTINE
TO DETERMINE THE PRESSURE RATIO AS A FUNCTION OF MACH NO. PARAM

PRESSURE RATIO = A1 * ANUX + A0


    MATRIX EQUATION

       0.60E+01     0.16E+00 A0      0.24E+00
       0.16E+00     0.46E-02 A1      0.67E-02

      A1 =     0.148012775550E+01    A0 =    -0.267131435600E-07

REFERENCE CONDITIONS FOR EACH RUN
AMBIENT PRESSURE   PLENUM PRESSURE   PLENUM TEMPERATURE   RUN NAME
 INCHES MERCURY     INCHES WATER      DEGREES CELSIUS

     30.0550         10.4000          17.4444             ST1SUCK.PRN
     30.0600         10.6000          21.3889             ST1BSUCK.PRN

 I =   1
 PRESSURE RATIO =     0.02593 MACH NUMBER PARAMETER =    0.3838E 01
 RUN NAME =  . ST1SUCK.PRN


         BEGIN NEWTON ITERATION

 ITERATION NUMBER  1   MACH NO. PARAM. = 0.114967      ERROR TERM =    0.8468E-02
 ITERATION NUMBER  2   MACH NO. PARAM. = 0.106497      ERROR TERM =    0.2709E-03
 ITERATION NUMBER  3   MACH NO. PARAM. = 0.106208      ERROR TERM =    0.3518E-06
 ITERATION NUMBER  4   MACH NO. PARAM. = 0.106208      ERROR TERM =    0.5149E-12

 VREF =         81.45063904852

 I =   2
 PRESSURE RATIO =     0.02641 MACH NUMBER PARAMETER =    0.3709E 01
 RUN NAME =    ST1BSUCK.PRN


         BEGIN NEWTON ITERATION

 ITERATION NUMBER  1   MACH NO. PARAM. = 0.114587      ERROR TERM =    0.7163E-02
 ITERATION NUMBER  2   MACH NO. PARAM. = 0.107483      ERROR TERM =    0.2065E-03
 ITERATION NUMBER  3   MACH NO. PARAM. = 0.107218      ERROR TERM =    0.1752E-06
 ITERATION NUMBER  4   MACH NO. PARAM. = 0.107218      ERROR TERM =    0.1261E-12

 VREF =         82.49811318969

 EXPERIMENT NUMBER     REFERENCE VELOCITY     NAME

        1                    81.4506          ST1SUCK.PRN
        2                    82.4981          ST1BSUCK.PRN
```

```
CCCCCCCCCCCCCCCCCCCCCCCCCCCCCCCCCCCCCCCCCCCCCCCCCCCCCCCCCCCCCCCCCCCCCCCCCCCCCCCCCCCCCC
C                                                                                    C
C                        OUTPUT FROM PROGRAM CALIBRATE                               C
C                                                                                    C
CCCCCCCCCCCCCCCCCCCCCCCCCCCCCCCCCCCCCCCCCCCCCCCCCCCCCCCCCCCCCCCCCCCCCCCCCCCCCCCCCCCCCC

     LEAST SQUARES STRAIGHT LINE CURVE FIT IS USED
     TO DETERMINE TUNNEL CHARACTERISTICS AT DIFFERENT SPEEDS

     NEWTON S METHOD IS USED TO DETERMINE THE REFERENCE VELOCITY
     FROM THE RECORDED AMBIENT PRESSURE AND TUNNEL PLENUM
     PRESSURE AND TEMPERATURE


BEGIN DETERMINING TUNNEL CHARACTERISTICS
FROM THE FOLLOWING MEASURED VALUES

   AXIAL VEL.          TANGENTIAL VEL.   AMBIENT PRESS.   PLENUM PRESS.   PLENUM TEMP.
   M PER SEC.            M PER SEC.      INCHES MERCURY   INCHES WATER     DEG. C.

    35.7320             32.5860            29.8700            4.3500          16.1111
    42.8170             39.0550            29.8900            6.1000          16.6667
    48.7490             44.4860            29.8900            8.0000          17.2222
    56.0220             53.9310            29.8900           10.3000          17.7778
    60.6650             55.0180            29.8900           12.1000          18.3333
    66.0340             57.7400            29.8900           14.3000          18.8889
    CALCULATED VALUES FOR THE TUNNEL CONFIGURATION

   TOTAL VALOCITY         MACH NUMBER             MACH NUMBER FUNCT.      PRESSURE RATIO

  0.48359313684E+02    0.63420487565E-01     0.13936425209E-01     0.11070955920E-01
  0.57953330482E+02    0.75929610932E-01     0.19888987657E-01     0.15455950541E-01
  0.65995978643E+02    0.86384226528E-01     0.25633301353E-01     0.20172983332E-01
  0.77762569691E+02    0.10168865418E+00     0.35263665072E-01     0.25822749833E-01
  0.81897634575E+02    0.10699390568E+00     0.38930076621E-01     0.30199415978E-01
  0.89046935691E+02    0.11622328940E+00     0.45697080117E-01     0.35495321071E-01
          CALLING LEAST SQUARES SUBROUTINE
TO DETERMINE THE PRESSURE RATIO AS A FUNCTION OF MACH NO. PARAM

PRESSURE RATIO = A1 * ANUX + A0


    MATRIX EQUATION

        0.60E+01     0.14E+00 A0       0.18E+00
        0.14E+00     0.36E-02 A1       0.47E-02

         A1 =     0.12975874005E+01    A0 =     0.25001140871E-02

REFERENCE CONDITIONS FOR EACH RUN
AMBIENT PRESSURE   PLENUM PRESSURE    PLENUM TEMPERATURE   RUN NAME
 INCHES MERCURY     INCHES WATER       DEGREES CELSIUS

      30.0500          12.1000             23.3300               S11A1209.PRN
      29.7600          11.9000             17.7778               S11B1207.PRN
   I =    1
   PRESSURE RATIO =     0.03004 MACH NUMBER PARAMETER =    0.3898E-01
   RUN NAME =    S11A1209.PRN


           BEGIN NEWTON ITERATION

   ITERATION NUMBER  1  MACH NO. PARAM. = 0.106008     ERROR TERM =   0.9857E-03
   ITERATION NUMBER  2  MACH NO. PARAM. = 0.107074     ERROR TERM =   0.4010E-05
   ITERATION NUMBER  3  MACH NO. PARAM. = 0.107070     ERROR TERM =   0.6620E-10
   VREF =          82.6555082634

   I =    2
   PRESSURE RATIO =     0.02984 MACH NUMBER PARAMETER =    0.3872E-01
   RUN NAME =    S11B1207.PRN


           BEGIN NEWTON ITERATION

   ITERATION NUMBER  1  MACH NO. PARAM. = 0.107096     ERROR TERM =   0.3972E-03
   ITERATION NUMBER  2  MACH NO. PARAM. = 0.106699     ERROR TERM =   0.6517E-06
   ITERATION NUMBER  3  MACH NO. PARAM. = 0.106698     ERROR TERM =   0.1756E-11
   VREF =          81.59340572006

   EXPERIMENT NUMBER     REFERENCE VELOCITY     NAME

          1                    82.6555              S11A1209.PRN
          2                    81.5934              S11B1207.PRN
```

```
C-----------------------------------------------------------------------
C
C     PROGRAM TO COMPUTE THE CALIBRATION CURVE FOR THE HPS LOW SPEED
C     CASCADE WIND TUNNEL.
C
C-----------------------------------------------------------------------
C
C     A STRAIGHT LINE IS FITTED THROUGH THE REFERENCE CONDITIONS OF
C     THE TUNNEL AT DIFFERENT SPEEDS.
C
C     THE REFERENCE VELOCITY IS THEN OBTAINED, BY NEWTON'S METHOD,
C     DEPENDING ON THE TUNNEL PLENUM PRESSURE AND TEMPERATURE
C
C-----------------------------------------------------------------------
      PROGRAM CALIBRATE
      IMPLICIT REAL*8(A-H,O-Z)
      PARAMETER (NP=6)
      DIMENSION VA(NP),VT(NP),PA(NP),PP(NP),TP(NP)
      DIMENSION VTOT(NP),X(NP),ANUX(NP),PR(NP)
      DIMENSION PAR(100),APR(100),TPR(100),PRR(100),ANUXR(100)
      DIMENSION VREF(100)
      CHARACTER*14 NAME(100)
C
      OPEN(UNIT=10,FILE='CALIB.DAT',STATUS='UNKNOWN')
      OPEN(UNIT=11,FILE='REFER.DAT',STATUS='UNKNOWN')
      OPEN(UNIT=12,FILE='CALIB.DOT',STATUS='UNKNOWN')
C
      PRINT BANNER
C
C
C                 VA = AXIAL VELOCITY              - MEASURED BY LDV (M/S)
C                 VT = TANGENTIAL VELOCITY         - MEASURED BY LDV (M/S)
C                 PA = AMBIENT PRESSURE                    (INCHES MERCURY)
C                 PP = PLENUM PRESSURE                       (INCHES WATER)
C                 TP = PLENUM STAGNATION TEMPERATURE                (DEG. C.)
C
      DO 1 I=1,NP
         READ(10,100)VA(I),VT(I),PA(I),PP(I),TP(I)
         WRITE(*,110)VA(I),VT(I),PA(I),PP(I),TP(I)
         WRITE(12,110)VA(I),VT(I),PA(I),PP(I),TP(I)
    1 CONTINUE
  100 FORMAT(1X,5F8.4)
  110 FORMAT(3X,F8.4,7X,F8.4,8X,F8.4,7X,F8.4,7X,F8.4)
C
C     CALC VTOT, X, ANUX AND PR
C
      WRITE(*,510)
      WRITE(12,510)
  510 FORMAT(//5X,'CALCULATED VALUES FOR THE TUNNEL CONFIGURATION',//,
     #3X,'TOTAL VELOCITY',6X,'MACH NUMBER',9X,'MACH NUMBER FUNCT.',3X,
     #'PRESSURE RATIO'//)
C
      DO 2 I=1,NP
         VTOT(I)=DSQRT(VA(I)**2+VT(I)**2)
         X(I)=VTOT(I)/DSQRT(2.D0*CPA*(TP(I)+273.16D0))
         ANUX(I)=(GAMMA/GM1)*(X(I)**2)*(1.D0-(X(I)**2))**(1.D0/(GM1))
         PR(I)=1.D0-(RHOHG*PA(I))/(RHOW*PP(I)+RHOHG*PA(I))
         WRITE(*,101)VTOT(I),X(I),ANUX(I),PR(I)
         WRITE(12,101)VTOT(I),X(I),ANUX(I),PR(I)
    2 CONTINUE
  101 FORMAT(4D20.11)
C
C     CALL THE LEAST SQUARES SUBROUTINE TO FIT A STRAIGHT LINE THROUGH THE
C     DATA; X-AXIS = PR, Y-AXIS = ANUX (MACH NO. PARAMETER)
C
      WRITE(*,520)
      WRITE(12,520)
  520 FORMAT(//10X,'CALLING LEAST SQUARES SUBROUTINE',//1X,
     #'TO DETERMINE THE PRESSURE RATIO AS A FUNCTION OF MACH NO. PARAM'
     #//1X,'PRESSURE RATIO = A1 * ANUX + A0',//)
C
      CALL LEASTSQUARE(NP,PR,ANUX,A0,A1)
C
      WRITE(*,530)A1,A0
      WRITE(12,530)A1,A0
  530 FORMAT(//10X,'A1 = ',D20.11,'    A0 = ',D20.11//)
C
C     READ IN REFERENCE CONDITIONS
C
      WRITE(*,199)
      WRITE(12,199)
  199 FORMAT(//1X,'REFERENCE CONDITIONS FOR EACH RUN'//
     #1X,'AMBIENT PRESSURE   PLENUM PRESSURE   PLENUM TEMPERATURE',
     #3X,'RUN NAME'/
     #1X,'  INCHES MERCURY      INCHES WATER       DEGREES CELSIUS'//)
C
C     THE NUMBER OF EXPERIMENTS
C
      READ(11,198)NE
  198 FORMAT(1X,I3)
C
C     THE REFERENCE CONDITIONS
```

```
      WRITE(*,500)
      WRITE(12,500)
  500 FORMAT(1X,78('C'),/1X,'C',76X,'C'/
     #1X,'C',20X,'OUTPUT FROM PROGRAM CALIBRATE',27X,'C'/1X,'C',76X,'C'/
     #1X,78('C')//
     #5X,'LEAST SQUARES STRAIGHT LINE CURVE FIT IS USED'/
     #5X,'TO DETERMINE TUNNEL CHARACTERISTICS AT DIFFERENT SPEEDS'//
     #5X,'NEWTON S METHOD IS USED TO DETERMINE THE REFERENCE VELOCITY'/
     #5X,'FROM THE RECORDED AMBIENT PRESSURE AND TUNNEL PLENUM'/
     #5X,'PRESSURE AND TEMPERATURE'/)
C
C     INITIALIZE AIR, MERCURY AND WATER PROPERTIES
C
      RHOW=1000.D0
      RHOHG=13000.D0
      RHOA=1.22560D0
      CPA=1005.D0
      GAMMA=1.4D0
      GM1=GAMMA-1.D0
C
C     BEGIN DETERMINING TUNNEL CHARACTERSTICS
C
      WRITE(*,501)
      WRITE(12,501)
  501 FORMAT(//1X,'BEGIN DETERMINING TUNNEL CHARACTERISTICS',
     #1X,'FROM THE FOLLOWING MEASURED VALUES',//
     #3X,'AXIAL VEL.               TANGENTIAL VEL.    AMBIENT PRESS.'
     #3X,'PLENUM PRESS.    PLENUM TEMP.'/
     #3X,'M PER SEC.               M PER SEC.          INCHES MERCURY'
     #3X,'INCHES WATER        DEG. C.'/)
C
C     READ IN DATA POINTS
C
C
      DO 77 I=1,NE
         READ(11,200)PAR(I),PPR(I),TPR(I),NAME(I)
         WRITE(*,201)PAR(I),PPR(I),TPR(I),NAME(I)
         WRITE(12,201)PAR(I),PPR(I),TPR(I),NAME(I)
   77 CONTINUE
  200 FORMAT(1X,3F8.4,A14)
  201 FORMAT(2(6X,F8.4),10X,F8.4,11X,A14)
C
C     CALCULATE THE PRESSURE RATIO
C
      DO 88 I=1,NE
         PRR(I)=1.D0-(RHOHG*PAR(I))/(RHOW*PPR(I)+RHOHG*PAR(I))
C
      ANUXR(I)=A0+A1*PRR(I)
C
      WRITE(*,550)I,PRR(I),ANUXR(I),NAME(I)
      WRITE(12,550)I,PRR(I),ANUXR(I),NAME(I)
  550 FORMAT(/1X,'I = ',I3,/
     #' PRESSURE RATIO = ',F10.5,' MACH NUMBER PARAMETER    ',F12.4,/
     #' RUN NAME - ',A14/)
C
C     NEWTON METHOD TO DETERMINE THE ROOTS OF THE EQUATION FOR ANUX
C
C     GUESS INITIAL VALUE OF VREF - VTOT(5)
C
      WRITE(*,560)
      WRITE(12,560)
  560 FORMAT(//10X,'BEGIN NEWTON ITERATION'/)
C
      KOUNT=1
      VREF(I)=VTOT(5)
      XR=VREF(I)/DSQRT(2.D0*CPA*(TPR(I)+273.16D0))
 1000 F=(GAMMA/GM1)*(XR**2)*(1.D0-(XR**2))**(1.D0/(GM1))-ANUXR(I)
      DFDX=(GAMMA/GM1)*2.D0*XR*((1.D0)-(XR**2))**(1.D0/(GM1))*
     #     (1.D0-(XR**2)*(1.D0/GM1)*(1.D0/(1.D0-(XR**2))))
      TERM=F/DFDX
C
      WRITE(*,570)KOUNT,XR,TERM
      WRITE(12,570)KOUNT,XR,TERM
  570 FORMAT(1X,'ITERATION NUMBER ',I2,'  MACH NO. PARAM. - ',F8.6,
     #'    ERROR TERM - ',D12.4)
C
      XR=XR-(F/DFDX)
      KOUNT=KOUNT+1
      IF(DABS(TERM).LT.1.D-10)GO TO 777
      IF(KOUNT.LT.10.OR.DABS(TERM).GT.1.D-10)GO TO 1000
C
C     CALCULATE THE REFERENCE VELOCITY
C
  777 VREF(I)=XR*DSQRT(2.D0*CPA*(TPR(I)+273.16))
      WRITE(*,580)VREF(I)
      WRITE(12,580)VREF(I)
  580 FORMAT(/1X,'VREF - ',F20.11/)
   88 CONTINUE
C
C     PRINT FINAL RESULT
C
      WRITE(12,585)
  585 FORMAT(/1X,'EXPERIMENT NUMBER     REFERENCE VELOCITY     NAME'/)
      DO 777 I=1,NE
      WRITE(12,590)I,VREF(I),NAME(I)
```

```
777   CONTINUE
590   FORMAT(8X,I2,16X,F8.4,10X,D14)
      STOP
      END
C-----------------------------------------------------------------------C
C                                                                       C
C                                                                       C
C     A LEAST SQUARES CURVE FIT FOR A STRAIGHT LINE THROUGH NOISY       C
C     DATA                                                              C
C                                                                       C
C     ALGORITHM TAKEN FROM: NUMERICAL METHODS, ROBERT W. HORNBECK       C
C                           PAGES 122 - 130, QUANTUM, 1975              C
C                                                                       C
C-----------------------------------------------------------------------C
      SUBROUTINE LEASTSQUARE(N,X,FX,A0,A1)
      IMPLICIT REAL*8(A-H,O-Z)
      DIMENSION COEFF(2,2),RHS(2),X(N),FX(N)
C
C     SET UP COEFFICIENT MATRIX AND RIGHT HAND SIDE.
C
      COEFF(1,1)=N
      COEFF(1,2)=0.D0
      COEFF(2,2)=0.D0
C
      RHS(1)=0.D0
      RHS(2)=0.D0
C
      DO 2 I=1,N
         COEFF(1,2)=COEFF(1,2)+X(I)
         COEFF(2,2)=COEFF(2,2)+X(I)**2
         RHS(1)=RHS(1)+FX(I)
         RHS(2)=RHS(2)+X(I)*FX(I)
    2 CONTINUE
      COEFF(2,1)=COEFF(1,2)
C
C      PRINT MATRIX EQUATION
C
      WRITE(*,110)
      WRITE(12,110)
  110 FORMAT(/5X,'MATRIX EQUATION',/)
      DO 3 I=1,2
         WRITE(*,102)(COEFF(I,J),J=1,2),I-1,RHS(I)
         WRITE(12,102)(COEFF(I,J),J=1,2),I-1,RHS(I)
    3 CONTINUE
  102 FORMAT(5X,2(2X,D10.2),' A',I1,3X,D10.2)
C
C     GAUSS ELIMINATION
C
      TERM=COEFF(1,1)/COEFF(2,1)
C
      COEFF(2,2)=COEFF(2,2)-COEFF(1,2)*TERM
      RHS(2)=RHS(2)-RHS(1)*TERM
C
      A1=RHS(2)/COEFF(2,2)
      A0=(RHS(1)-COEFF(1,2)*A1)/COEFF(1,1)
C
      RETURN
      END
```

APPENDIX C. PROBE CALIBRATION

This Appendix contains the following:

1. Yaw probe calibration and plot.
2. Static probe correction.

C1. YAW PROBE CALIBRATION

The calibration of the yaw probe, pressure ports 10 and 11, located at the midspan of the rake probe was accomplished by mounting it in a free jet and subjecting it to three different dynamic pressures. The range of dynamic pressure was 12.2 in. H_2O, 14.1 in. H_2O and 16 in. H_2O. The probe was yawed from -5° to $+5^{\circ}$ in one degree increments. A line was fitted to the data for each test and finally an average equation was fitted. It was noticed that the variation of $(P_{10}-P_{11})$ was not the same for positive and negative incidence due to manufacture imperfection. The uncertainty in the probe calibration was calculated to be 0.5° . The average equation is found in Appendix B.

The data are presented on the following pages and followed by the plot of the data with each equation.

C2. STATIC PROBE CORRECTION

The static probe displayed a deviation of 1.98 in.

H_2O for the first calibration run and 2.34 in. H_2O for the other two runs. Therefore, a line was fitted to correct the rake-measured static pressure for the tunnel velocity variations. The Reynolds number referenced to the probe diameter was between 6000 and 7000, therefore, Reynolds number effect was considered to be negligible. The correction equation is found in Appendix B.

RAKE PROBE CALIBRATION 10/16/92

PA= 29.99 IN Hg Tt=112 F

REFERENCE PA=49.9 IN H20 Q=12.2 IN H20

ALPHA	PT	PROBE (P9)	PROBE (P10)	PROBE (P11)	PROBE (P12)	ATMOS
-5	37.7	47.7	38.6	40.3	37.7	49.9
-4	37.7	47.75	38.7	40.15	37.7	49.9
-3	37.7	47.85	38.95	39.9	37.7	49.9
-2	37.7	47.9	39.05	39.7	37.7	49.9
-1	37.7	47.9	39.25	39.45	37.7	49.9
0	37.7	47.9	39.3	39.3	37.7	49.9
1	37.7	47.9	39.35	39.15	37.7	49.9
2	37.7	48.1	39.5	39	37.7	49.9
3	37.7	48.2	39.8	38.9	37.7	49.9
4	37.7	48.2	39.9	38.8	37.7	49.9
5	37.7	48.2	40.1	38.65	37.7	49.9

Q=14.1 IN H20

ALPHA	PT	PROBE (P9)	PROBE (P10)	PROBE (P11)	PROBE (P12)	ATMOS
-5	35.8	47.35	36.9	38.9	35.8	49.9
-4	35.8	47.4	37.05	38.65	35.8	49.9
-3	35.8	47.5	37.25	38.4	35.8	49.9
-2	35.8	47.55	37.45	38.15	35.8	49.9
-1	35.8	47.6	37.65	37.9	35.8	49.9
0	35.8	47.6	37.7	37.7	35.8	49.9
1	35.8	47.6	37.7	37.5	35.8	49.9
2	35.8	47.85	38.1	37.4	35.8	49.9
3	35.8	47.7	38.35	37.2	35.8	49.9
4	35.8	47.85	38.6	37.05	35.8	49.9
5	35.8	47.7	38.8	36.95	35.8	49.9

Q=16 IN H20

ALPHA	PT	PROBE (P9)	PROBE (P10)	PROBE (P11)	PROBE (P12)	ATMOS
-5	33.9	47.5	35.2	37.35	33.9	49.9
-4	33.9	47.6	35.3	37	33.9	49.9
-3	33.9	47.7	35.55	36.75	33.9	49.9
-2	33.9	47.7	35.7	36.5	33.9	49.9
-1	33.9	47.7	35.9	36.15	33.9	49.9
0	33.9	47.7	36	36	33.9	49.9
1	33.9	47.7	36.2	35.7	33.9	49.9
2	33.9	47.6	36.45	35.55	33.9	49.9
3	33.9	47.6	36.8	35.4	33.9	49.9
4	33.9	47.55	37	35.2	33.9	49.9
5	33.9	47.5	37.3	35.2	33.9	49.9

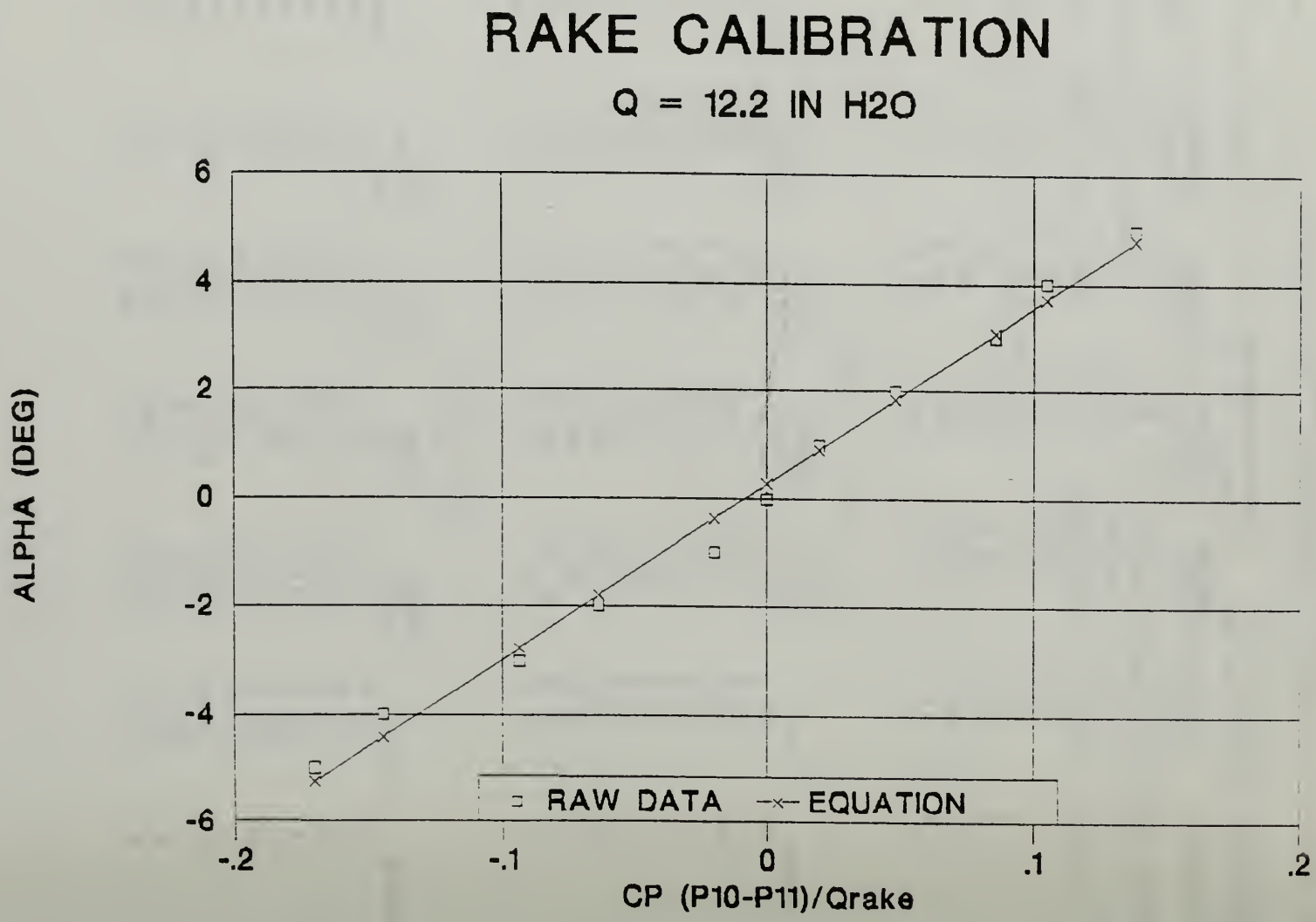
RAKE CALIBRATION
Q = 12.2 IN H2O
ALPHA (DEG)
6
4
2
0
-2
-4
-6
-.2
-.1
0
.1
.2
CP (P10-P11)/Qrake
RAW DATA
EQUATION

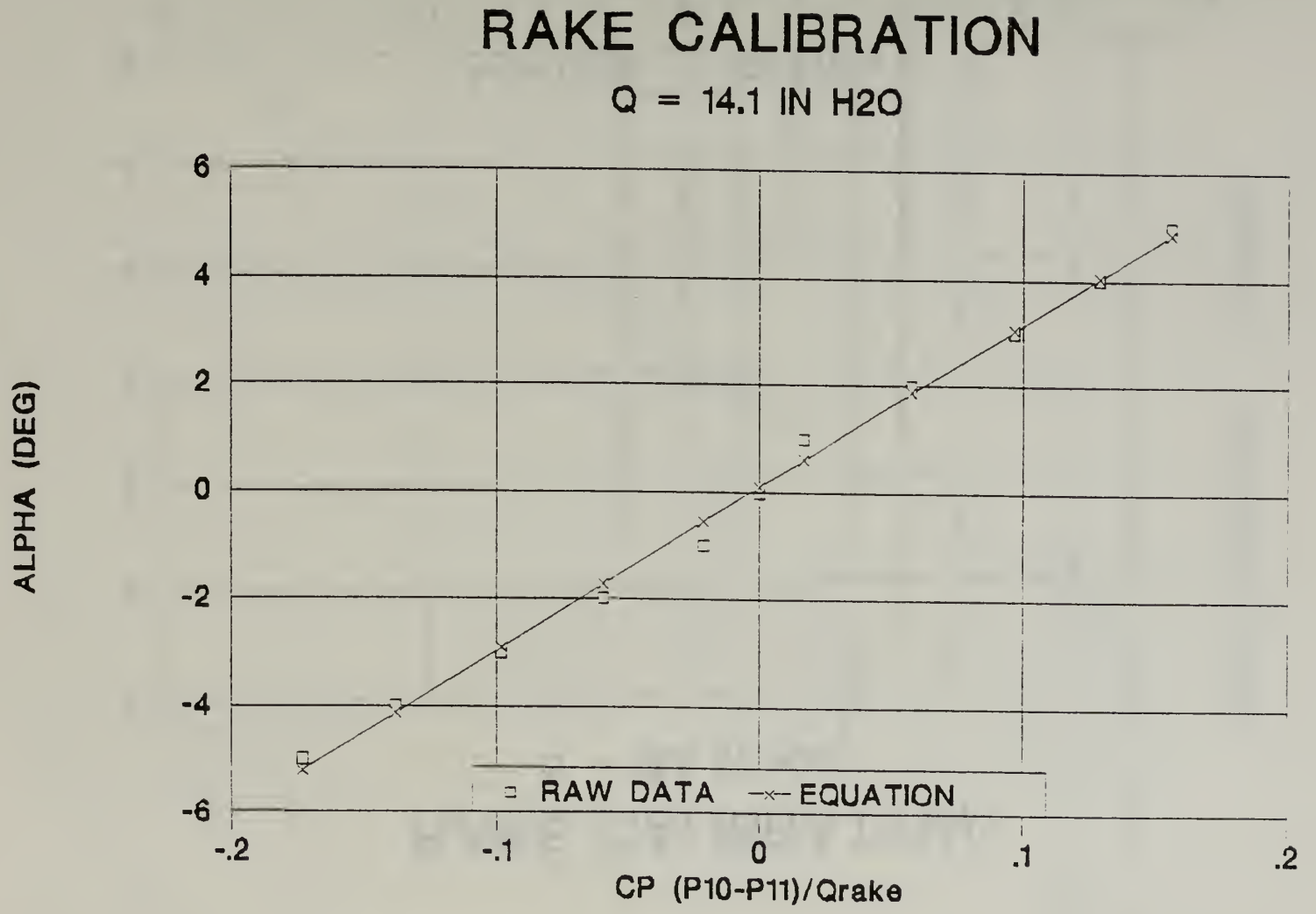
RAKE CALIBRATION
Q = 14.1 IN H2O
ALPHA (DEG)
6
4
2
0
-2
-4
-6
-.2
-.1
0
.1
.2
CP (P10-P11)/Qrake
RAW DATA
EQUATION

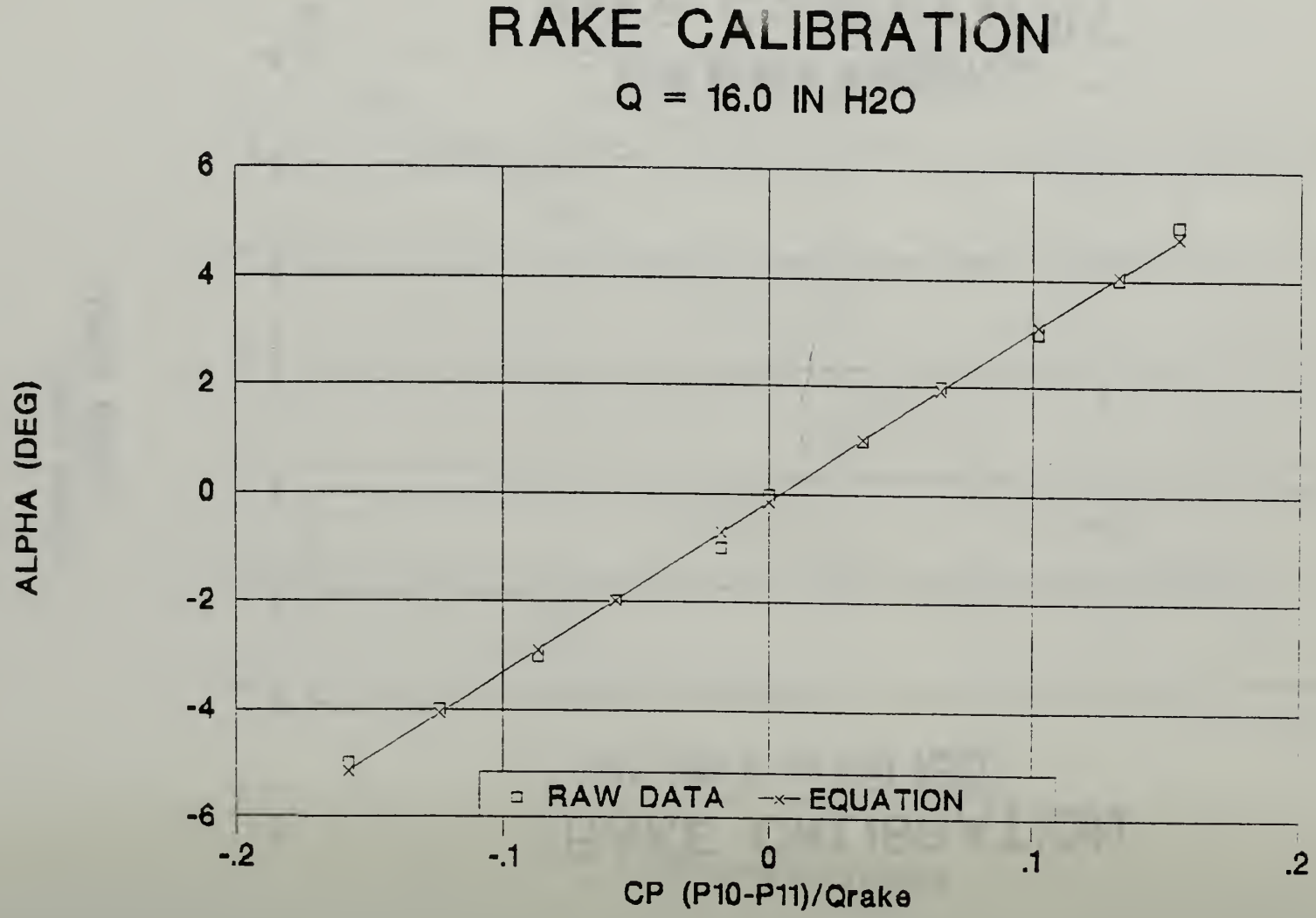
RAKE CALIBRATION
Q = 16.0 IN H2O
ALPHA (DEG)
6
4
2
0
-2
-4
-6
-.2
-.1
0
.1
.2
CP (P10-P11)/Qrake
RAW DATA
EQUATION

APPENDIX D. ENGINEERING DRAWINGS

This Appendix contains all detailed drawings cited in the body of this document. They are displayed in the following order:

1. Inlet guide vanes
2. Suction slot
3. Suction slot adjustable mounting brackets
4. Porous baffle
5. Suction manifold cross section
6. Rake probe plan view
7. Rake probe spanwise dimensions

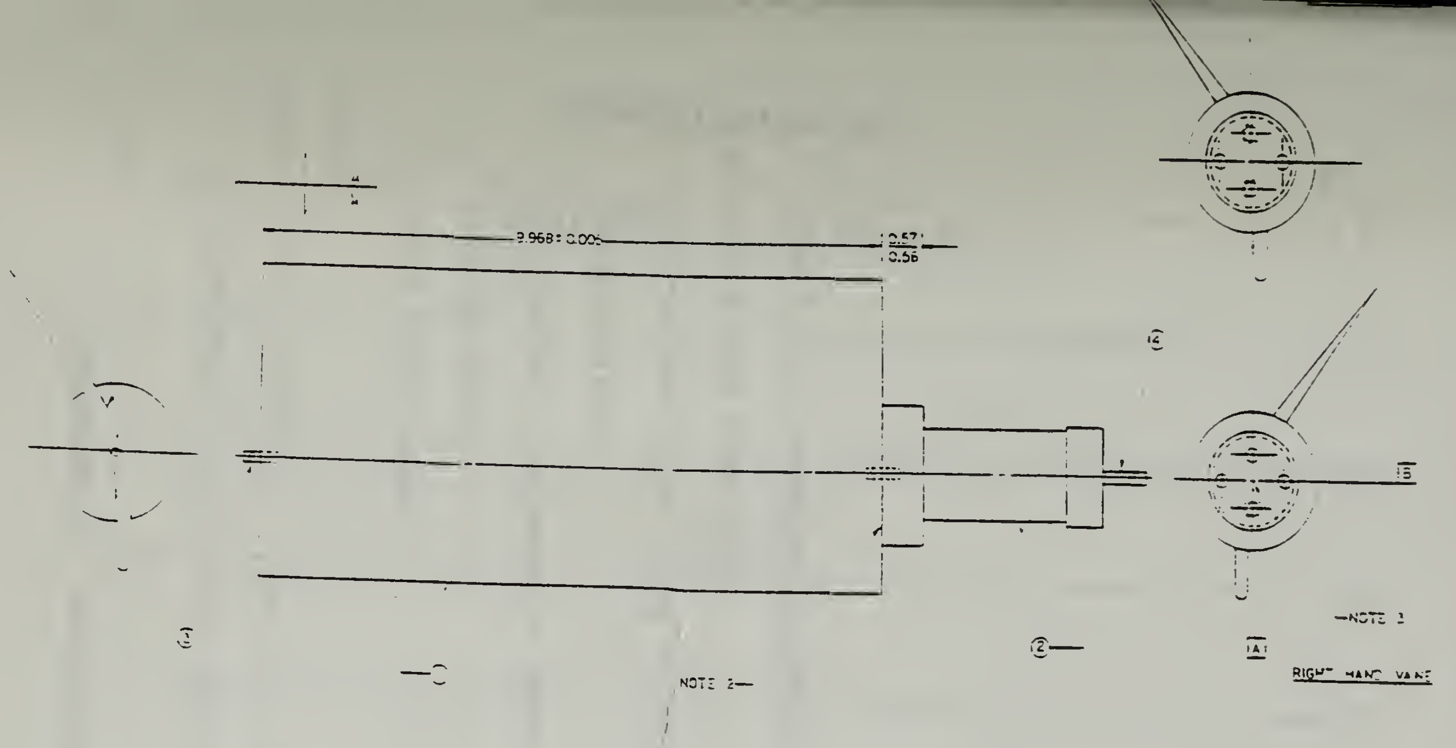

NOTE 30 LEFT HAND AND 30 RIGHT HAND TURNING VANES REQ'D. RIGHT HAND/LEFT HAND VANE SHOWN

2. REFERENCE AXES (1) AND (2) IN COMPLETED PART SHALL BE COINCIDENT TO ±0.005, END TO END

3. ACTUATING PIN REFERENCE PLANE [B] SHALL BE PERPENDICULAR TO REFERENCE PLANE [A] WITHIN 0.25° ON FINISHED PART. INSTALLED ACTUATING PINS SHALL MATCH ACTUATING ARM PROVIDED.

TOLERANCES:

0.X =±0.05
0.XX =±0.005
0.XXX =±0.001
XX° =±0.2°

PART NO	Q'TY	PART NAME	MAT.
4	120	ACTUATING PIN	STEEL
3	120	CENTERING PIN	STEEL
2	60	TURNING VANE SHANK	6061-T6 ALUM
1	60	TURNING VANE	6061-T6 ALUM

TURNING VANE ASS'Y — 6022 — SHEET NO. 1/2

RELEASED — FULL

US NAVAL POSTGRADUATE SCHOOL
DEPT OF AERONAUTICS
MONTEREY CA

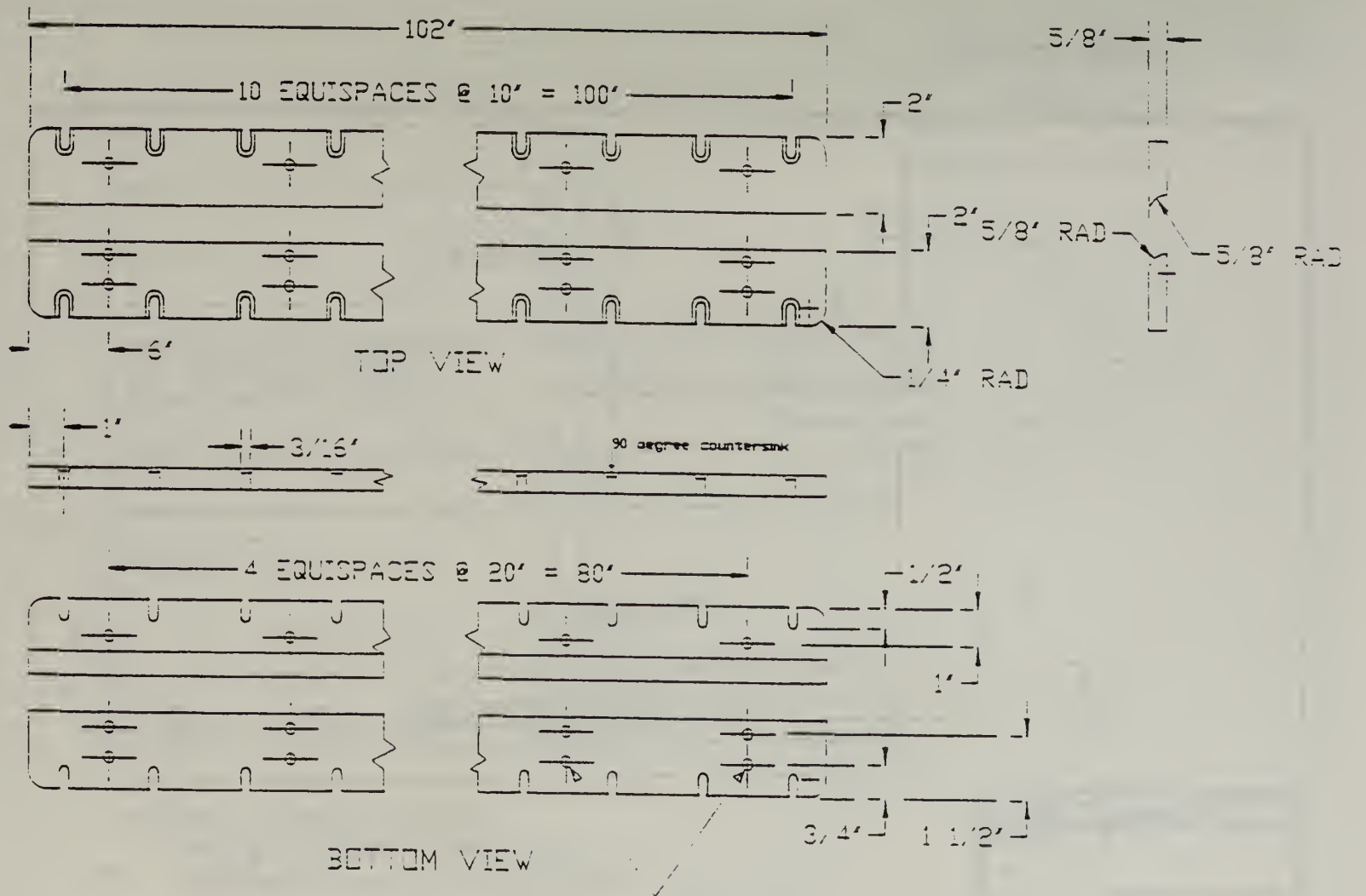

CASCADE ENDWALL SLOTS

Material: Aluminum Alloy
6061-T6
Quantity: Two sets

Garth Hobson 03/20/01

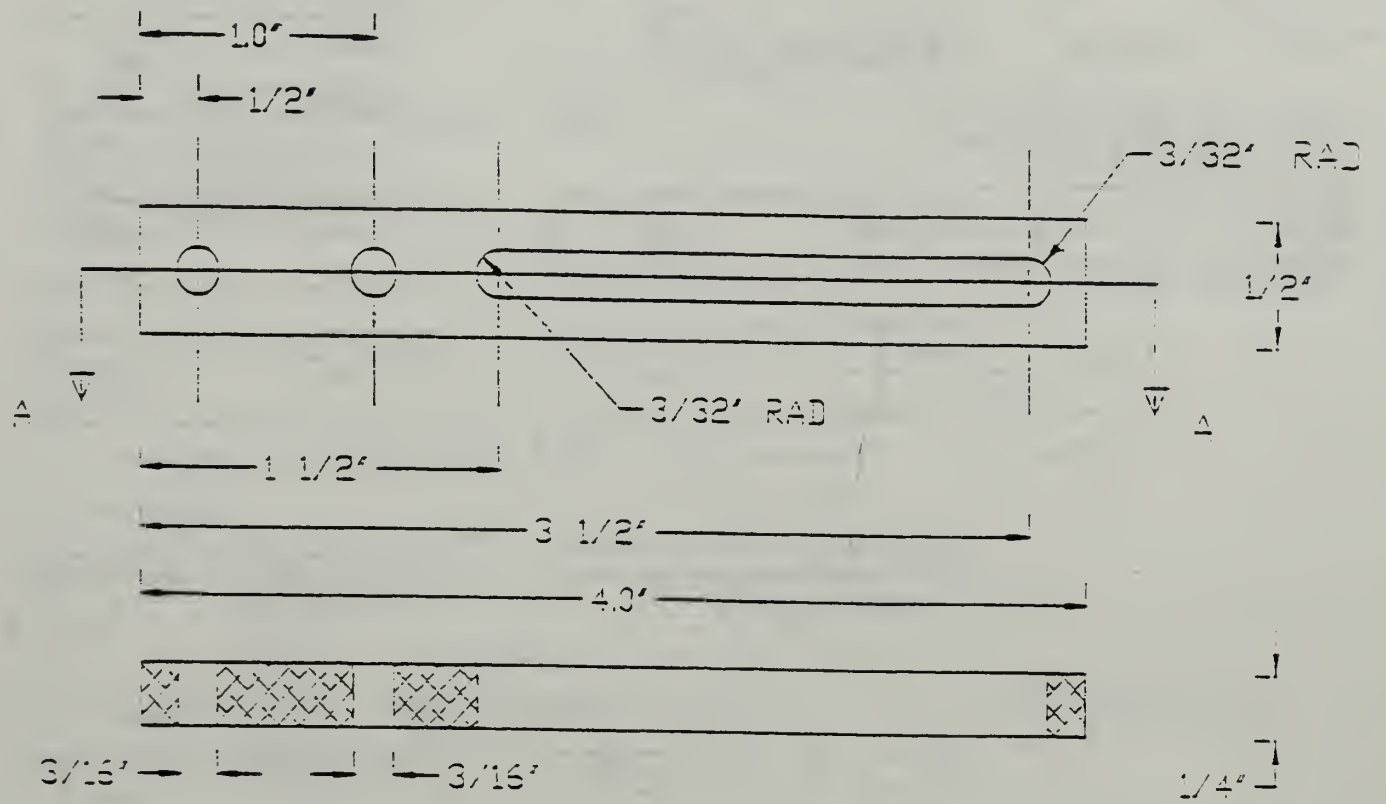

SECTION A-A

GUIDES

Material: Aluminum Alloy

Quantity: 10

09/20/91

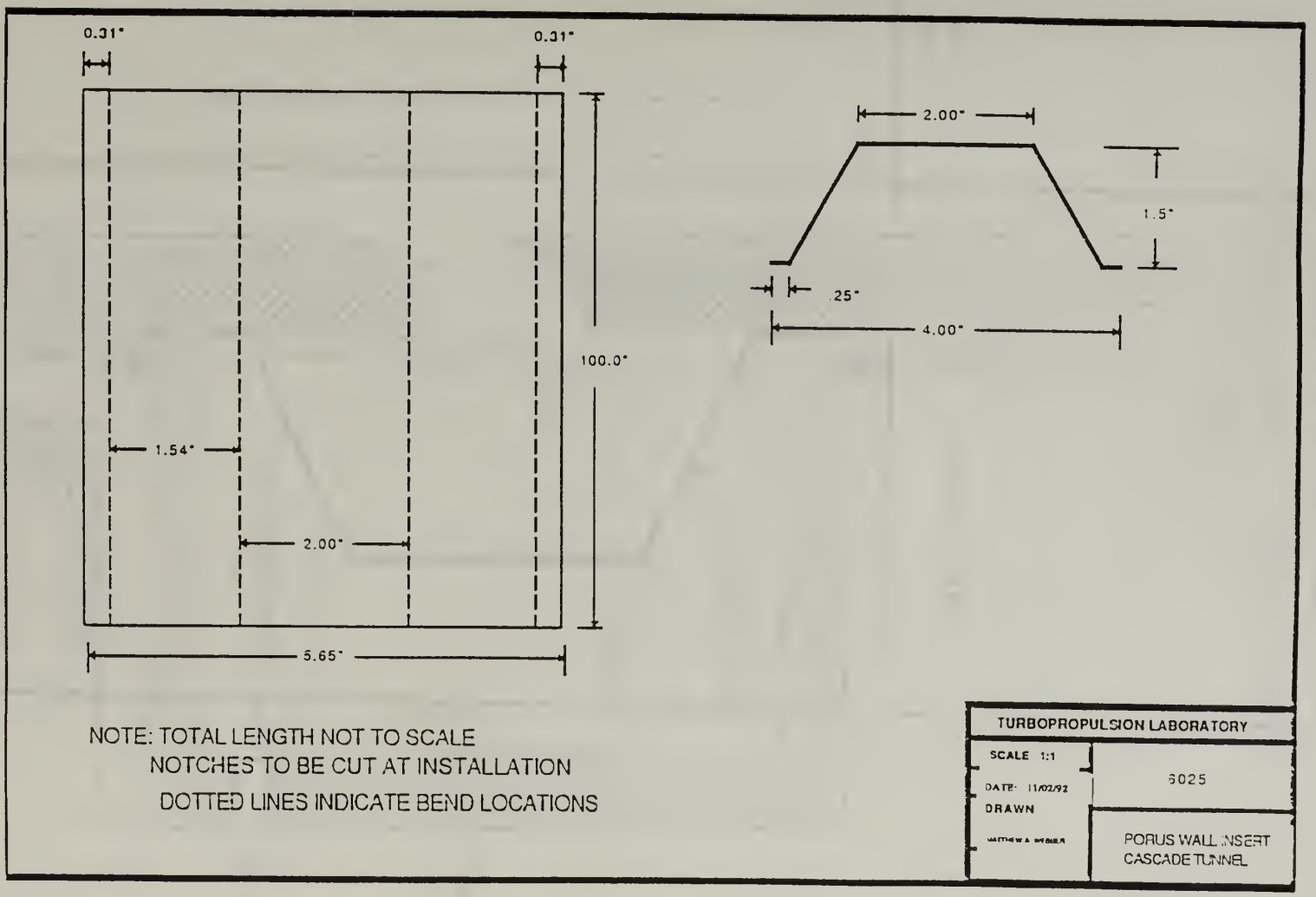
0.31"
0.31"
100.0"
1.54"
2.00"
5.65"
2.00"
1.5"
.25"
4.00"
NOTE: TOTAL LENGTH NOT TO SCALE
NOTCHES TO BE CUT AT INSTALLATION
DOTTED LINES INDICATE BEND LOCATIONS
TURBOPROPULSION LABORATORY
SCALE 1:1
DATE: 11/02/92
DRAWN
6025
POROUS WALL INSERT
CASCADE TUNNEL

CROSS-SECTION OF SUCTION MANIFOLD

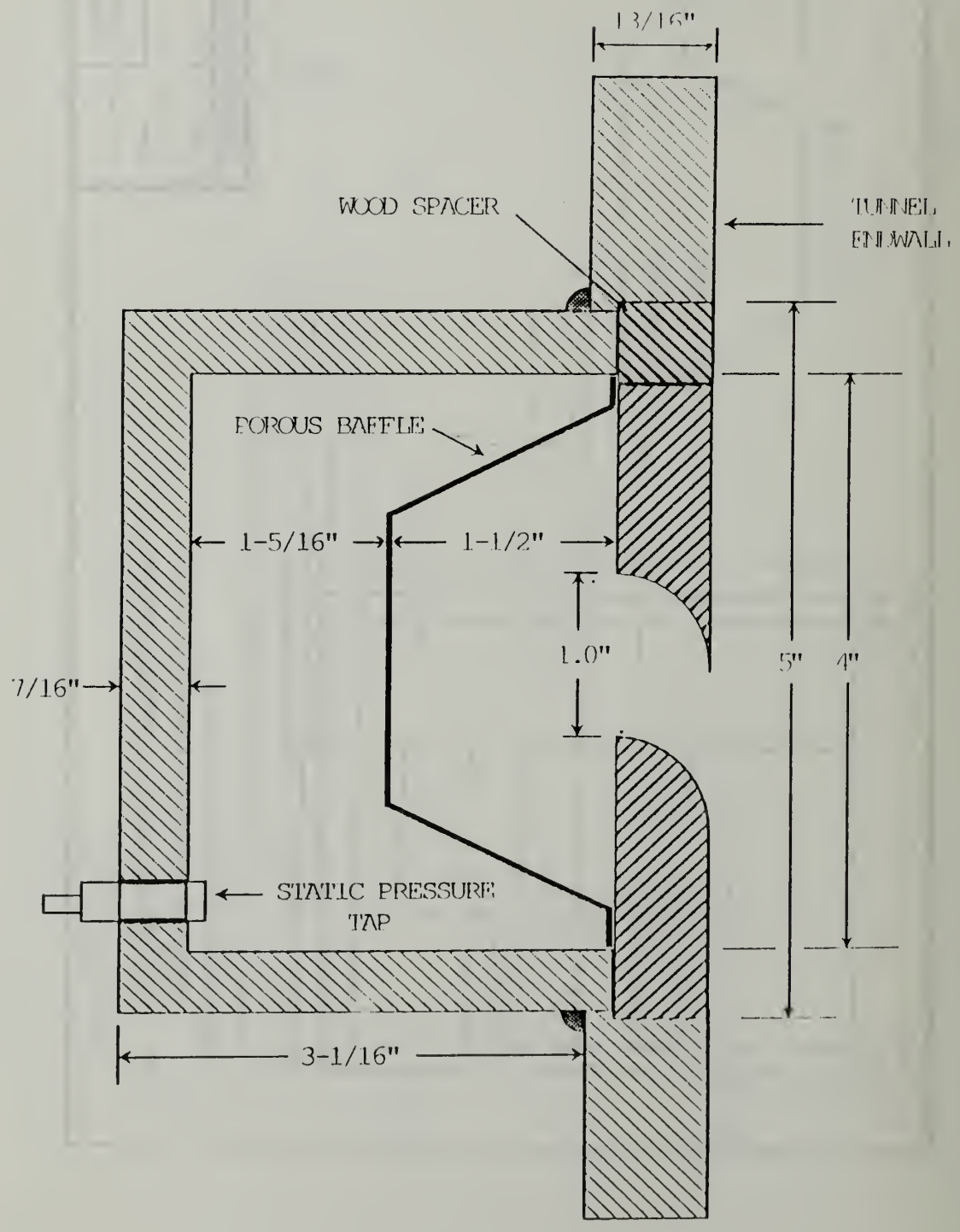

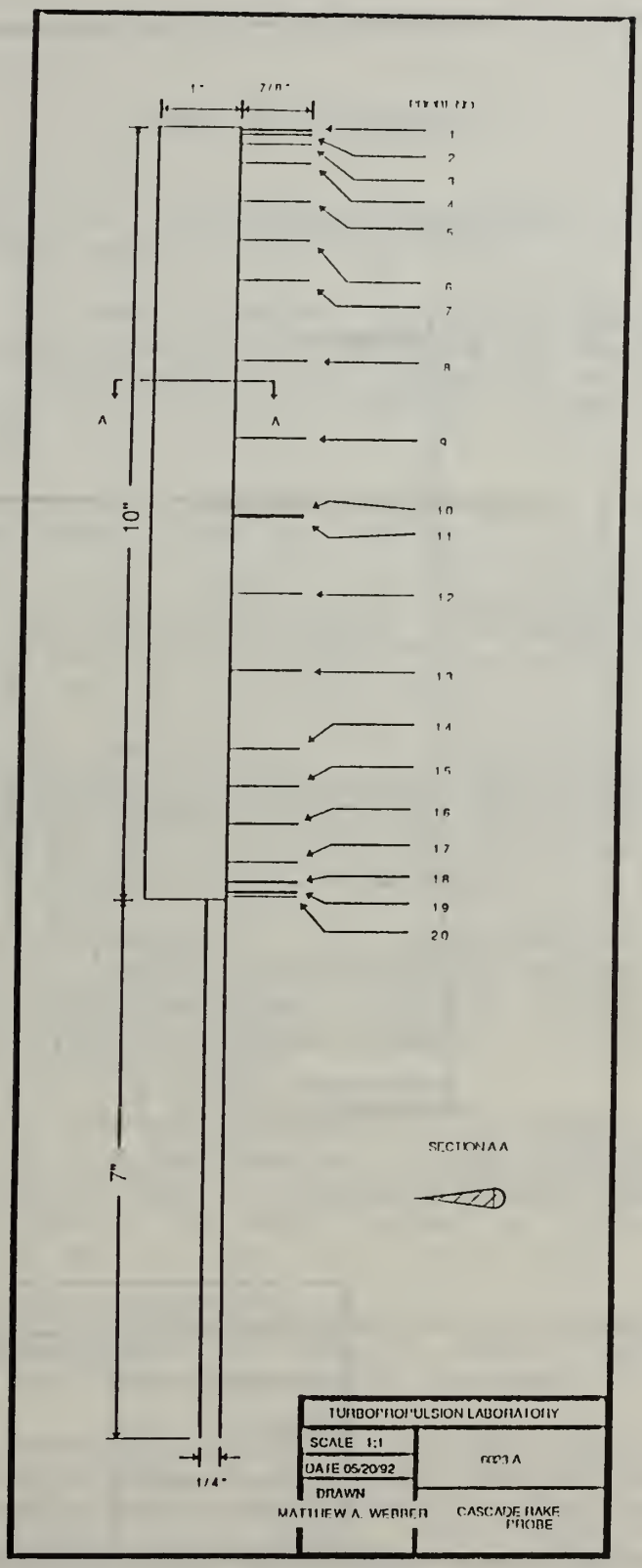
1
2
3
4
5
6
7
8
9
10
11
12
13
14
15
16
17
18
19
20
A
A
10"
7"
1/4"
SECTION A A
TURBOPROPULSION LABORATORY
SCALE 1:1
DATE 05/20/92
DRAWN
MATTHEW A. WEBBER
CASCADE RAKE PROBE

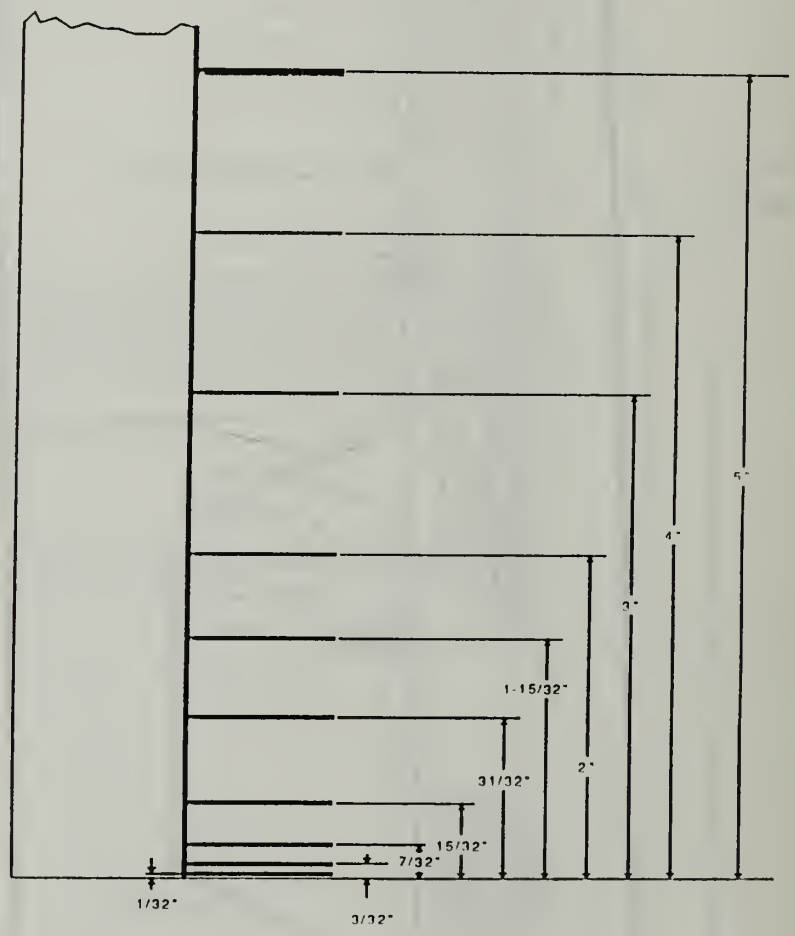

TURBOPROPULSION LABORATORY	
SCALE 1:2	6023 B
DATE 05/20/92	
DRAWN MATTHEW A WEBBER	RAKE PROBE - PROBE DIMENSIONS

LIST OF REFERENCES

1. Horlock, J. H., Axial Flow Compressors, Krieger Publishing Company, 1958, pp. 73-75.

2. Rodger, P., and Sjolander, S., Establishing Two-Dimensional Flow in a Large Scale Planar Turbine Cascade, AIAA paper 92-3066 presented at the 28th Joint Propulsion Conference and Exhibit, Nashville, TN, July 6-8, 1992.

3. Gostelow, J. P., Cascade Aerodynamics, 1st Ed., Permagon Press, 1984, pp. 35-40.

4. Barnwell, R. W., Effect of Sidewall Suction on Flow in Two-Dimensional Wind Tunnels, AIAA paper 84-0242 presented at the AIAA 22nd Aerospace Sciences Meeting, Reno, NV, Jan. 9-12, 1984.

5. Deutsch, S., and Zierke, W. C., The Measurement of Boundary layers on a Compressor Blade Cascade Part I: A Unique Experimental Facility, ASME paper 87-GT-248 presented at the Gas Turbine Conference and Exhibition, Anaheim, CA, May 31 - June 4, 1987.

6. Hobbs, D. E., Wagner, J. H., Dannenhoffer, J. F., and Dring, R. P., Wake Experiments and Modeling for Fore- and Aft-Loaded Compressor Cascades, Pratt and Whitney Aircraft Group Government Products Division, West Palm Beach, FL, Sept., 1980.

7. Sanger, N. L., and Shreeve, R. P., Comparison of Calculated and Experimental Cascade Performance for Controlled-Diffusion Compressor Stator Blading, Transactions of the ASME, Journal of Turbomachinery, Vol. 108, No. 1, pp. 42-50, July 1986.

8. Dreon, J. W., Controlled Diffusion Compressor Blade Wake Measurements, M.S. Thesis, Naval Postgraduate School, Monterey, California, September 1986.

9. Elazar, Y., A Mapping of the Viscous Flow Behavior in a Controlled Diffusion Compressor Cascade Using Laser Doppler Velocimetry and Preliminary Evaluation of Codes for the Prediction of Stall, Ph.D. Dissertation, Naval Postgraduate School, Monterey, California, March 1988.

10. Classick, M., Off-Design Loss Measurements in a Compressor Cascade, M.S. Thesis, Naval Postgraduate School, Monterey, California, September 1989.

11. Hobson, G., and Shreeve, R., Inlet Turbulence Distortion and Viscous Flow Development in a Controlled-Diffusion Compressor Cascade at Very High Incidence, AIAA paper 91-2004 presented at the 27th Joint Propulsion Conference, Sacramento, CA, June 24-26, 1991.

12. Rose, C., and Guttormson, D. L., Installation and Test of a Rectilinear Cascade, M.S. Thesis, Naval Postgraduate School, Monterey, California, 1964.

13. McGuire, A., Determination of Boundary Layer Transition and Separation on Double Circular Arc Compressor Blades in a Large Subsonic Cascade, M.S. Thesis, Naval Postgraduate School, Monterey, California, September 1983.

14. Murray, K., Automation and Extension of LDV Measurements of Off-Design Flow in a Subsonic Cascade Wind Tunnel, M.S. Thesis, Naval Postgraduate School, Monterey, California, June 1989.

15. Dober, D., 3-Dimensional Fiber-Optic LDV Measurements in the Endwall Region of a Linear Cascade of Controlled-Diffusion Stator Blades, M.S. Thesis, Naval Postgraduate School, Monterey, California, March 1993.

INITIAL DISTRIBUTION LIST

		No. Copies
1.	Library, Code 0142 Naval Postgraduate School Monterey, California 93943-5002	2
2.	Defense Technical Information Center Cameron Station Alexandria, Virginia 22304-6145	2
3.	Department Chairman, AA Department of Aeronautics Naval Postgraduate School Monterey, California 93943	1
4.	Garth V. Hobson, Turbopropulsion Laboratory Code AA/Hg Department of Aeronautics Naval Postgraduate School Monterey, California 93943	7
5.	Naval Air Systems Command AIR-536T (Attn: Mr. Paul F. Piscopo) Washington, District of Columbia 20361-5360	1
6.	Naval Air Warfare Center Aircraft Division (Trenton) PE-31 (Attn: S. Clouser) 250 Phillips Blvd Princeton Crossroads Trenton, New Jersey 08628-0176	1
7.	Matthew A. Webber U. S. Naval Air Facility PSC 477, Box 25 FPO AP 96306-1225	1

DUDLEY KNOX LIBRARY
NAVAL POSTGRADUATE SCHOOL
MONTEREY CA 93943-5101

DUDLEY KNOX LIBRARY
3 2768 00307397 4